MODELLING, ASSESSMENT AND SCHEDULING FOR USING BUILDING ENERGY FLEXIBILITY AS SPINNING RESERVE IN POWER SYSTEMS

HAN BINGLONG

PhD

The Hong Kong Polytechnic University

2025

The Hong Kong Polytechnic University

Department of Building Environment and Energy Engineering

Modelling, Assessment and Scheduling for Using Building Energy Flexibility as Spinning Reserve in Power Systems

Han Binglong

A thesis submitted in partial fulfillment of the requirements for the degree of Doctor of Philosophy

Aug 2024

CERTIFICATE OF ORIGINALITY

I hereby declare that this thesis is my own work and that, to the best of my knowledge and belief, it reproduces no materials previously published or written, nor material that has been accepted for the award of any other degree or diploma, except where due acknowledgement has been made in the text.

_____(Signed)

Han Binglong (Name of student)

ABSTRACT

Abstract of thesis entitled: Modelling, assessment and scheduling for using building energy flexibility as spinning reserve in power systems

Submitted by : Han Binglong

For the degree of : Doctor of Philosophy

at The Hong Kong Polytechnic University in August, 2024

The growing adoption of renewable energy and the increasingly frequent extreme weather events pose great challenges to the supply-demand balance and the reliability of power systems. Spinning reserve is an essential means to manage power imbalance due to renewable forecast uncertainties and generator failures. Traditionally, spinning reserve is provided by standby generators operating at part load. However, more spinning reserve capacity is needed while fewer standby generators are available due to increased renewable penetration. Buildings, particularly their air-conditioning systems, have great potential to provide spinning reserve due to their large electricity use and energy flexibility. However, there are several problems and challenges when using this alternative spinning reserve resource. First, effective methods are needed to model and quantify the energy flexibility capacity of buildings for providing spinning reserve. Second, the impacts of using building energy flexibility for spinning reserve on power systems and buildings need to be assessed. Third, the power system reserve scheduling should be optimized to utilize building energy flexibility in a reliable and economic manner.

This PhD study, therefore, aims to comprehensively and systematically investigate the modelling, assessment and scheduling of building energy flexibility for providing spinning reserve in power systems.

Analytical solutions are developed for energy flexibility modelling of building air-conditioning systems. Five straightforward equations are derived from a commonly used second-order building thermodynamic model, which quantify the load reduction and subsequent load rebound of buildings at both individual and aggregated levels. The solutions avoid time-consuming iterative and finite difference computations of the existing numerical method, facilitating the integration of flexibility quantification in power system scheduling and dispatch. The high accuracy and computational efficiency of analytical solutions are verified through numerical simulations.

The impacts of using building energy flexibility for spinning reserve are assessed and compared with that for load shifting, considering the operation of both power systems and buildings. An integrated grid-buildings model is developed to capture the dynamic interaction between buildings and the power supply side. The model is applied to the Hong Kong power system in 2035. The results show that spinning reserve provision not only offers higher operating cost savings for the power system but also has much less interference to building operation compared to load shifting. Therefore, spinning reserve is proposed as a priority use of building energy flexibility in smart grids.

Buildings may fail to achieve their committed spinning reserve provision in actual operation due to various uncertainties. A probabilistic model is proposed for real-time quantification of building energy flexibility, considering uncertainties in model inputs, model bias, and building response failures. An analytical equation is used to quantify the flexibility of each building, which effectively captures the distinct characteristics

of diverse buildings. Test results show that the proposed model accurately quantifies the aggregated energy flexibility of 150 buildings in 6.7 seconds, up to 537 times faster than existing probabilistic models.

A risk-averse reserve scheduling framework is proposed for power systems that engage building energy flexibility, considering the trade-off between cost savings and the risk of using building energy flexibility as spinning reserve. The framework leverages the outputs of the probabilistic model of building energy flexibility to provide risk-based decision-making. A new risk indicator, namely expected reserve shortage, is proposed for more accurate risk assessment. Test results show that adopting building energy flexibility as spinning reserve can reduce both the operation costs and risks of the power system, compared to using conventional generators solely.

An optimal reserve scheduling strategy is proposed for power systems that engage building energy flexibility, considering the load rebound effect after demand response. The strategy accounts for the uncertainties in both renewable forecasts and generator failures, enabling more effective utilization of building flexibility potential. A two-stage robust optimization problem is formulated for reserve scheduling considering load rebound. Test results show that the proposed strategy reduces the power system operation cost by 7.54%, compared to the strategy without considering load rebound.

PUBLICATIONS ARISING FROM THIS THESIS

Journal Papers

[1] **Binglong Han**, Hangxin Li, Shengwei Wang. (2024). Analytical solution for energy flexibility modelling of building air-conditioning system. *IEEE Transactions on Smart Grid (PES letter)*, 2024.

[2] **Binglong Han**, Hangxin Li, Shengwei Wang. (2024). A probabilistic model for real-time quantification of building energy flexibility. *Advances in Applied Energy*, Volume 15, 2024, 100186.

[3] **Binglong Han**, Hangxin Li, Shengwei Wang. (2024). Robust reserve scheduling for power systems engaging building energy flexibility by considering load rebound. *Journal of Energy Storage*. (Under second review)

[4] **Binglong Han**, Hangxin Li, Shengwei Wang. (2024). Comparative assessment of using building energy flexibility as spinning reserve in power systems. *Applied energy*. (Under review).

Conference Paper

[1] **Binglong Han**, Hangxin Li, Shengwei Wang. (2025). Incorporating building energy flexibility in power system spinning reserve: A risk-averse scheduling framework. IEEE 8th International Electrical and Energy Conference.

ACKNOWLEDGEMENTS

First and foremost, I would like to express my appreciation to Professor Shengwei Wang, my supervisor, for his supervision, valuable suggestions, and continuous support during my PhD study. His rich experience and extensive knowledge have led me in the right direction for my research. His patient guidance and stringent academic requirements have helped me achieve satisfactory outcomes. I would like to thank Professor Fu Xiao and Dr. Hangxin Li for their suggestions throughout the entire period of my PhD studies.

I would also like to thank all colleagues in my research group, especially Mingkun Dai, Zhisen Chen, Xingyu Zang, and Dr. Hang Yu, who have shared their experiences and thoughts on both research and life with me. I will remember the days spent with all my friends.

Finally, I would like to thank the reviewer of my first manuscript. The comments inspired me to rethink the scope, direction, and advantages of my research. I would like to express my appreciation to my girlfriend, Min Zuo, for her support over the past years and for the rest of my life. Additionally, I would like to dedicate this thesis to my parents for their unconditional support throughout my life.

TABLE OF CONTENTS

LIST OF FIGURES

LIST OF TABLES

NOMENCLATURE

C	Thermal capacitance/Cost
CCGT	Combined cycle gas turbine
COP	Coefficient of performance
e	Model bias
E	Energy state
EF	Energy flexibility
EERS	Expected energy not served
ERS	Expected reserve shortage
HVAC	Heating, ventilation, and air conditioning
MC	Minimum load cost
MDT	Minimum shutdown duration
MOT	Minimum online duration
OCGT	Open cycle gas turbine
p	Probability
P	Power
Q	Cooling load
ra/rc	Reserve activation/commitment price
R	Thermal resistance
RE	Renewable energy
RU/RD	Ramping up/down
SC	Startup cost
SR	Spinning reserve
T	Temperature
TOR	Temperature offset ratio
t	Time
VC	Variable cost
x	Model inputs

Subscripts

ac	Air-conditioning
act	Activation
agr	Aggregate
base	Baseline
bui	Building
ch	Charging
com	Commitment
dem	Demand
dis	Discharging
em	Emergency action
ES	Energy storage
gen	Generator
GF	Generator failure
i	Index of generator cluster
in	Indoor air
j	Index of time interval
k	Index of buildings
LS	Load shifting
m	Internal mass
max	Maximum
min	Minimum
nor	Normal
on	Online
out	Outdoor air
RE	Renewable energy
req	Required
shut	Shutdown
SR	Spinning reserve
start	Start up
reb	Rebound
s	Reduction

Greek symbols

α	Load reduction coefficient
β	Load rebound coefficient
γ	Disturbance vector
ω	Response state of buildings
u	Deviation
σ	Uncertainty budget
η	Charging efficiency
φ	Function

CHAPTER 1 INTRODUCTION

This chapter presents an outline of this thesis. The background and motivation of the study are presented in Section 1.1. The aim and objectives are presented in Section 1.2. Section 1.3 presents the organization of this thesis.

1.1 Background and motivation

Renewable energy sources, such as wind and solar power, are increasingly integrated into electrical power systems to facilitate energy transitions and achieve decarbonization targets (Qin et al. 2023). However, the stochastic and uncontrollable nature of renewable generation poses significant challenges in maintaining the power balance and reliable operation of power systems. Extreme weather events, such as heat waves, exacerbate these challenges by causing higher peak loads and increased failure rates of power system components such as conventional generators. Spinning reserve is an essential means to manage power imbalances due to renewable forecast uncertainties and unexpected generator failures (Roos and Bolkesjø 2018). For instance, during the significant power supply failure in Europe in 2021, spinning reserve was instrumental in preventing a widespread blackout. Traditionally, spinning reserve has been provided by conventional generators operating at part load that can rapidly adjust power outputs (Frew et al. 2021). However, as renewable penetration increases, the need for significantly increased spinning reserve capacity arises, while the availability of conventional generators decreases. Although utility-scale energy storage can provide spinning reserve by discharging electricity as needed, its widespread adoption is still hindered by the high costs and safety concerns (Wald et al. 2023).

Buildings have significant potential and advantages in providing spinning reserve due to their large electricity use and inherent energy flexibility. The building sector accounts for approximately 40% of energy consumption worldwide and 90% of electricity consumption in Hong Kong (Tang and Wang 2023). Numerous studies have demonstrated that the heating, ventilation, and air conditioning (HVAC) systems in buildings can achieve a rapid demand reduction in response to power grid requests, with negligible or acceptable sacrifices in indoor thermal comfort. In fact, buildings can respond to power grid requests much more rapidly than the 10 minutes required for spinning reserve provision (Wang, Wang, and Tang 2019). Moreover, buildings usually incur much lower standby costs compared to conventional generators when providing spinning reserve. Therefore, building energy flexibility has emerged as a feasible and cost-effective resource for providing spinning reserve in power systems, especially in systems with increasing renewable energy penetration that require greater spinning reserve capacity. However, there are still many significant problems and challenges impeding the adoption of building energy flexibility for spinning reserve, as summarized below.

1. To achieve optimized grid-buildings coordination when using buildings for spinning reserve, a large number of flexibility quantification are needed concerning the load reduction and load rebound of buildings. However, existing studies rely on finite difference and iterative computations, which are computationally intractable when integrating building flexibility quantification in grid scheduling and dispatch.
2. The impacts of spinning reserve provision by buildings are not fully investigated. Existing studies usually assume building flexibility as a price-taker in grid service markets and focus on cost savings of power systems, without assessing the impact

of reserve provision on building operation. A comparison of using building energy flexibility for spinning reserve and load shifting is not found in the literature.

3. Buildings may fail to achieve their committed spinning reserve provision in actual operation due to various uncertainties, such as building model inputs, model bias, and building response failures. Most existing studies overlook the impact of these uncertainties and the diversity of buildings. An effective probabilistic model is still lacking for real-time building flexibility quantification under uncertainties.
4. There is a lack of an effective framework for identifying the best reserve schedule incorporating building energy flexibility, concerning its impact on power system operation cost and risk. Existing studies usually use power-based risk indicators which are difficult to quantify. They also overlook the risk from conventional generators, which may lead to an underutilization of building energy flexibility.
5. Load rebound often occurs after activating building flexibility for spinning reserve. Most existing studies overlook the load rebound effect or assume it as a hypothetical value, which may adversely affect reliability and economy of power systems. They focus on uncertainties in either renewable forecasts or generator failures, leading to suboptimal utilization of building energy flexibility.

1.2 Aim and objectives

This PhD study aims to investigate the modelling and quantification of building energy flexibility for spinning reserve, assess the impacts of reserve provision by buildings on both power systems and buildings, and develop optimized reserve scheduling to leverage building energy flexibility in a reliable and economic manner. This will be accomplished by addressing the following objectives and research tasks:

1. Develop accurate and computationally efficient analytical solutions for energy flexibility modelling of building air-conditioning systems. Quantify the load reduction and load rebound of buildings at both individual and aggregated levels.
2. Assess the impact of using building energy flexibility as spinning reserve on both power systems and buildings. Develop an effective integrated grid-buildings model for impact assessment. Conduct a systematic comparison of using building energy flexibility for providing spinning reserve and load shifting.
3. Develop a probabilistic model for real-time quantification of building energy flexibility under uncertainties. The model will comprehensively consider the major uncertainties involved in flexibility quantification while adequately capturing the diversity of individual buildings.
4. Develop a risk-averse reserve scheduling framework for power systems engaging building energy flexibility. This framework can provide quantified power system operation cost and risk for identifying the best reserve schedule. Additionally, develop a new risk indicator for computationally efficient and accurate risk assessment.
5. Develop an optimal reserve scheduling strategy that considers load rebound for power systems engaging building energy flexibility. Create a robust optimization problem that efficiently incorporates the load rebound effect in reserve scheduling, considering uncertainties in both renewable forecasts and generator failures.

1.3 Organization of this thesis

Chapter 1 introduces the background and motivations for studying the use of building energy flexibility as spinning reserve. The aim and objectives of this study, as well as the organization of this thesis, are also presented.

Chapter 2 presents a comprehensive literature review on the related existing studies. An overview of using building energy flexibility for providing grid services is presented first. Then, studies on building energy flexibility quantification and impact assessment are discussed, followed by those on reserve scheduling of power systems engaging building energy flexibility. The research gaps are also summarised following the literature review.

Chapter 3 presents the analytical solutions for energy flexibility modelling of building air-conditioning systems at both individual and aggregated levels. Five straightforward equations are derived from a commonly used second-order building thermodynamic model in demand response conditions. Both load reduction and the following load rebound of buildings are quantified as functions of regulation durations and indoor air temperature offsets. Tests are conducted to validate the solutions.

Chapter 4 presents a comparative assessment of using building energy flexibility for spinning reserve and load shifting, considering the operation of both buildings and the power system. An integrated grid-buildings model is developed to capture the dynamic interaction between building flexibility and the power supply side. The model is applied to the Hong Kong power system in 2035, considering different generation mix scenarios, to comprehensively assess the impacts of building energy flexibility.

Chapter 5 presents a probabilistic model for the real-time quantification of building energy flexibility. The model uses an analytical equation to quantify the flexibility of individual buildings, capturing their diversity. It comprehensively considers the major uncertainty factors in flexibility quantification. Tests are conducted to verify the computational efficiency and accuracy of the proposed probabilistic model.

Chapter 6 presents a risk-averse day-ahead reserve scheduling framework for power systems engaging building energy flexibility. The framework leverages the outputs of the probabilistic model of building energy flexibility and identifies the best alternative reserve schedule by balancing power system operation costs and risks. A new risk indicator, namely expected reserve shortage, is proposed for risk assessment. Tests are conducted to validate the proposed risk-averse framework.

Chapter 7 presents an optimal day-ahead reserve scheduling strategy for power systems engaging building energy flexibility, considering the load rebound effect after demand response. A two-stage robust optimization problem is formulated for optimal reserve scheduling, taking into account both the load rebound and uncertainties in renewable forecasts and generator failures. Tests are conducted to validate the effectiveness of the proposed strategy in managing load rebound proactively.

Chapter 8 summarizes the main contributions of this PhD study and offers recommendations for future research on the related subjects.

The connections among the main chapters are illustrated as shown in Figure 1.1.

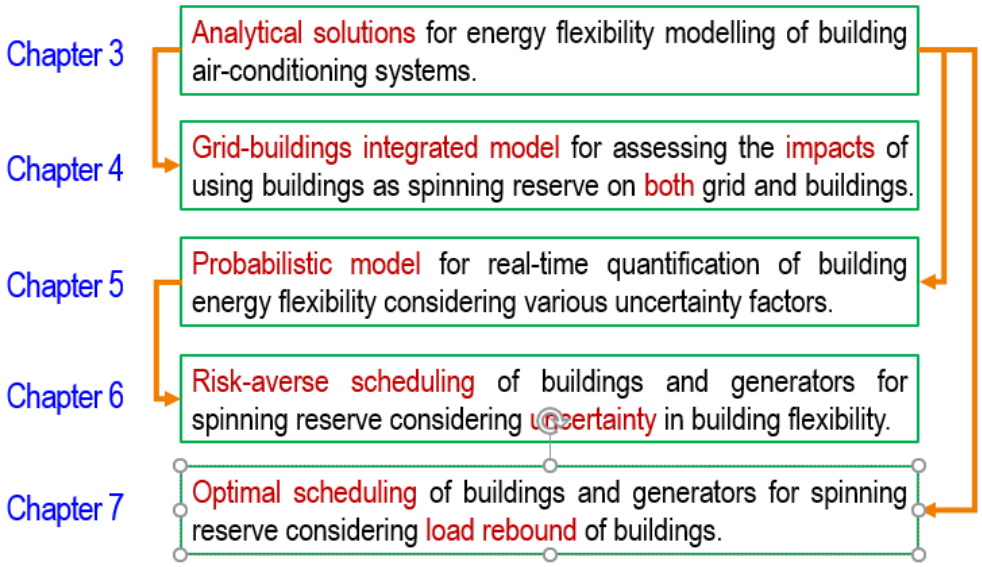

Figure 1.1 Connections among the main chapters of the thesis

CHAPTER 2 LITERATURE REVIEW

Buildings have significant potential for energy flexibility, which can be utilized to provide spinning reserve to manage supply-demand imbalances in power systems. Accurate and real-time quantification of building energy flexibility is essential for the reliable and optimal operation of both buildings and power systems. Understanding the impact of reserve provision by buildings is crucial for adopting this approach on a large scale. Optimized reserve scheduling is necessary to achieve optimal power system operation, taking into account the coordination between building energy flexibility and conventional generators.

This chapter presents a comprehensive literature review on the use of building energy flexibility as spinning reserve. Section 2.1 presents an overview of how building energy flexibility can be used to provide grid services. Section 2.2 discusses studies on the modelling and quantification of building energy flexibility. Section 2.3 examines the impact of using building flexibility for spinning reserve. Section 2.4 explores studies on reserve scheduling in power systems that incorporate building energy flexibility. Section 2.5 summarizes the research gaps identified in the aforementioned areas.

2.1 Overview of using building energy flexibility for grid services

Buildings have significant potential and advantages for providing grid services due to their large electricity consumption and inherent energy flexibility. In Hong Kong, the building sector accounts for about 90% of electricity consumption, with heating, ventilation, and air conditioning (HVAC) systems consuming about 30% of electricity in non-residential buildings (Tang, Wang, and Li 2021). Moreover, the operating

power of HVAC systems can be flexibly controlled within an acceptable range due to the buffer effect of thermal inertia (passive thermal mass storage) of buildings (Jingjing Liu et al. 2022). With advancements in grid-interactive control, buildings can rapidly and consistently adjust their power demand in response to power grid requests, making them technically qualified to provide various grid services, including load shifting and spinning reserve.

Load shifting is a conventional and well-discussed use of building energy flexibility. It involves shifting power demand from high-price periods to lower-price periods to reduce building electricity costs (Yang, Gao, and You 2024). Precooling building thermal mass is a common measure for shifting the flexible cooling load of buildings, which can reduce the power demand during peak periods. Such peak reduction can help defer the investment of power generation capacity and maintain power system reliability during extreme conditions such as heat waves (Liang et al. 2024). Additionally, load shifting can reshape power system load profiles, reducing renewable curtailment and the overall power system operating cost (Patteeuw et al. 2015).

The large-scale, real-world implementation of building load shifting remains limited, particularly when exploiting the flexibility of HVAC systems (Seatle and McPherson 2024). Buildings users usually require high incentives to regulate HVAC systems for providng grid flexibility, which can cause a sacrifice in thermal comfort for occupants (Z. Wang et al. 2023). Recent studies have shown that the cost savings of power systems from load shifting may not outweigh the payments required to incentivize buildings (Barani et al. 2023). Moreover, load shifting could lead to unnecessary energy loss and additional electricity cost if the predicted peak does not occur in real-time operation (Tina, Aneli, and Gagliano 2022).

Another promising use of building energy flexibility is providing spinning reserve. Spinning reserve is an essential grid service for managing uncertainties in generator failures and renewable forecasts. It has traditionally been provided by generators operating at part load, which can adjust their power output rapidly. Buildings can also provide spinning reserve by quickly curtailing power demand upon grid requests. Field tests have demonstrated the response quality of HVAC systems providing spinning reserve, with a response speed faster than the 10-min required by grid operators (MacDonald 2014). Unlike load shifting, which requires frequent and actual flexibility activation, spinning reserve only requires buildings to be in a standby state most of the time, with a low probability of actual response in real-time operation (Gade et al. 2024).

A series of control strategies have been proposed to achieve fast and stable operating power reduction of HVAC systems to proivide spinning reserve. A fast demand response control strategy was proposed by shutting down operating chillers (Xue et al. 2015). However, conventional HVAC controls could lead to excessive speeding up of chilled water pumps in situations with reduced cooling supply, resulting in a diminished effect of load reduction. A supply-based feedback control was proposed for achieving a stable power reduction during demand response (Wang and Tang 2017). Dai et al. (Dai et al. 2024) proposed a reconfigurable feedback control strategy to achieve smooth control transition between normal operation and demand response modes.

The above literature indicates the needs and feasibility of using building energy flexibility for providing various grid services including spinning reserve. However, the modelling, impact assessment and scheduling of building energy flexibility requires further investigation to promote its adoption as a provider of spinning reserve for power systems in a reliable and economic way.

2.2 Studies on quantification of building energy flexibility

Accurate and real-time quantification of building energy flexibility is crucial for the reliable and optimal operation of both buildings and power grids. Currently, building flexibility must demonstrate a high level of performance predictability to provide grid services. For example, buildings must guarantee a minimum success probability of 95% when providing spinning reserve (Vindel et al. 2023). Failing to meet this mandatory requirement results in disqualification from providing spinning reserve service. The flexibility quantification needs to be rapid for buildings to participate in grid service markets. This is because load aggregators are required to quantify building flexibility and submit bids to the grid service market based on the updated information of buildings (Song et al. 2020).

The basis of building energy flexibility quantification is the development of effective models that accurately describe the dynamics of individual buildings. These models can be physics-based, data-driven, or a combination of both (grey-box) (Li and Hong 2022). Physics-based models consider detailed building physics but are time-consuming to solve. Data-driven models utilize statistical or machine learning methods, offering faster computational speed (Bampoulas et al. 2023). A data-driven building thermodynamic model was used to control a cluster of heat pumps for spinning reserve provision (Bünning et al. 2023). However, data-driven models require extensive training data and may lack generalization beyond the training dataset.

Grey-box models incorporate the basic principles of building physics while requiring less data for calibration, thus facilitating real-world implementation. Among various grey-box models, resistance and capacitance (RC) models are widely used. The first-order RC model assumes the entire building thermal mass as a single thermal

capacitance. Despite their simple structure, these models have been proven to be inaccurate for flexibility quantification (Reynders, Diriken, and Saelens 2014). Second-order RC models characterize the dynamics of indoor air and internal mass separately, offering adequate accuracy (Zhan, Dong, and Chong 2023). The aggregated flexibility of buildings is quantified by modeling each building with a second-order model (Amadeh, Lee, and Max Zhang 2023) (Dong et al. 2018).

In the aforementioned studies, the RC models are solved numerically based on a discrete-time state space formulation, which is time-consuming. Moreover, because the values of temperature cannot be aggregated directly, it poses challenges to simultaneously optimize the collective operation of numerous buildings characterized by diversified specifications. If each building is individually modelled as an agent with time-dependent states, i.e., the indoor air temperature, it becomes intractable to solve the optimization problem due to the involvement of a considerable number of decision variables and constraints (Dong et al. 2024).

A well-established building dynamic model does not guarantee accurate prediction of actual building flexibility due to various uncertainties such as uncertainties in model inputs, model bias, and potential building response failures (Luo, Peng, and Yin 2023). These uncertainties can cause buildings to fail to achieve the expected flexibility in actual operation. Quantifying building flexibility under uncertainties is challenging due to the high computational burden. Some studies estimate the aggregated flexibility of buildings using archetype-based models (Martinez, Vellei, and Le Dréau 2022a) (Wang, Li, and You 2018) (Hu and Xiao 2020). These studies use a few building archetypes to represent the entire building cluster to reduce computational time. The archetypes representing these groups are used to estimate aggregated flexibility.

Although archetype-based models can serve as tools for preliminary planning purposes, they may lack adequacy and accuracy for control applications in highly diverse building clusters where buildings have distinct characteristics. To address this issue, the first-order RC model is transformed into an equivalent virtual battery model, so that the flexibility of individual buildings can be quantified analytically (Song et al. 2018). Several studies have quantified the aggregated flexibility of buildings by modelling each building as a virtual battery, considering uncertainties in model inputs and response failures (Qi et al. 2023) (Zhang and Domínguez-García 2018). However, these studies rely on the first-order RC model that ignores the dynamic interaction between the indoor air and building internal mass, thus lacking sufficient accuracy.

The above literature indicates that there is a lack of an accurate and efficient model for quantifying building energy flexibility under uncertainties. Existing models are either archetype-based, which inadequately capture the distinct characteristics of diverse buildings, or developed based on the first-order RC model that has been proven inaccurate. Several studies quantify the aggregated flexibility by characterizing each building using second-order models, but these models are solved numerically, which is computationally intractable for power grid scheduling and dispatch.

2.3 Studies on impacts of using building energy flexibility as spinning reserve

Using building energy flexibility as spinning reserve may have significant impacts on the operation of both power grids and buildings. Understanding such impacts is crucial for informing market design, policy support, and technology development. The financial benefits for buildings from reserve provision have been assessed based on

service market prices (Zhou, Hale, and Present 2022) (Gade et al. 2024). But these studies are limited to specific scenarios with a small number of buildings, because they do not consider the impact of building flexibility engagement on market prices.

Some studies have used power grid dispatch models to assess cost savings from using large-scale demand flexibility for spinning reserve (Roos and Bolkesjø 2018) (Karangelos and Bouffard 2012) (Mimica, Boras, and Krajačić 2023). But these studies inadequately consider the temporal availability of building flexibility, treating it as a static proportion of total building power use. Moreover, they focus solely on power system cost savings without assessing the impact on building operation. Adjustments in power use profiles for providing spinning reserve can interfere with the normal operation of HVAC systems. Currently, no studies evaluate the year-round operational impact on buildings when they provide spinning reserve.

Both load shifting and spinning reserve provision can engage buildings in facilitating power balance. However, it is still unclear which service is more suitable and beneficial for utilizing building energy flexibility. Load shifting relies on reshaping load profiles for managing generation-demand mismatches that can be roughly predicted, while spinning reserve requires buildings to manage uncertain power imbalances that have a low probability of occurring in real-time operation (Aryandoust and Lilliestam 2017). Therefore, it seems more acceptable for building users to provide spinning reserve compared to load shifting, concerning the potential interference to building operations.

Some studies have compared the technical capacity of massive buildings for providing spinning reserve and load shifting, considering shifting duration constraints (Müller and Möst 2018). Other studies have compared the revenues that buildings can obtain

from grid service provision under service market prices (Gade et al. 2024) (Sun et al. 2022). However, their results are not applicable to scenarios with a large number of buildings, since the buildings may alter the market prices (Qin et al. 2023). It was claimed that building flexibility providing spinning reserve yields higher cost savings for power systems compared to load shifting (Roos and Bolkesjø 2018). But this study lacks a quantitative comparison. A quantitative comparison of using large-scale building energy flexibility for spinning reserve and load shifting is not found in the literature.

2.4 Studies on reserve scheduling of power systems engaging building flexibility

2.4.1 Problem reformulation of reserve scheduling

When massive buildings are engaged in spinning reserve provision, the coordination between buildings and traditional reserve providers (i.e., conventional generators) is crucial for achieving optimal system performance. Scenario-based stochastic optimization was applied for coordinating buildings and conventional generators to provide spinning reserve for managing renewable forecast uncertainties (Zhang et al. 2022) (Le et al. 2022). However, these studies overlook the reserve for unexpected generator failures, although such failures have a significant adverse impact on power system reliability.

A robust scheduling strategy was proposed for demand flexibility to provide both types of spinning reserve (Ji et al. 2021). The optimal reserve schedule was obtained by solving a robust optimization problem. Stochastic reserve scheduling was also proposed for integrated electricity and heating systems, with flexibility provision by

heat pumps considering both types of spinning reserve (Tan et al. 2021). The optimal schedule was obtained by solving a chance-constrained programming problem. However, these studies lack detailed modelling of building energy flexibility. Furthermore, the cost of using building flexibility (e.g., the compensation to buildings) is not considered.

2.4.2 Managing uncertainties related to demand response

There are different alternative reserve schedules when considering building flexibility as a spinning reserve provider (Zhao et al. 2013). All alternative reserve schedules can fulfill power system reserve requirements, but they correspond to different reserve commitment combinations of buildings and conventional generators. Therefore, it is essential to quantify the risks of these alternative schedules for optimized decision-making (Herding et al. 2024).

Typical risk indicators such as expected energy not served (EENS) are used, as found in (Jia et al. 2019) (Ding et al. 2019). However, such indicators focus on power imbalances. It is time-consuming to capture and quantify power imbalance events due to uncertain reserve provision, because spinning reserve is activated infrequently (Q. Wang et al. 2023). Some studies have used reserve shortages to quantify the risk of scheduling improper reserve capacities within power systems, where reserve shortages are considered as deterministic values (Q. Wang et al. 2023) (Lavin et al. 2020). A probabilistic formulation of reserve shortage was proposed (Stover, Karve, and Mahadevan 2023). However, this study solely focuses on the uncertain reserve requirements of power systems. Moreover, conventional generators also have a response failure probability when their committed reserve is called on. However, none of the studies consider the response failures of conventional generators, which may

lead to underutilization of building energy flexibility (Herre, Pinson, and Chatzivasileiadis 2022).

2.4.3 Managing load rebound after demand response

The load rebound associated with building energy flexibility is acritical issue that has been widely overlooked in the literature. Load rebound refers to the phenomenon where building power demand often exceeds the normal levels after a load reduction, when the HVAC system controls return to their normal setting (Burgio et al. 2023). It occurs because of the increased indoor air temperature of buildings during the period of reduced cooling supply (Georges et al. 2017). This load rebound, if not managed effectively, may cause new power imbalance in real-time operation.

Load rebound can be balanced by increasing the power output of online conventional generators in real-time operation (Ding et al. 2019). However, conventional generators may operate at high partial load levels without sufficient regulation capacity to manage load rebound, leading to severe power imbalances. Some studies have incorporated the load rebound effect into the power system reserve scheduling problem (Karangelos and Bouffard 2012) (Liu and Tomsovic 2014) (Paterakis et al. 2018). These studies suggest that considering load rebound leads to a reduced reserve commitment for buildings. But these studies assume load rebound as a hypothesis proportion of the previous load reduction, limiting their practical applicability.

To explicitly model the load rebound of buildings, a dynamic load baseline method was proposed by (Wei et al. 2020) to establish a coupling between the load rebound and the previous load reduction. But this method is not suitable for large-scale power systems, as power grid operators cannot directly incorporate the thermal dynamics of massive buildings into their daily dispatch schedules. To address this issue, the first-

order building thermodynamic model was transformed into an equivalent virtual energy storage model (Hao et al. 2018). By doing so, only the aggregated power information (e.g., the maximum load reduction of buildings) is communicated to grid operators. Trovato et al. (Trovato, Teng, and Strbac 2018) quantified the aggregated load rebound of buildings by modelling buildings as a single virtual energy storage based on their averaged parameters, which is not suitable for highly diverse building clusters.

The literature review above shows that most existing studies focus on using building energy flexibility for spinning reserve, considering either renewable forecast uncertainties or generator failures, leading to suboptimal flexibility utilization. These studies usually overlook the uncertainties in building demand response or the response failures of conventional generators, which hinders the identification of the best reserve schedule. The load rebound effect associated with utilizing building HVAC systems is seldom considered, which may adversely affect the reliability and economy of power systems. Although a few studies consider load rebound in reserve scheduling, they estimate the magnitude of load rebound based on either hypothetical values or averaged parameters of buildings, lowering their applicability.

2.5 Summary of research gaps

This chapter presents a comprehensive review of existing studies on the modeling, quantification, impact assessment, and scheduling of using building energy flexibility for providing spinning reserve in power systems. From this review, several research gaps can be identified and summarized:

1. Model Complexity and Computation Efficiency: Most existing studies use a first-order building thermodynamic model for flexibility quantification, which may lack accuracy. Some studies use second-order (or even higher-order) building thermodynamic models, but these rely on numerical method, specifically finite difference and iterative computations. Such approaches are time-consuming for real-time online applications.
2. Uncertainty and Building Diversity: While most studies overlook the impact of uncertainties in quantifying building energy flexibility, the major uncertainties are seldom comprehensively considered. Although some studies address these uncertainties, they depend on archetype-based models to reduce computational times, which may not adequately characterize building diversity.
3. Impact on Building Operations: The impacts of using building energy flexibility as spinning reserve are not fully investigated. Existing studies primarily focus on the cost savings of power systems and seldom assess the impact of reserve provision on building operation. A comprehensive and quantitative comparison between spinning reserve provision and load shifting by buildings is still lacking.
4. Risk Assessment and Framework Development: An effective framework is needed to identify the best reserve schedule, considering the trade-off between cost savings and the risk of using building flexibility. Existing risk indicators struggle to quantify the risks from buildings. Moreover, no study considers the risk from conventional generators in reserve scheduling, which may lead to the underutilization of building energy flexibility.
5. Simultaneous Uncertainties and Load Rebound: Existing studies on reserve scheduling seldom consider uncertainties in renewable forecast and generator failures simultaneously. This oversight could lead to the underutilization of

building energy flexibility. The load rebound effect is often overlooked or assumed to be a hypothetical value in reserve scheduling, which may adversely affect the reliability and economy of power systems.

CHAPTER 3 ANALYTICAL SOLUTIONS FOR ENERGY FLEXIBILITY MODELLING OF BUILDING AIR-CONDITIONING SYSTEMS

This chapter presents the analytical solutions for modelling the energy flexibility of building air-conditioning systems at both individual and aggregated levels. Five straightforward equations are derived from a commonly used second-order building thermodynamic model in demand response conditions. Both load reduction and the subsequent load rebound of buildings are quantified, facilitating the integration of building flexibility quantification into power grid scheduling and real-time dispatch. Section 3.1 discusses the problem formulation and the current numerical solution method. Section 3.2 introduces the analytical solutions. Section 3.3 evaluates the performance evaluation of these analytical solutions. Section 3.4 provides a summary of this chapter.

3.1 Problem formulation and numerical solution

3.1.1 Problem formulation

We are considering a demand response problem involving a large number of heterogeneous buildings, each cooled by a HVAC system with continuously adjustable operating power. The dynamic process of a building's demand response event is illustrated in Figure 3.1. It consists of a load reduction for a duration Δt_s followed by a load rebound for a duration Δt_r. For convenience, the start and end time of the load reduction period are denoted as t_0 and t_1, respectively. The end time of the

load rebound period is denoted as t_2. Accordingly, the indoor air temperature increases first by ΔT^{in} from time t_0 to t_1, and then returns to the baseline value $T^{in,base}$ at time t_2.

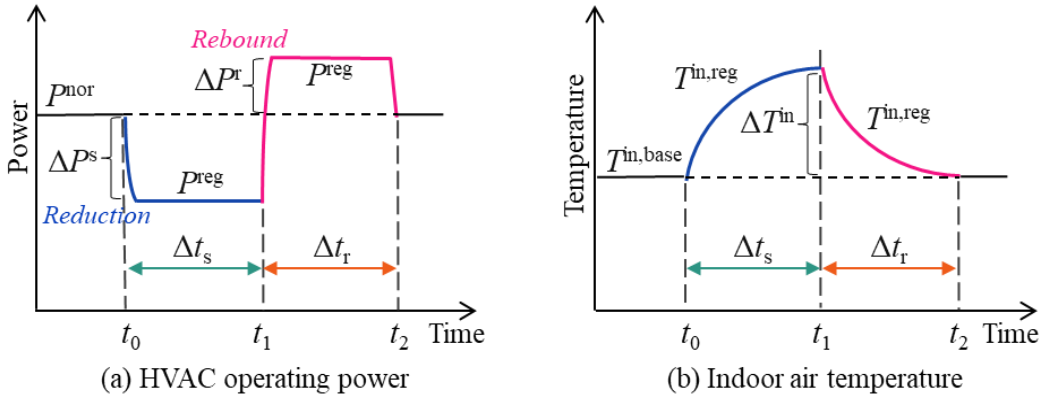

Figure 3.1 Illustration of the load reduction and load rebound of a building

The following assumptions are made, as commonly used in energy flexibility quantification: (i) the indoor air temperature remains at its baseline value in the normal operation scenario (i.e., without the demand response event); (ii) in demand response scenario, the reduction and rebound of HVAC operating power are kept constant during the respective durations, which aligns with the common practice in electricity market clearing and power system scheduling problems (Salgado-Bravo, Negrete-Pincetic, and Kiprakis 2023); (iii) the building heat gains are not affected by the implementation of demand response. Note that in Figure 3, constant power lines are used only for illustration purpose. The flexibility quantification methods discussed in this study are valid under time-varying boundary conditions (e.g., outdoor weather).

The fundamental problem is to quantify the magnitude of load reduction ΔP^{s} and load rebound ΔP^{r} for individual buildings during the reduction and rebound durations (Δt_s and Δt_r), respectively, at a given indoor air temperature offset ΔT^{in}, as shown in Eqs. (3.1) and (3.2). The aggregated energy flexibility of buildings can then be quantified based on the energy flexibilities of individual buildings. Note that Δt_s is typically

assigned by power grid operators. ΔP^{r} or Δt_{r} should be properly set to avoid either a high load rebound for the power grid or slow temperature restoration for buildings.

$$\Delta P^{\mathrm{s}} = P^{\mathrm{nor}}(\Delta t_{\mathrm{s}}) - P^{\mathrm{dr}}(\Delta t_{\mathrm{s}}) \tag{3.1}$$

$$\Delta P^{\mathrm{r}} = P^{\mathrm{dr}}(\Delta t_{\mathrm{r}}) - P^{\mathrm{nor}}(\Delta t_{\mathrm{r}}) \tag{3.2}$$

3.1.2 Building thermodynamic model

Building HVAC systems are considered to provide energy flexibility, because they are the major power consumers in buildings and can effectively utilize building thermal mass. Unlike the first-order building thermodynamic model used in most existing studies, second-order building thermodynamic models take into account the dynamic interaction of indoor air and building internal mass, which results in significantly improved modeling accuracy (Zhang et al. 2013). This study adopts a commonly used second-order building thermodynamic model to characterize the thermal dynamics of buildings and determine the operating power of HVAC systems, as illustrated in Figure 3.2.

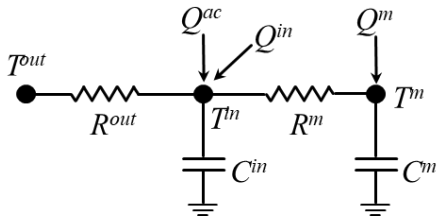

Figure 3.2 Illustration of the second-order building thermodynamic model

The governing equations of the second-order building thermodynamic model are shown in Eqs. (3.3) and (3.4).

$$C^{\mathrm{in}}\frac{dT^{\mathrm{in}}}{dt} = \frac{T^{\mathrm{out}} - T^{\mathrm{in}}}{R^{\mathrm{out}}} + \frac{T^{\mathrm{m}} - T^{\mathrm{in}}}{R^{\mathrm{m}}} + Q^{\mathrm{in}} - COP \cdot P^{\mathrm{ac}} \tag{3.3}$$

$$C^{\mathrm{m}}\frac{dT^{\mathrm{m}}}{dt} = \frac{T^{\mathrm{in}} - T^{\mathrm{m}}}{R^{\mathrm{m}}} + Q^{\mathrm{m}} \tag{3.4}$$

Where, t is the time. R, C and T refer to thermal resistance, thermal capacitance, and temperature, respectively. The superscripts, i.e., *in*, *m*, and *out*, denote the indoor air, building structure mass, and outdoor air, respectively. Q^{in} and Q^{m} are the heat gains of indoor air and building structure mass, respectively. P^{ac} and COP represent the operating power and the overall coefficient of performance of the HVAC system, respectively.

The model is appropriate for buildings in cooling-dominated regions, which typically feature light outer walls but relatively heavy internal mass. If the building thermal mass is primarily in the outer walls, other second-order RC models would be more suitable (Dong et al. 2018). Note that this study employs a deterministic building thermodynamic model because it focuses on quantifying energy flexibility based on given building parameters. In real-world applications, a challenge in identifying building thermal parameters lies in the presence of data noise. To address this, a stochastic building thermodynamic model employing stochastic differential equations could enable more robust parameter estimation using actual operational data (Bacher and Madsen 2011).

A limitation of building thermodynamic model used in this study is that it overlooks the effect of humidity on HVAC operation power. Hong Kong is hot and humidity, and dehumidification energy consumption could be significant. Future work could consider the humidity/latent load in building thermodynamic model.

A single second-order building thermodynamic model may not accurately reflect the thermal dynamics of individual thermal zones of a complex multi-zone building. However, a “single-zone equivalent” second-order model would adequately represent the volume-averaged zone temperature and the total cooling load of these zones, as

demonstrated in (Shamsi et al. 2021) (Guo et al. 2021). For buildings with highly diverse thermal zones, multiple second-order models could be used to model the representative zones. In such cases, the last term of Eq. (3.3), i.e., $COP \cdot P^{ac}$, could be replaced by the cooling load of individual zones. The impact of varied *COP* during demand response periods can be addressed using Eq. (3.3) to calculate the cooling load. As this study concentrates on the aggregated flexibility of a large number of buildings, a constant *COP* is assumed for each HVAC system during demand response periods.

3.1.3 Numerical solution

The problem presented in Section 3.1.2 is currently solved using a numerical approach. The building thermodynamic model is transformed into its discrete-time state space formulation, as shown in Eq. (3.5).

$$x(j+1) = Ax(j) + B \cdot P^{\mathrm{ac}}(j) + C\gamma(j) \tag{3.5}$$

where, $x=[T^{\mathrm{in}}, T^{\mathrm{m}}]^{\mathrm{T}}$ is the state vector. j is the time step. $\gamma=[T^{\mathrm{out}}, Q^{\mathrm{in}}, Q^{\mathrm{m}}]^{\mathrm{T}}$ is the disturbance vector. The disturbances include the outdoor aim temperature and the heat gains of the indoor air and building structure mass. Matrices *A, B,* and *C* can be easily derived from Eqs. (3.3) and (3.4).

The indoor air temperature at time t_1 can be determined using the finite difference method, as commonly used for implementing model predictive control (Zhan et al. 2023). Iterative computations (e.g., binary search) are then employed to find the appropriate ΔP^{ac} that corresponds to the desired ΔT^{in}. To clarify, with the initial condition $x(t_0)$ and a trial value of P^{ac}, the indoor air temperature at time t_1, i.e., $T^{\mathrm{in}}(t_1)$, can be determined using Eq. (3.5) by tracking the temperature evolution in the load

reduction duration Δt_s. The value of P^{ac} is adjusted until $T^{in}(t_1)$ matches the specified ΔT^{in}. The load rebound ΔP^r is quantified using similar methods.

The above numerical solution relies on time-consuming iterative and finite difference computations. However, it is not feasible to integrate building energy flexibility quantification into power grid scheduling and real-time dispatch. This is because a large number of flexibility quantification computations are necessary for optimizing the coordination between buildings and conventional generators, particularly concerning the load reduction and load rebound of buildings. Furthermore, multiple flexibility quantifications are required to optimize the regulation tasks of individual buildings and to coordinate their contribution to providing the required demand response in real-time operation. Therefore, there is an urgent need for a computationally efficient and accurate solution for energy flexibility modelling and quantification.

3.2 Analytical solutions

This section presents the analytical solutions of the energy flexibility quantification problem introduced in Section 3.1. First, analytical solutions for the energy flexibility of individual building are derived. Then, analytical solutions for the aggregated energy flexibility of a large number of buildings are derived.

3.2.1 Solution for individual buildings

Revisiting the second-order building thermodynamic model

The second-order building thermodynamic model can be expressed by a second-order differential equation, as shown in Eq. (3.6), and solved as shown in Eq. (3.7) (Amadeh et al. 2023).

$$a\frac{d^2T^{\text{in}}}{dt^2} + b\frac{dT^{\text{in}}}{dt} + cT^{\text{in}} = d \tag{3.6}$$

$$T^{\text{in}}(t) = A_1 e^{r_1 t} + A_2 e^{r_2 t} + d/c \tag{3.7}$$

where, $a = C^{\text{in}}C^{\text{m}}R^{\text{m}}$, $b = (1 + R^{\text{m}}/R^{\text{out}})C^{\text{m}} + C^{\text{in}}$

$c = 1/R^{\text{out}}$, $d = T^{\text{out}}/R^{\text{out}} + Q^{\text{m}} + Q^{\text{in}} - COP \cdot P^{\text{ac}}$

$r_1 = (-b + \sqrt{b^2 - 4ac})/2a$, $r_2 = (-b - \sqrt{b^2 - 4ac})/2a$

$A_1 = \left[dT^{\text{in}}/dt\,(0) + \left(d/c - T^{\text{in}}(0)\right)r_2\right]/(r_1 - r_2)$

$A_2 = \left[dT^{\text{in}}/dt\,(0) + \left(d/c - T^{\text{in}}(0)\right)r_1\right]/(r_2 - r_1)$.

Remark: For Eq. (3.7), the parameters *a*, *b*, *c*, r_1 and r_2 are constants, depending on the thermal parameters of a building. These parameters have no physical meaning. The time-derivative term $dT^{\text{in}}/dt(0)$ is determined by Eq. (3.3). The variables *d*, A_1 and A_2 depend on the HVAC system operating power P^{ac}. Therefore, for a given initial time (condition), the indoor air temperature after a duration of Δt is a function of two variables, denoted as $\varphi\,(\Delta t, P^{ac})$.

Load reduction of individual building

The HVAC operating power is first reduced by ΔP^{ac} from its normal value $P^{\text{ac,base}}$ for a duration of Δt_s in the demand response scenario. In contrast, the indoor air temperature remains at the baseline value in the normal operation scenario. Considering t_0 as the initial time, the indoor air temperature at t_1 in the two scenarios can be described as follows.

$$T^{\text{in,reg}}(t_1) = \varphi(\Delta t_{\text{s}}, P^{\text{nor}} - \Delta P^{\text{s}}),\ T^{\text{in,reg}}(t_0) = T^{\text{in,base}} \tag{3.8}$$

$$T^{\text{in,nor}}(t_1) = \varphi(\Delta t_{\text{s}}, P^{\text{nor}}),\ \ T^{\text{in,nor}}(t_0) = T^{\text{in,base}} \tag{3.9}$$

The implementation of load reduction results in an increase of indoor air temperature by ΔT^{in}, which gives Eq. (3.10).

$$T^{\text{in,reg}}(t_1) - T^{\text{in,nor}}(t_1) = \Delta T^{\text{in}} \tag{3.10}$$

The load reduction ΔP^{ac} is quantified as shown in Eq. (3.11), by combining Eqs. (3.7)-(3.10). It is a function of the indoor air temperature offset ΔT^{in}, the load reduction duration Δt_s, and the parameters of a building. This finding aligns with the numerical simulation results reported by (Wang et al. 2019). Note, analytical solutions of other second-order thermodynamic models can be easily derived in a similar approach.

$$\Delta P^{\text{ac}} = \alpha(\Delta t_{\text{s}})\, \Delta T^{\text{in}} \tag{3.11}$$

where α is denoted as the load reduction coefficient.

$$\alpha(\Delta t_{\text{s}}) = \frac{(r_1 - r_2) C^{\text{in}} \Delta T^{\text{in}}}{[e^{r_1 \Delta t} - e^{r_2 \Delta t} + C^{\text{in}} R^{\text{out}} (r_1 - r_2 + r_2 e^{r_1 \Delta t} - r_1 e^{r_2 \Delta t})] \cdot COP}$$

Load rebound of individual building

After the load reduction period ends, the HVAC operating power will be higher than that in the normal operation scenario in order to restore the indoor air temperature to its baseline value. The load rebound ΔP^{r} for the rebound duration Δt_{r} causes the restoration of indoor air temperature at time t_2.

$$T^{\text{in,reg}}(t_2) = T^{\text{in,nor}}(t_2) \tag{3.12}$$

Considering t_1 as the initial time, the indoor air temperature at t_2 in the two scenarios can be described as follows.

$$T^{\text{in,reg}}(t_2) = \varphi(\Delta t_{\text{r}}, P^{\text{nor}} + \Delta P^{\text{r}}), \;\; T^{\text{in,reg}}(t_1) = T^{\text{in,base}} + \Delta T^{\text{in}} \tag{3.13}$$

$$T^{\text{in,nor}}(t_2) = \varphi(\Delta t_{\text{r}}, P^{\text{nor}}), \quad T^{\text{in,nor}}(t_1) = T^{\text{in,base}} \tag{3.14}$$

Solving Eqs. (3.13)-(3.14) involves the difference in $dT^{\text{in}}/dt(t_1)$ between the demand response scenario and the normal operation scenario. This difference can be determined based on Eq. (3.3) and is expressed by Eq. (3.15).

$$\frac{dT^{\text{in}}}{dt}(t_1)\Big|_{\text{nor}}^{\text{reg}} = \frac{1}{C^{\text{in}}}\left(\frac{\Delta T^{\text{m}}}{R^{\text{m}}} - \frac{\Delta T^{\text{in}}}{R^{\text{out}}} - \frac{\Delta T^{\text{in}}}{R^{\text{m}}} - COP \cdot \Delta P^{\text{r}}\right) \tag{3.15}$$

where, ΔT^{m} is the difference in the temperature of the building internal mass at time t_1 between the two scenarios. It is determined by applying the energy balance equation for the entire building, as shown in Eq. (3.16).

$$C^{\text{m}}\Delta T^{\text{m}} + C^{\text{in}}\Delta T^{\text{in}} + \int_{t_0}^{t_1} \frac{T^{\text{out}} - T^{\text{in}}}{R^{\text{out}}} = \Delta P^{\text{s}}\Delta t_{\text{s}}\, COP \tag{3.16}$$

where, the left side represents the cooling energy released from the indoor air and building internal mass, and the reduced heat gain from ambient during the reduction duration Δt_{s}. The right side is the accumulated reduction in the HVAC cooling supply.

The load rebound ΔP^{r} is quantified as shown in Eq. (3.17), by combining Eqs. (3.12)-(3.16).

$$\Delta P^{\text{r}} = \beta(\Delta t_{\text{s}}, \Delta t_{\text{r}})\, \Delta T^{\text{in}} \tag{3.17}$$

where, β is denoted as the load rebound coefficient.

$$\beta(\Delta t_{\text{s}}, \Delta t_{\text{r}}) = \frac{[C^{\text{in}}\alpha(\Delta t_{\text{s}}) \cdot p(\Delta t_{\text{s}}) \cdot c \cdot COP/a - h](e^{r_1\Delta t_{\text{r}}} - e^{r_2\Delta t_{\text{r}}}) + C^{\text{in}}q(\Delta t_{\text{r}})}{[e^{r_1\Delta t_{\text{r}}} - e^{r_2\Delta t_{\text{r}}} + C^{\text{in}}R^{\text{out}}(r_1 - r_2 - q(\Delta t_{\text{r}}))] \cdot COP}$$

$$p(\Delta t_{\text{s}}) = \frac{(1 - e^{r_1\Delta t_{\text{s}}})\left(\frac{1}{C^{\text{in}}} + r_2 R^{\text{out}}\right)}{(r_1 - r_2)r_1} + \frac{(1 - e^{r_2\Delta t_{\text{s}}})\left(\frac{1}{C^{\text{in}}} + r_1 R^{\text{out}}\right)}{(r_2 - r_1)r_2}$$

$$q(\Delta t_{\text{r}}) = r_1 e^{r_2\Delta t_{\text{r}}} - r_2 e^{r_1\Delta t_{\text{r}}},\ h = \frac{C^{\text{in}}}{C^{\text{m}}R^{\text{m}}} - \frac{1}{R^{\text{out}}} - \frac{1}{R^{\text{m}}}$$

3.2.2 Solution for aggregated buildings

To quantify the aggregated flexibility of a large number of buildings, the temperature offset ratio (TOR) is introduced to coordinate the actual indoor air temperature offset ΔT^{in} of individual buildings (Dong et al. 2023). The TOR is defined by Eq. (3.18).

$$TOR_k = \Delta T_k^{\text{in}} / \Delta T_k^{\text{in,max}} \tag{3.18}$$

where, k is the index of a building. $\Delta T^{\text{in,max}}$ is the maximum allowable indoor air temperature offset of a building.

To ensure the fairness in the thermal comfort compromise among individual buildings, the TOR and the durations of load reduction and load rebound are controlled to be identical for all buildings.

$$\overline{TOR} = TOR_1 = TOR_2 = \cdots = TOR_N \tag{3.19}$$

The aggregated load reduction P^{sr} and load rebound P^{reb} are quantified by Eqs. (3.20) and (3.21) respectively. They are the sum of load reduction and load rebound, respectively, of all individual buildings.

$$P^{\text{sr}} = \sum_k \Delta P_k^{\text{s}} = \sum_k \alpha_k(\Delta t_{\text{s}}) \Delta T_k^{\text{in}} \tag{3.20}$$

$$P^{\text{reb}} = \sum_k \Delta P_k^{\text{r}} = \sum_k \beta_k(\Delta t_{\text{s}}, \Delta t_{\text{r}}) \Delta T_k^{\text{in}} \tag{3.21}$$

Combining Eqs. (3.19)-(21), the consensus TOR of buildings is determined as shown in Eq. (3.22).

$$\overline{TOR} = \frac{P^{\text{sr}}}{\sum_k \alpha_k(\Delta t_{\text{s}}) \Delta T_k^{\text{in, max}}} \tag{3.22}$$

The regulation tasks of individual buildings in the load reduction and rebound periods are then determined by Eqs. (3.23) and (3.24), respectively.

$$\Delta P_k^{\mathrm{s}} = \frac{\alpha_k(\Delta t_{\mathrm{s}})\Delta T_k^{\mathrm{in,max}}}{\sum_k \alpha_k(\Delta t_{\mathrm{s}})\Delta T_k^{\mathrm{in,max}}} P^{\mathrm{sr}} \tag{3.23}$$

$$\Delta P_k^{\mathrm{r}} = \frac{\beta_k(\Delta t_{\mathrm{s}}, \Delta t_{\mathrm{r}})\Delta T_k^{\mathrm{in,max}}}{\sum_k \alpha_k(\Delta t_{\mathrm{s}})\Delta T_k^{\mathrm{in,max}}} P^{\mathrm{sr}} \tag{3.24}$$

The coupling between the aggregated load reduction and load rebound of buildings is explicitly represented by Eq. (3.25).

$$\frac{P^{\mathrm{reb}}}{P^{\mathrm{sr}}} = \frac{\sum_k \beta_k\,(\Delta t_{\mathrm{s}}, \Delta t_{\mathrm{r}})\Delta T_k^{\mathrm{in,max}}}{\sum_k \alpha_k\,(\Delta t_{\mathrm{s}})\Delta T_k^{\mathrm{in,max}}} \tag{3.25}$$

Remark: Eqs. (3.11) and (3.17) quantify the load reduction and rebound, respectively, of individual buildings as functions of load reduction/redound durations and indoor air temperature offset. Eqs. (3.23) and (3.24) enable the convenient allocation of an assigned demand response task among buildings. Eq. (3.25) enables the convenient incorporation of aggregated building energy flexibility of a large number of buildings into power grid scheduling and real-time dispatch. Note that the proposed analytical solutions are not suitable for real-time dynamic load control problems, such as power tracking for frequency regulation, while buildings need to follow a time-varying signal. The flexibility computations for real-time control can be fulfilled by numerical method.

3.3 Performance evaluation of analytical solutions

Numerical simulations are performed to verify the accuracy and computational efficiency of proposed analytical method using 5000 buildings. The parameters of buildings and HVAC systems are based on (Dong et al. 2023). All buildings have an indoor air temperature of 24℃ in normal operation, with a maximum allowable offset of 2 K. Outdoor conditions are chosen as a typical summer day in Hong Kong. Both

load reduction and rebound durations are set to 3600 seconds. The simulations are conducted using MATLAB on a PC with an eight-core Intel Core i7 CPU.

3.3.1 Accuracy

We first validate the proposed analytical model by comparing its outputs with those of the high-resolution numerical solution method. For this purpose, the time step of the numerical solution method is set to 1 second. We find that the differences between the temperatures and aggregated energy flexibility of buildings computed by the two methods are less than 0.0001 K and 0.01%, respectively. Such negligible differences prove that the analytical solutions are accurate and correct.

The analytical solutions are valid under time-varying boundary conditions (e.g., outdoor temperature), although constant boundary conditions are assumed for individual buildings when deriving the second-order differential equation, Eq. (3.6). This is because, as observed from Eq. (3.6), the evolution of indoor air temperature of a building has two time constants, which only depend on building parameters, not on boundary conditions. Besides, the indoor air temperature offset is determined based on the normal operation and demand response scenarios, where terms related to boundary conditions are offset. Therefore, the assumption of constant boundary conditions does not affect the validity of the solution.

To validate the solution, numerical simulation is conducted on a building under time-varying boundary conditions. The time-varying outdoor temperature and building heat gains are generated using trigonometric functions. The HVAC power reduction is assumed to be constant during demand response, according to typical requirement of power grid operators. The demand response event is assumed to begin at 3600s and ends at 7200s. The subsequent load rebound ends at 14400s. Firstly, the load reduction

and load rebound of the building are computed using analytical solutions, considering an indoor air temperature offset of 2 K. The HVAC operating power in the demand response scenario is obtained, as shown in Figure 3.3 (a). Using the operating power as input to Eqs. (3.3) and (3.4), the evolution of indoor air temperature during demand response periods is computed numerically. As shown in Figure 3.3 (b), the indoor air temperature increases from 24 ℃ to 26 ℃ at the end of load reduction period, and then restores to 24 ℃ at the end of load rebound period. This indicates the solution is valid under time-varying boundary conditions.

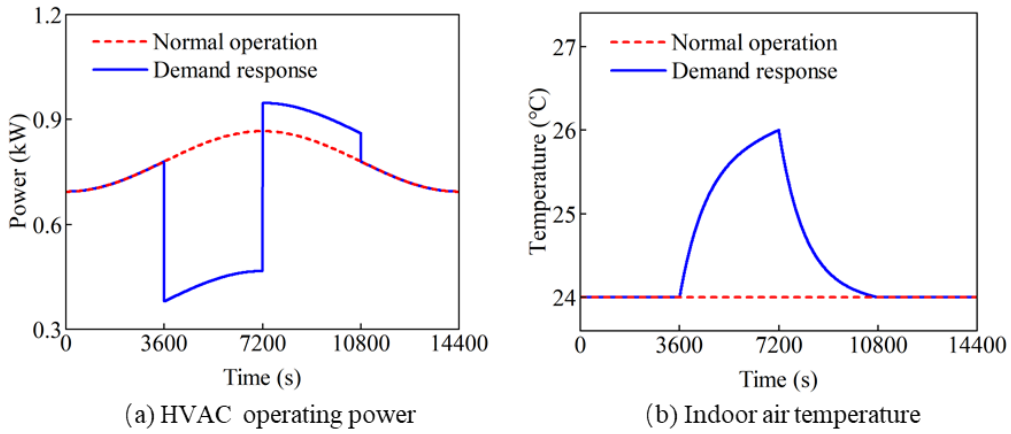

Figure 3.3 HVAC operating power and indoor air temperature in demand response

3.3.2 Computational efficiency

Firstly, we consider a demand response event with an indoor air temperature offset of 2 K for all buildings. We quantify the aggregated energy flexibility of buildings using the analytical solutions and conventional numerical solution, respectively. The time step of the numerical solution method is set to 5 minutes to properly balance the accuracy and computational efficiency. As shown in Table 3.1, the numerical solution takes 8.83 seconds to obtain flexibility quantification results, while the analytical solutions only take 0.000009 seconds, which is 980,000 times faster than the

numerical solution. Note that a shorter time step (1 second) for numerical method can give more accurate results but longer computational time. The higher computational efficiency of our analytical solutions is particularly advantageous in optimized power grid scheduling and real-time dispatch, where a large number of flexibility quantification computations are involved (Liu et al. 2024). Furthermore, the requirement for data storage is lower due to the significantly fewer variables involved.

Table 3.1 Computational results of flexibility quantification

Method	P^{sr} (MW)	P^{reb} (MW)	Time (s)
Analytical	2.042	0.449	0.000009
Numerical-1s	2.042	0.449	525.3
Numerical-5min	2.066	0.446	8.83

We further examine a scenario that involves a regulation task allocation among buildings. It is assumed that an aggregated load reduction target of 1.6 MW is assigned to buildings in real-time operation. The task allocation problem is equivalent to determining the consensus TOR for buildings. As shown in Table 3.2, the analytical solution gives a solution of TOR in 0.000006 second, facilitating timely demand response in real-time operation. In contrast, the numerical solution method takes 57.6 seconds to find a solution, because it requires time-consuming iterations to quantify the aggregate load reduction of buildings and to find the correct TOR under the given load reduction target.

Table 3.2 Computational results in regulation task allocation

Method	TOR	Time (s)
Analytical	0.783	0.000006
Numerical-5min	0.774	57.6

3.4 Summary

This chapter presents the analytical solutions for energy flexibility modeling and quantification of building air-conditioning systems. Five straightforward equations are derived from a second-order building thermodynamic model. The first two equations quantify the load reduction and the subsequent load rebound of individual buildings, respectively, as functions of regulation durations and indoor air temperature offsets. The next two equations allocate the aggregated load reduction and rebound tasks, respectively, among buildings. The fifth equation explicitly represents the coupling between the aggregated load reduction and load rebound of buildings.

The analytical solutions can accurately quantify the energy flexibility of buildings at both individual and aggregated levels with dramatically reduced computation time, facilitating the integration of building flexibility quantification into power grid scheduling and real-time dispatch. Numerical experiments show that the analytical solutions only take 0.000009 seconds to quantify the flexibility of 5000 buildings, which is 980,000 times faster than the numerical solution method.

CHAPTER 4 COMPARISON OF USING BUILDING ENERGY FLEXIBILITY FOR SPINNING RESERVE AND LOAD SHIFTING

This chapter presents a comparative assessment of using building energy flexibility for providing spinning reserve and load shifting (conventional demand response), considering the operation of both buildings and power systems. Unlike existing studies relying on predefined service market prices, an integrated grid-buildings optimization model is developed to capture the dynamic interaction between buildings and the power supply side. The model is applied to the Hong Kong power system in 2035, considering different generation mix scenarios. The results can provide more extensive and practical insights into building flexibility utilization.

Section 4.1 outlines the integrated grid-buildings model. Section 4.2 presents the optimization problem formulation. Section 4.3 presents the models for the power system and buildings. Section 4.4 introduces the Hong Kong power system and buildings. Section 4.5 presents the assessment results of using building energy flexibility for spinning reserve and load shifting. Section 4.6 discusses the policy implications. Section 4.7 gives a summary of this chapter.

4.1 Outline of integrated grid-buildings model

An integrated grid-buildings optimization model is developed to assess the impact of using building flexibility for providing grid services, as illustrated in Fig. 4.1. Firstly, a building load model is used to quantify the flexibility capacity of buildings. With the generation mix and quantified building flexibility capacity as inputs, an hourly-

resolution grid dispatch model is then used to simulate the optimal dispatch of supply-side resources (e.g., conventional generators) and building flexibility. The simulation is conducted for an entire year to capture the variability of renewable generation, electricity demand and building flexibility over different days and seasons. The main outputs include the operating cost of the power system and the total amount of activated building flexibility (MWh). The impacts of using building flexibility for providing grid services are quantified by comparing the outputs (operating cost and activated flexibility) before and after engaging building flexibility. Building flexibility is incorporated into the grid dispatch model through reserve balance constraint and power balance constraint, respectively, to assess the impact of reserve provision and load shifting by buildings. The model is applicable for other cities and regions, with only adjustments in the parameters representing the power system and buildings, such as the generation mix of power systems.

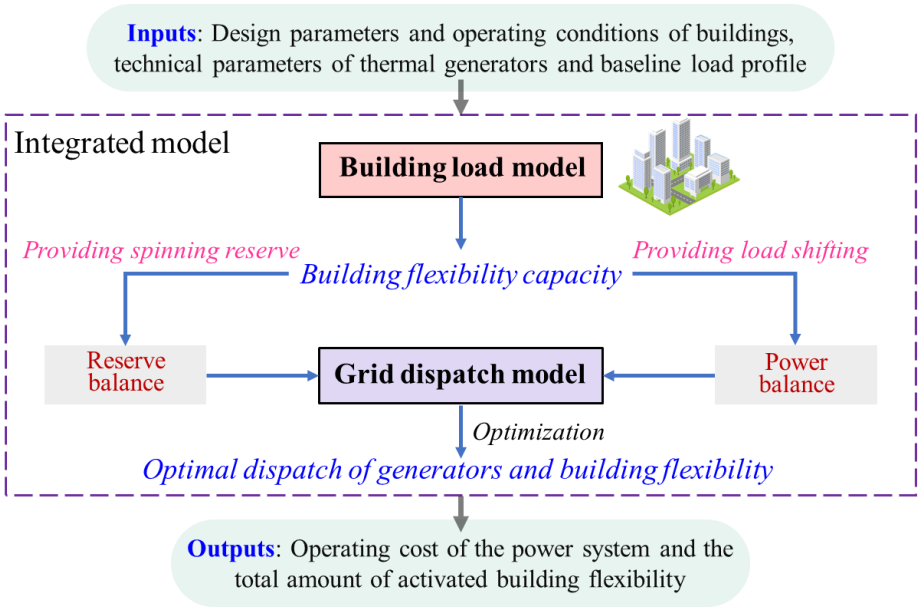

Figure 4.1 Outline of the integrated grid-buildings model

Compared to existing counterparts, the model incorporates a more detailed description of the characteristics of conventional generators (e.g., startup cost) and building

energy flexibility (e.g., temporal availability). To assess the operating cost savings of the power system under different levels of building flexibility activation (MWh), the model considers the cost of activating building flexibility by introducing an incentive paid to buildings for flexibility activation (€/MWh). As a preliminary assessment, this study only leverages this incentive to adjust the cost-effectiveness of building flexibility to grid operators. Increasing the incentive can result in a lower amount of building flexibility utilized by grid operators but does not affect the flexibility capacity that buildings are willing to provide. When the incentive is set to zero, the cost savings quantified by the model are equivalent to those in existing studies, where building flexibility is freely activated for power system cost minimization.

4.2 Optimization problem formulation

In this study, two optimization problems are formulated to obtain the optimal operation of the power system using building flexibility for providing grid services.

Spinning reserve provision

The objective function for using building flexibility to provide spinning reserve, as shown in Eq. (4.1), aims to minimize the total power system cost. This includes the operating cost of conventional generators (C^{gen}) and the cost of activating building flexibility for spinning reserve provision ($C^{\text{bui,SR}}$). It is subject to spinning reserve balance constraint, as shown in Eq. (4.2).

$$\min \sum_{j} (C_j^{\text{gen}} + C_j^{\text{bui,SR}}) \tag{4.1}$$

$$SR_j^{\text{gen}} + SR_j^{\text{bui}} + SR_j^{\text{ES}} = SR_j^{\text{req}} \tag{4.2}$$

where, j represents the time interval. SR^{gen}, SR^{bui} and SR^{ES} are the spinning reserve

provided by conventional generators, building flexibility, and utility-scale energy storage, respectively. SR^{req} is the spinning reserve requirement of the power system.

This study focuses on the energy flexibility of HVAC systems in buildings. The spinning reserve capacity of buildings (SR^{bui}), as shown in Eq. (4.3), is constrained by the maximum load reduction of HVAC systems for a predefined service duration (1 hour in this study). Note that only upward reserve is considered because downward reserve can be easily obtained by ramping down conventional generators or curtailing renewable generation (Roos and Bolkesjø 2018).

$$SR_j^{\mathrm{bui}} \leq P_j^{\mathrm{ac,\,base}} - P_j^{\mathrm{ac,\,min}} \tag{4.3}$$

where $P^{ac,base}$ and $P^{ac,min}$ are the baseline and minimum operating power of HVAC systems, respectively, considering the baseline setting and the allowable maximum offset of indoor air temperature during demand response.

The cost of using building flexibility for spinning reserve is determined by Eq. (4.4), using the method proposed by (Trovato 2023). Here, p^{SR} is the probability of spinning reserve activation, which can be derived from historical data of the power system. c^{act} is the incentive for activating flexibility of buildings (€/MWh).

$$C_j^{\mathrm{bui,SR}} = p^{\mathrm{SR}} c^{\mathrm{act}} SR_j^{\mathrm{bui}} \tag{4.4}$$

Load shifting

The objective function when using building flexibility for load shifting, as shown in Eq. (4.5), aims to minimize the total power system cost, including the operating cost of conventional generators (C^{gen}) and the cost of activating building flexibility for load shifting ($C^{bui,LS}$), subject to power balance constraint, as shown in Eq. (4.6). At each time interval, the system power balance must be maintained by coordinating the

dispatch of conventional generators, renewable generation, utility-scale energy storage and building energy flexibility.

$$\min \sum_j (C_j^{\text{gen}} + C_j^{\text{bui,LS}}) \tag{4.5}$$

$$P_j^{\text{dem}} + P_j^{\text{bui,ch}} + P_j^{\text{ES,ch}} = P_j^{\text{gen}} + P_j^{\text{RE}} + P_j^{\text{ES,dis}} + P_j^{\text{bui,dis}} \tag{4.6}$$

where, P^{dem} is the electricity demand of the power system. $P^{\text{bui,ch}}$ and $P^{\text{bui,dis}}$ represent the load increase and reduction of buildings from the baseline load profile, respectively. $P^{\text{ES,ch}}$ and $P^{\text{ES,dis}}$ are the charging power and discharging power of utility-scale storage, respectively. P^{gen} and P^{RE} are the power supply from conventional generators and renewable energy, respectively.

To model the load shifting associated with regulating HVAC systems, the passive thermal mass storage of buildings is modeled as a generic virtual energy storage, as also adopted by (Barani et al. 2023) (Seatle and McPherson 2024). The governing equations are shown in Eqs. (4.7)-(4.10).

$$E_j^{\text{bui}} = E_{j-1}^{\text{bui}} + \eta P_j^{\text{bui,ch}} - P_j^{\text{bui,dis}} \tag{4.7}$$

$$E_j^{\text{bui,min}} \leq E_j^{\text{bui}} \leq E_j^{\text{bui,max}} \tag{4.8}$$

$$0 \leq P_j^{\text{bui,ch}} \leq P_j^{\text{ac, max}} - P_j^{\text{ac, base}} \tag{4.9}$$

$$0 \leq P_j^{\text{bui,dis}} \leq P_j^{\text{ac, base}} - P_j^{\text{ac, min}} \tag{4.10}$$

where, E^{bui} represents the energy state of building passive thermal mass storage. $P^{\text{ac,max}}$ is the maximum operating power of HVAC systems in buildings. η represents the energy loss percentage when shifting the HVAC load through precooling the building thermal mass. This parameter reflects the energy storage efficiency of building thermal mass, and can be easily calculated using analytical solutions in Chapter 3. A building

with heavier thermal mass has a larger value of η.

The cost of activating building flexibility for load shifting is determined by Eq. (4.11). The total amount of activated building flexibility is half of the accumulated values of $P^{\text{bui,ch}}$ and $P^{\text{bui,dis}}$, because the other half represents the load recovery of buildings (Barani et al. 2023).

$$C_j^{\text{bui,LS}} = c^{\text{act}}(P_j^{\text{bui,ch}} + P_j^{\text{bui,dis}})/2 \tag{4.11}$$

4.3 Models for the power system and buildings

4.3.1 Building load model

This study focuses on the energy flexibility of HVAC systems in commercial buildings, given that HVAC systems are major electricity consumers in Hong Kong, a high-density and cooling-dominated city. A commonly-used second-order R-C (resistance–capacitance) model is used to determine building thermal dynamics and the operating power of HVAC systems. The governing equations of the model are shown in Eqs. (4.12) and (4.13).

$$C^{\text{in}}\frac{dT^{\text{in}}}{dt} = \frac{T^{\text{out}} - T^{\text{in}}}{R^{\text{out}}} + \frac{T^{\text{m}} - T^{\text{in}}}{R^{\text{m}}} + Q^{\text{in}} - COP \cdot P^{\text{ac}} \tag{4.12}$$

$$C^{\text{m}}\frac{dT^{\text{m}}}{dt} = \frac{T^{\text{in}} - T^{\text{m}}}{R^{\text{m}}} + Q^{\text{m}} \tag{4.13}$$

where, t is the time. R, C and T refer to thermal resistance, thermal capacitance, and temperature, respectively. The superscripts, i.e., '*in*', '*m*', and '*out*', denote the indoor air, building structure mass, and outdoor air, respectively. Q^{in} and Q^{m} are the heat gains of indoor air and building structure mass, respectively. P^{ac} and COP are the operating power and the overall coefficient of performance of the HVAC system, respectively.

4.3.2 Grid dispatch model

A typical unit commitment model is employed to simulate the dispatch of the power supply side, accounting for operational constraints of conventional generators, as detailed in (Mallapragada, Sepulveda, and Jenkins 2020). In this model, individual generators are grouped into clusters based on their types, assuming that the generators in each cluster have identical characteristics (e.g., capacity size). A single integer variable (N^{on}) is used to represent the number of online generators in each cluster.

The day-ahead commitment cost of each cluster is determined using Eq. (4.14). Where, *i* represents the cluster type and *j* represents the time interval. *SC*, *MC* and *VC* are the startup cost, operating cost at minimum power output, and output-dependent operating cost of generators, respectively. N^{start} is the number of generators being started.

$$C_{i,j}^{\text{gen}} = SC_i N_{i,j}^{\text{start}} + MC_i N_{i,j}^{\text{on}} + VC_i P_{i,j}^{\text{gen}} \tag{4.14}$$

The number of online generators (N^{on}) is constrained by the installed number of generators in the cluster, as shown in Eq. (4.15). The constraints for generator startup and shutdown actions are shown in Eq. (4.16). The maximum and minimum power output constraints for each cluster are given by Eq. (4.17). The minimum up and down time constraints for each cluster are shown in Eqs. (4.18) and (4.19), respectively.

$$N_{i,j}^{\text{on}} \leq N_i^{\text{install}} \tag{4.15}$$

$$N_{i,j}^{\text{on}} = N_{i,j-1}^{\text{on}} + N_{i,j}^{\text{start}} - N_{i,j}^{\text{shut}} \tag{4.16}$$

$$N_{i,j}^{\text{on}} P_i^{\text{min}} \leq P_{i,j}^{\text{gen}} \leq N_{i,j}^{\text{on}} P_i^{\text{max}} \tag{4.17}$$

$$N_{i,j}^{\text{on}} \geq \sum_{j=j+1-MOT_i}^{j} N_{i,j}^{\text{start}} \tag{4.18}$$

$$N_i^{\text{install}} - N_{i,j}^{\text{on}} \geq \sum_{t=j+1-MDT_i}^{j} N_{i,j}^{\text{shut}} \tag{4.19}$$

The capacity of each cluster for providing spinning reserve (SR^{gen}) is constrained by

the upward ramping capacity of online generators in the cluster, considering the required response time issued by grid operators (10 min in this study), as shown in Eq. (4.20). The ramping up and down capacity constraints for each cluster between two consecutive time intervals are shown in Eqs. (4.21) and (4.22), respectively.

$$SR_{i,j}^{\text{gen}} \leq min\left(N_{i,j}^{\text{on}} P_i^{\max} - P_{i,j}^{\text{gen}}, N_{i,j}^{\text{on}} RU_i^{10\text{min}}\right) \tag{4.20}$$

$$P_{i,j+1}^{\text{gen}} - P_{i,j}^{\text{gen}} \leq N_{i,j}^{\text{on}} RU_i + N_{i,j+1}^{\text{start}} P_i^{\min} - N_{i,j}^{\text{shut}} P_i^{\min} \tag{4.21}$$

$$P_{i,j}^{\text{gen}} - P_{i,j+1}^{\text{gen}} \leq (N_{i,j}^{\text{on}} - N_{i,j}^{\text{start}} + N_{i,j}^{\text{shut}}) RD_i - N_{i,j}^{\text{start}} P_i^{\min} \tag{4.22}$$

4.4 Outline of the Hong Kong power system and buildings

4.4.1 Description of the power system

The power system in Hong Kong, a relatively standalone and mid-scale power system, is used as a reference case. The supply side consists of wind power, solar photovoltaic (PV), biopower, nuclear power, gas-fired power, including combined cycle gas turbine (CCGT) and open cycle gas turbine (OCGT), and utility-scale energy storage. Given the high uncertainty in renewable energy adoption in Hong Kong, four different generation mix scenarios for the year of 2035 are studied, as illustrated in Figure 4.2.

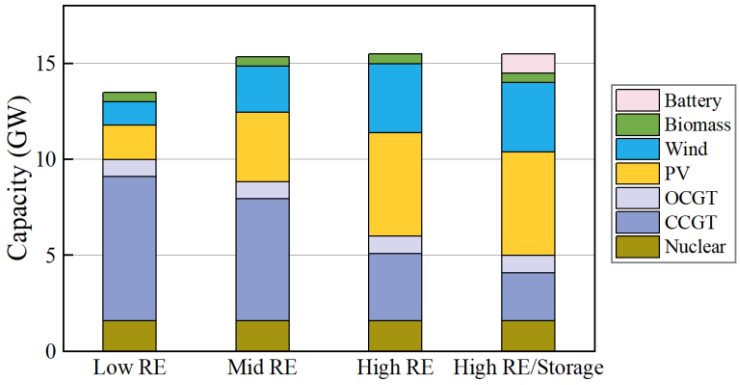

Figure 4.2 Generation mix scenarios of the Hong Kong power system

The low RE scenario corresponds to the installed capacities of solar and wind power planned by the Hong Kong Climate Action Plan. The Mid RE and High RE scenarios are derived by scaling up the installed capacities of renewables in the Low RE scenario by factors of two and three, respectively. The annual renewable penetrations under these three scenarios are approximately 15%, 25%, and 35%, respectively, which are below the maximum renewable penetration potential of about 39% in Hong Kong (Jia Liu et al. 2022).

To investigate the impact of utility-scale energy storage on the benefit and utilization of building energy flexibility, we further examine a High RE/Storage scenario that includes 4-hour battery storage with a 1 GW capacity, corresponding to approximately 10% of power system peak loads. This storage capacity is considered sufficiently high given the examined renewable penetration of 15-35% (Mallapragada et al. 2020). The installed capacity of nuclear power is set to the value in the year 2024.

The peak loads of Hong Kong are about 10 GW, which usually occur in summer due to the high cooling load of buildings. The electricity demand profiles of Hong Kong are obtained by scaling up the measured hourly demand profiles to the year 2035, based on the projected variation in total electricity demand. The power system spinning reserve requirement is set at the installed capacity of the largest generator (600 MW) plus a fraction of hourly renewable generation, following common practices in utility management. The average probability of spinning reserve activation is based on the historical data from U.S. power systems (MacDonald 2014). The technical specifications of conventional generators are shown in Table 4.1 (Mallapragada et al. 2020) (Chyong and Newbery 2022).

Table 4.1 Technical specifications of conventional generators

Technology	Plant Size (MW)	Rated Efficiency	Startup Cost [€/MW]	Min. Stable Output	Hourly Ramp Rate	Min. Up/Down Time [h]
Nuclear	500	/	1,000	50%	25%	12/12
OCGT	100	0.36	25.7	20%	80%	1/1
CCGT	350	0.56	64	40%	60%	4/4

4.4.2 Description of reference buildings

Commercial buildings account for over 70% of electricity use in Hong Kong, an international high-density city with a service-oriented economy and thousands of high-rise buildings. In this study, HVAC systems in commercial buildings are engaged in providing grid services, which are suitable for grid-interactive control due to existing building automation systems. First, using the building load model, the hourly load profiles (including baseline, maximum and minimum load profiles) of a prototype commercial building (i.e., International Commerce Centre) are simulated for the full year. This building is chosen because its design parameters and electricity usage pattern are typical and representative of the high-density city (Jia Liu et al. 2022). The densities and schedules of occupants, lighting, equipment and air-conditioning can be found in (Wang et al. 2019). The baseline indoor air temperature is set at 24 ℃, with an offset of up to 2 K allowed during flexibility activation. The maximum load shifting duration is chosen as two hours to avoid an unacceptable sacrifice in indoor thermal comfort (Aryandoust and Lilliestam 2017). Based on this, the aggregated load profiles of the entire commercial building sector in Hong Kong are obtained by scaling the load profiles of the prototype building to match publicly available data. The aggregated energy flexibility of buildings for providing spinning reserve is also quantified.

4.5 Assessment results

4.5.1 Benefits of using building flexibility for spinning reserve

This section analyzes the impact of using building energy flexibility for spinning reserve on power system operations across different generation mix scenarios. As shown in Figure 4.3(a), the commercial building sector can contribute up to 520 MW of spinning reserve during cooling seasons, which meets up to 86.7% of the spinning reserve required to manage unexpected generator failures (600 MW) in Hong Kong.

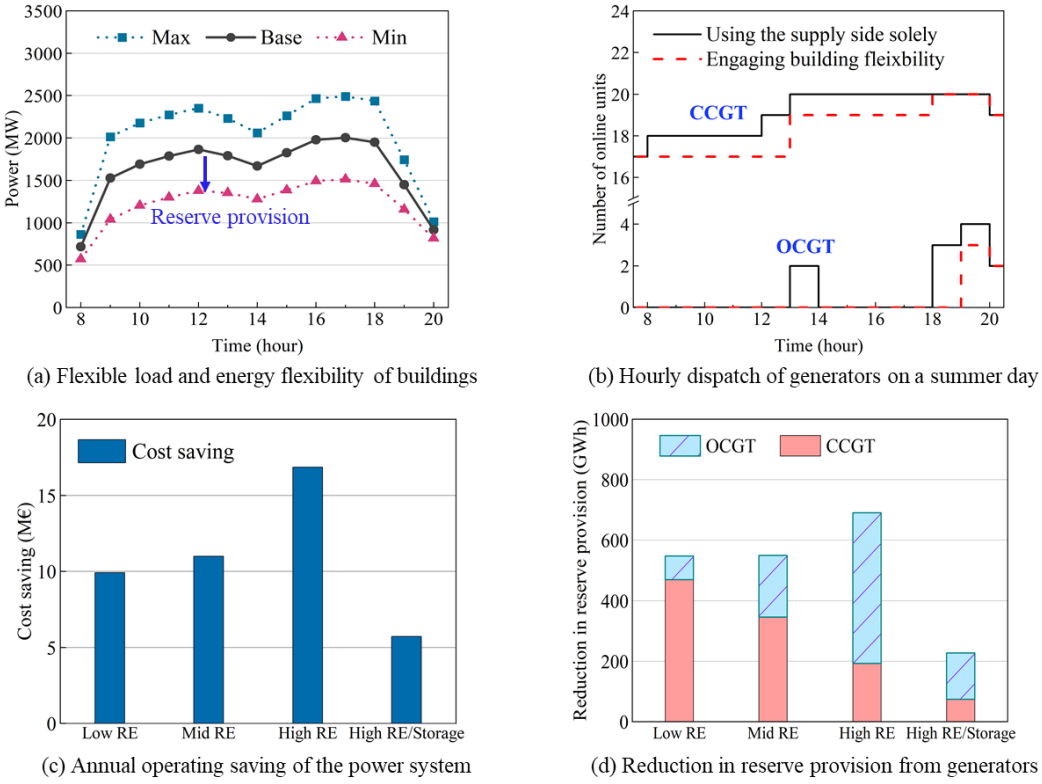

(a) Flexible load and energy flexibility of buildings

(b) Hourly dispatch of generators on a summer day

(c) Annual operating saving of the power system

(d) Reduction in reserve provision from generators

Figure 4.3 Capacity and impacts of building flexibility providing spinning reserve

By engaging building flexibility in spinning reserve provision, fewer thermal generators are committed and operated at part load, resulting in reduced start-up costs and part-load efficiency losses, as illustrated in Figure 4.3(b). This also allows enhanced renewable integration by lowering curtailment of renewables that would otherwise be displaced by gas-fired reserve generation. Consequently, the annual

operating cost of the power system decreases by 0.60%-1.55% (5.7-16.9 M€) compared to relying solely on the power supply side, as seen in Figure 4.3(c).

It is important to note that the cost savings achieved by utilizing buildings for spinning reserves are highly robust. Unlike building thermodynamic models, which rely on numerous simplifications of physical processes and propagate many uncertainties, the power system dispatch model used in this study involves far less uncertainty propagation. The operating cost of thermal generators is primarily driven by factors such as fuel cost and part-load efficiency, which are well supported by real-world data.

In scenarios without utility-scale energy storage, the cost saving increases as renewable penetration increases. This is because fewer baseload generators (CCGTs) are required for electricity supply, while more spinning reserve capacity is needed to manage renewable forecast uncertainties. In this case, high-cost peaking generators (OCGTs) are frequently dispatched to address short-duration reserve shortages. The engagement of building energy flexibility mainly displaces peaking OCGTs rather than baseload CCGTs, as seen in Figure 4.3(d), which increases the value of per-unit building flexibility as spinning reserve.

However, the cost saving decreases after adopting utility-scale storage in the High RE/Storage scenario. Energy storage replaces thermal generators as the primary provider of spinning reserve due to its near-zero operating cost during reserve provision. Consequently, less gas-fired reserve generation can be displaced by building flexibility providing spinning reserve, as seen in Figure 4.3(d). Nonetheless, the cost saving is still considerable at 5.7 M€. It should be noted that the 1 GW storage capacity in the High RE/Storage scenario is already a sufficiently high value.

Therefore, grid operators can anticipate sustainable and substantial cost savings by adopting building energy flexibility as spinning reserve.

4.5.2 Comparison of spinning reserve provision and load shifting

This section presents a comparison of the impacts of using building flexibility for spinning reserve versus load shifting on both the power system and buildings. Unlike most previous studies that assume building flexibility can be freely activated, our analysis incorporates the potential payment to buildings for activating flexibility, which varies from 0.001 to 150 €/MWh, to achieve different levels of flexibility activation (i.e., interference to building operation).

As shown in Figure 4.4, using building flexibility for providing spinning reserve leads to a relatively consistent annual operating cost saving of the power system, even when the incentive varies significantly. Providing spinning reserve only requires buildings to be on standby in most time periods, with actual activation occurring infrequently (typically 20 times per year). In contrast, as the incentive increases from 0.001 to 50 €/MWh, the cost saving of the power system from load shifting decreases dramatically, as does the total amount of activated building flexibility. Each instance of load shifting requires actual activation of building energy flexibility. Consequently, a large portion of technically available flexible load is not economically viable to be shifted. For instance, no observed load shifting occurs to reduce part-load efficiency losses of baseload CCGTs, when a 50 €/MWh incentive is assumed. On the other hand, high-value load shifting actions, such as those for absorbing curtailed renewables, can provide a relatively consistent cost saving for the power system, even when the incentive is increased from 100 to 150 €/MWh.

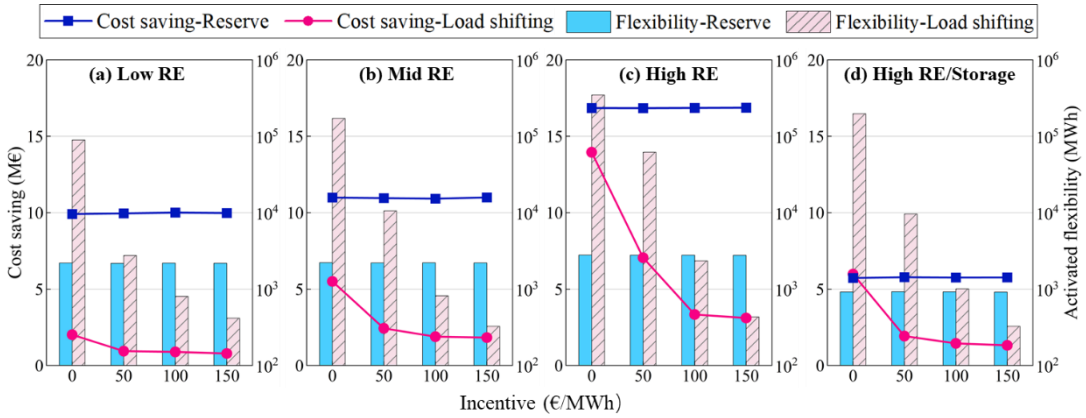

Figure 4.4 Comparison of using building energy flexibility for spinning reserve and load shifting

The power system operating cost saving from load shifting is much lower than that obtained from using building flexibility for spinning reserve in most examined generation mix scenarios, particularly when setting a high incentive for activating flexibility in buildings. For instance, in the Low RE scenario with an incentive of 0.001 €/MWh, the annual operating cost saving from using building flexibility for spinning reserve is 4.9 times that for load shifting, while the total accumulated amount of activated building flexibility for spinning reserve provision is only 2.4% of that for load shifting. Although the operating cost saving from load shifting is slightly higher (less than 5%) in the High RE/Storage scenario, the resulting total amount of activated building flexibility is 215 times that from providing spinning reserve, as shown in Figure 4.4.

Considering a comparable level of building flexibility activation (i.e., interference to building operation), such as setting the incentive at 100 €/MWh in the High RE and High RE/Storage scenarios, the cost savings from using building flexibility for spinning reserve are approximately 5 and 4 times those from load shifting, respectively. This indicates that utilizing building flexibility for spinning reserve offers a higher

operating cost saving for the power system but also interferes far less with building operations compared to load shifting.

To further illustrate the advantage of providing spinning reserve over load shifting when utilizing building flexibility, we estimate the cost saving associated with per-unit activated building flexibility (€/kWh) by assuming building flexibility can be freely activated and all cost savings from demand response go back to buildings (Seatle and McPherson 2024). This metric is calculated as the power system cost saving divided by the total amount of activated building flexibility throughout the year. For load shifting, the unit cost saving ranges from 22 to 40 €/MWh. Given that the typical incentive for activating building flexibility is 150 €/MWh in real-world load shifting programs, implementing load shifting in daily operation seems economically unviable (Seatle and McPherson 2024). In contrast, the unit cost saving from spinning reserve provision is 4522-6315 €/MWh, up to 205 times that for load shifting. This shows that spinning reserve provision has much better economic viability than load shifting in real-world scenarios where a reward must be paid to buildings for activating flexibility.

4.6 Policy implications

Based on the assessment results presented in Section 6.3, we discuss the following key policy implications.

Building energy flexibility as an alternative reserve resource for power systems

Engaging building energy flexibility in spinning reserve provision can offer several operational benefits to power systems beyond the cost saving. First, it can reduce power system carbon emissions by enhancing renewable absorption and part-load

efficiency of thermal generators. Second, it can enable faster frequency restoration in the power system after contingency events (e.g., generator failures), because buildings can respond more rapidly to grid requests than most power generators with ramping limits (Wang et al. 2019). Third, it can reduce the variability of electricity prices by reducing the dispatch of high-cost peaking generators, thereby benefiting all electricity consumers. Fourth, aggregating massive diverse buildings can provide a more reliable spinning reserve capacity compared to conventional generators, even though individual buildings have higher response failure rates than individual generators (Herre et al. 2022).

Spinning reserve as a priority use of building energy flexibility in smart grids

In addition to the higher operating cost benefit and lower interference with building operation, using building flexibility for spinning reserve has several advantages over load shifting. First, load shifting often involves precooling building thermal mass to reduce the power demand during subsequent peak periods. This could cause unnecessary energy loss and additional electricity cost if the predicted peak does not occur in real-time due to forecast uncertainties (Tina et al. 2022). In contrast, providing spinning reserve requires buildings to be on a standby state and avoids the cost of precooling. Second, load shifting may increase carbon emissions when the flexible load is shifted towards cheaper but carbon-intensive coal-fired power. In contrast, buildings providing spinning reserve can reduce both operating cost and carbon emissions, which avoids the trade-off between cost reduction and emission increase, facilitating engineering practice. Third, the actual response duration of spinning reserve provision is typically much shorter than that of load shifting, which enhances the acceptance of building owners. For instance, 80% of reserve activation in the US

markets last less than 20 minutes, but load shifting typically requires a response duration of 2 hours (MacDonald 2014).

Prioritizing spinning reserve does not mean disregarding the benefits of load shifting.

Spinning reserve is a more effective use of building flexibility in daily operation, however, this does not mean that spinning reserve provision can completely replace load shifting. Our analysis only examines the operational impacts of building flexibility, without considering the impact on long-term planning. Load shifting (e.g., precooling buildings) can effectively reduce power system peak loads. Such peak reduction can not only help defer the investment of power generation capacity but also maintain power system reliability during extreme conditions (e.g., heat waves) (Navidi, El Gamal, and Rajagopal 2023). There are also certain cases where load shifting can provide a high operating cost benefit with minimal interference with building operation, e.g., precooling buildings during unoccupied periods with curtailed renewables. Therefore, more focused rather than broad implementation of load shifting is recommended, as also suggested by (Müller and Möst 2018).

Generality of the presented results to other power systems

As the first comparative impact assessment of city-scale building flexibility, this study assumes that the entire commercial building sector participates in grid service provision, representing an upper bound of the associated cost saving. The results are case-specific and influenced by contextual factors such as supply-side flexibility. The cost saving may be lower than estimated if electricity trading with neighbours and utility-scale energy storage capacity exceed the levels examined.

The qualitative insights from this study can be applied to other power systems with comparable generation mixes and building flexibility potential. The findings suggest

that providing spinning reserve is a more suitable use of building energy flexibility, particularly when building users request high incentives to activate flexibility. Currently, most spinning reserve markets do not allow building flexibility to participate. Therefore, market reforms and policy support are recommended to engage buildings in spinning reserve markets, thereby better exploiting building energy flexibility. Besides, spinning reserve provision requires rapid demand reduction in response to grid requests. Unlike conventional load shifting (precooling), such fast demand response control necessitates further research to enable buildings for spinning reserve provision.

4.7 Summary

This chapter presents a comparative assessment of using large-scale building energy flexibility for spinning reserve and load shifting, focusing on the Hong Kong power system in 2035 as a reference case. An integrated grid-buildings optimization model is developed to capture how building energy flexibility affects the operations of both the power system and buildings.

The results show that adopting the flexibility of commercial buildings for spinning reserve can reduce the annual operating cost of the power system by 0.60%-1.55% (5.7-16.9 M€), compared to using conventional generators exclusively. The cost savings depend on the generation mix scenario. These savings increase as renewable energy penetration increases, but decrease after the adoption of utility-scale energy storage.

The annual cost saving from using building flexibility for spinning reserve are up to 4.9 times greater than those for load shifting, while the total accumulated amount of

activated building flexibility for spinning reserve provision is only 2.4% of that for load shifting. This indicates that spinning reserve provision not only offers higher cost savings for the power system but also causes much less interference with building operation compared to load shifting. Therefore, spinning reserve is proposed as a priority use of building energy flexibility in smart grids.

CHAPTER 5 A PROBABILISTIC MODEL FOR REAL-TIME QUANTIFICATION OF BUILDING ENERGY FLEXIBILITY

This chapter presents a probabilistic model for real-time quantification of building energy flexibility under uncertainties. The model considers the major uncertainties involved in flexibility quantification, enabling buildings to serve as a reliable provider of grid flexibility. An explicit equation is used to analytically quantify the flexibility of individual buildings, effectively capturing the characteristics of diverse buildings. The model is computationally efficient for real-time online application, facilitating the participation of building energy flexibility in grid service markets.

Section 5.1 presents the proposed probabilistic model. Section 5.2 presents the validation test arrangement. Section 5.3 presents the test results to validate the performance of the proposed model. Section 5.4 discusses the real-world implementation of the proposed model. Section 5.5 summarizes this chapter.

5.1 Proposed probabilistic model

5.1.1 Outline of the model

The proposed probabilistic model for quantifying the aggregated energy flexibility of a cluster of buildings under uncertainties is outlined in Figure 5.1. This model combines a straightforward equation to directly quantify the flexibility of each individual building with a sampling-based uncertainty analysis to obtain the distribution of their aggregated flexibility. To the best of our knowledge, this model

represents the first attempt to achieve real-time flexibility quantification of building clusters using a bottom-up approach, while comprehensively considering the major uncertainties in flexibility quantification and second-order building thermal dynamics.

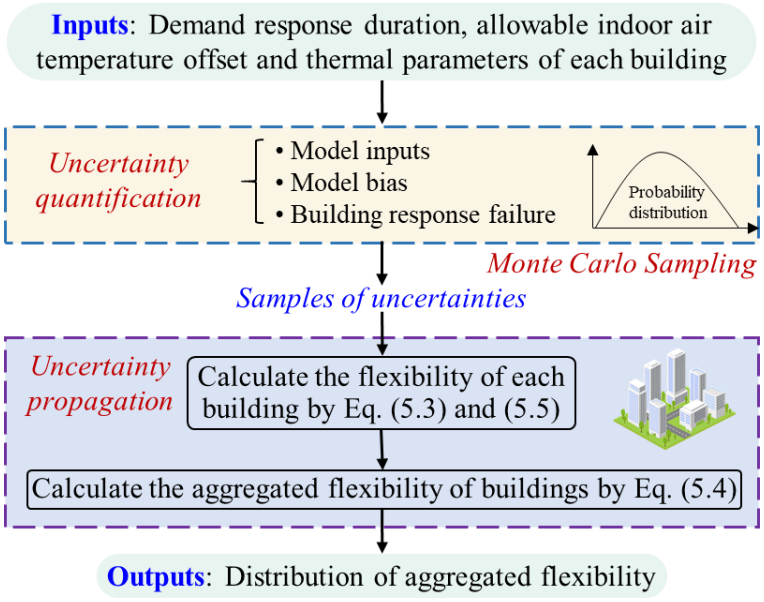

Figure 5.1 Outline of the proposed probabilistic model

5.1.2 Basic deterministic model of building energy flexibility

Modelling individual buildings is the basis for quantifying their aggregated flexibility. In this study, the thermal dynamics of each building and the operating power of each HVAC system (P^{ac}) are characterized by a second-order thermodynamic model. The governing equations of the model are shown in Eqs. (5.1) and (5.2).

$$C^{in}\frac{dT^{in}}{dt} = \frac{T^{out} - T^{in}}{R^{out}} + \frac{T^{m} - T^{in}}{R^{m}} + Q^{in} - COP \cdot P^{ac} \tag{5.1}$$

$$C^{m}\frac{dT^{m}}{dt} = \frac{T^{in} - T^{m}}{R^{m}} + Q^{m} \tag{5.2}$$

where, t is the time. R, C and T refer to thermal resistance, thermal capacitance, and temperature, respectively. The superscripts, i.e., *in, m,* and *out*, denote the indoor air,

building structure mass, and outdoor air, respectively. More details can be found in Section 3.1.

Existing studies (Wang et al. 2018) (Hu and Xiao 2020) usually rely on a few building archetypes to represent the entire building cluster in order to reduce the computational time of quantifying the aggregated flexibility of massive buildings under uncertainties. However, this approach inadequately considers the distinct characteristics of diverse buildings, compromising the modeling accuracy.

To address this issue, we apply the analytical solution to quantify the load reduction ΔP^{ac} of each individual building, as shown in Eq. (5.3). The derivation process of this equation has been presented in Section 3.2.1. The load reduction of a building is a function of the indoor air temperature offset ΔT^{in}, demand response duration Δt, and the parameters of this building.

$$\Delta P^{\mathrm{ac}} = \frac{(r_1 - r_2) C^{\mathrm{in}} \Delta T^{\mathrm{in}}}{[e^{r_1 \Delta t} - e^{r_2 \Delta t} + C^{\mathrm{in}} R^{\mathrm{out}} (r_1 - r_2 + r_2 e^{r_1 \Delta t} - r_1 e^{r_2 \Delta t})] \cdot COP} \tag{5.3}$$

where, $a = C^{\mathrm{in}} C^{\mathrm{m}} R^{\mathrm{m}}$, $b = (1 + R^{\mathrm{m}}/R^{\mathrm{out}}) C^{\mathrm{m}} + C^{\mathrm{in}}$, $c = 1/R^{\mathrm{out}}$,

$$r_1 = (-b + \sqrt{b^2 - 4ac})/2a, \; r_2 = (-b - \sqrt{b^2 - 4ac})/2a$$

Eq. (5.3) only characterizes the magnitude of load reduction ΔP^{ac} of a building. In practice, individual buildings may fail to respond to power grid requests in real-time operation due to various reasons, such as the random behaviour of building occupants, grid-building communication failure due to malicious cyberattacks, and malfunction of building control systems. Besides, the second-order building thermodynamic model is only an approximation of the real system, due to missing physics, overlooked input variables, numerical approximations, and incorrect hypotheses. These two factors should also be considered when quantifying building energy flexibility.

The aggregated energy flexibility of a cluster of buildings (EF^{agr}) is quantified using Eq. (5.4). It is determined by the sum of flexibilities of all individual buildings in the building cluster. This bottom-up approach can better represent the specific characteristics of diverse buildings, compared to the archetype-based approach. Moreover, the building response failure and the model bias are considered in Eq. (5.5), enabling a more realistic flexibility quantification.

$$EF^{\text{agr}} = \sum_{k=1}^{N^{\text{bui}}} EF_k^{\text{bui}} \tag{5.4}$$

$$EF_k^{\text{bui}} = \omega_k \Delta P^{\text{ac}}(x_k) + e_k \tag{5.5}$$

$$f(\omega_k) = \begin{cases} p_k^{\text{bui}}, & \omega_k = 0 \\ 1 - p_k^{\text{bui}}, & \omega_k = 1 \end{cases} \tag{5.6}$$

where, k refers to the index of individual buildings. N^{bui} is the number of buildings in the building cluster. The binary variable, ω_k, represents the response activation state of the building, which is modeled as a Bernoulli distribution, as shown in Eq. (5.6). A value of 0 indicates a failed response, and a value of 1 indicates a successful response. p^{bui} is the response failure rate of the building, which can be derived from empirical or historical data. x_k and e_k are the inputs and bias of the building thermodynamic model.

5.1.3 Probabilistic modelling based on Monte Carlo simulation

The above deterministic model can provide a deterministic output for the aggregated building flexibility based on a given set of inputs. To account for the impact of uncertainties, a sampling-based uncertainty analysis method, i.e., Monte Carlo simulation, is applied to obtain the distribution of the aggregated building flexibility.

The uncertainty analysis consists of four procedures, as illustrated in Figure 5.1. First, the major uncertain parameters are quantified, including the inputs and bias of the building thermodynamic model, and the response failure rates of buildings. Each

uncertain parameter is assigned an appropriate probability distribution based on the available data. Second, Latin Hypercube Sampling is used to generate a set of samples, each representing a possible realization of these uncertain parameters, which are sampled randomly from their respective probability distributions. Third, the uncertain parameters in each sample are imported into the deterministic quantification model to propagate the combined effect of uncertainties. Finally, the values of aggregated flexibility across all samples are collected, and the distribution of aggregated building flexibility of buildings is obtained.

The probability that buildings can successfully achieve a specific committed flexibility capacity (EF^{com}) in actual operation can be determined using Eq. (5.7), where, p^{agr} is the distribution of the aggregated building flexibility.

$$P(EF^{\text{agr}} \geq EF^{\text{com}}) = \int_{EF^{\text{com}}}^{+\infty} p^{\text{agr}} \tag{5.7}$$

By varying the demand response duration, a set of probability-capacity curves can be obtained. These curves serve as a valuable tool for effectively designing demand response programs. By setting the success probability to a desired confidence level (e.g., 99.9%), building energy flexibility can be leveraged in a reliable manner, similar to conventional generators.

5.2 Validation test arrangement

5.2.1 Description of reference buildings

In this study, a building cluster consisting of 150 large-sized commercial buildings is chosen to provide demand-side flexibility. Commercial buildings are considered due to their feasibility of implementing advanced grid-interactive control using existing building automation systems. The building cluster is generated based on a prototype

commercial building in Hong Kong, following the method adopted by (Dong et al. 2018). The design parameters and normal usage pattern (e.g., occupancy profile) of the prototype building can be found in (Wang et al. 2019). The overall COP of the HVAC system of the prototype building is assumed to be equal to 3. With simulation data from the software TRNSYS, the thermal parameters of the prototype building are estimated for characterizing its second-order thermal dynamics.

For the building cluster, the parameters (e.g., thermal resistance and COP) of each building are randomly sampled from uniform distributions, with a ±20% variation range around the parameters of the prototype building. This large variation range is chosen to ensure diversity among individual buildings. The randomization process for generating the building cluster is conducted only once. After randomization, each building has unique thermal parameters, HVAC system, and normal usage pattern. The validation tests are conducted using the weather data on a typical summer day in Hong Kong, when the building HVAC systems are in operation. The maximum allowable indoor air temperature offset for each building is assumed to be 2 K during the demand response period. Individual buildings are assumed to have independent controls, enabling them to respond to grid requests independently.

5.2.2 Description of major uncertainties

Building energy flexibility quantification involves various uncertainties. Based on the previous studies on sensitivity analysis of building parameters (Martinez, Vellei, and Le Dréau 2022b), the following uncertain inputs of the second-order building thermodynamic model are considered: the thermal resistance between the indoor air and the building structure mass, and the actual indoor air temperature offset during the

demand response. These uncertainties are assumed to follow normal distributions with mean values corresponding to their deterministic values.

In practical operation, buildings may fail or choose not to respond to power grid requests due to communication and control issues. The uncertainty in response failures is quantified using the response failure rate, which is assumed to follow a binomial distribution based on data from a real-world demonstration project in Germany (Müller and Jansen 2019). The bias of the second-order building thermodynamic model is assumed to follow a normal distribution with a zero mean and a standard deviation that is 5% of the deterministic predicted value (Amadeh, Lee, and Zhang 2022). Table 5.1 provides detailed information on the probability distributions of major uncertain parameters involved in flexibility quantification.

Table 5.1 Major uncertain parameters and their distributions

Group	Parameter	Probability distribution
Building parameters	Thermal resistance	Normal (R_{det} ,0.05 R_{det})
	Indoor air temperature offset	Normal (ΔT^{in}_{det} ,0.25)
Response state	Response failure rate	Binomial (N^{bui}, 0.1)
Model bias	Building model bias	Normal (0, 0.05 P_{det})

Note: Normal (μ, σ) refers to a normal distribution with mean μ and standard deviation σ.

5.2.3 Outline of flexibility quantification models

Four different models are tested and compared to verify the effectiveness and advantages of the proposed model in quantifying the aggregated flexibility of buildings, as listed below.

- *Deterministic model*: This model does not consider uncertainties in flexibility quantification. It quantifies the aggregated flexibility by modeling each individual building in the building cluster, as described in 5.1.2.

- *Proposed model*: This model considers the major uncertainties in flexibility quantification. It quantifies the aggregated flexibility by modeling each individual building, using the analytical equations introduced in Section 5.1.3.
- *Probabilistic numerical model*: This model is extended from the deterministic model by considering the major uncertainties. It quantifies the aggregated flexibility by modeling each individual building, using the numerical solution method described in Section 3.1.2.
- *Archetype-based model*: This model considers the major uncertainties. It estimates the aggregated flexibility by classifying the building cluster into a few groups (i.e., archetypes) (Wang et al. 2018). The flexibility of each archetype is quantified using the numerical solution method described in Section 3.1.2.

5.3 Performance evaluation of proposed model

This section presents the flexibility quantification results of the proposed probabilistic model. The accuracy and computational efficiency of the proposed model are demonstrated and compared with the deterministic model and other probabilistic models respectively. All flexibility quantification models are implemented in Matlab on a PC with an eight-core Intel Core i7 CPU. The number of samples for the Monte Carlo simulation is chosen as 5,000 to ensure convergence. This number provides a proper balance between computational efficiency and the accuracy of the results.

5.3.1 Quantification results and comparison with deterministic model

Figure 5.2 shows the distribution and cumulative distribution function (CDF) of the aggregated building flexibility of the building cluster during a 1-hour demand response event, as quantified by the proposed probabilistic model. The aggregated

flexibility capacity ranges from about 160 MW to 210 MW under uncertainties. In contrast, the deterministic model, which overlooks uncertainties, gives a single output of 183 MW, which corresponds to 47.5% of the CDF. This indicates a high probability (i.e., 52.5%) of overestimating the aggregated flexibility when using the deterministic model, posing a significant risk to the power grid if such flexibility capacity is committed by buildings. Therefore, it is necessary to consider and quantify the impact of uncertainties on building energy flexibility.

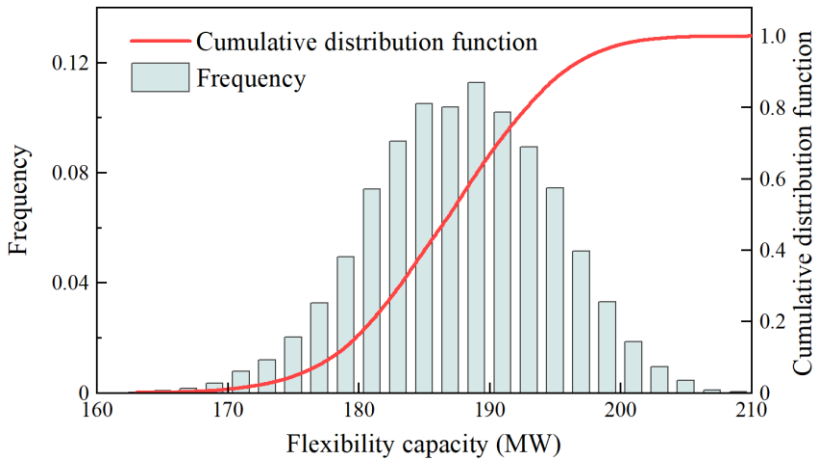

Figure 5.2 Distribution of the aggregated flexibility of buildings

Based on the quantified distribution of aggregated building flexibility, probability-capacity curves are generated for different demand response durations, as shown in Figure 5.3. It can be observed that for a given demand response duration, a higher committed flexibility capacity corresponds to a lower probability of successfully achieving the committed flexibility in actual operation. On the other hand, for the same desired success probability, buildings can provide more energy flexibility with shorter demand response durations, which aligns with the findings reported in (Zhang and Domínguez-García 2018). Therefore, the demand response duration should be carefully determined to optimize the coordination of building energy flexibility and power grids.

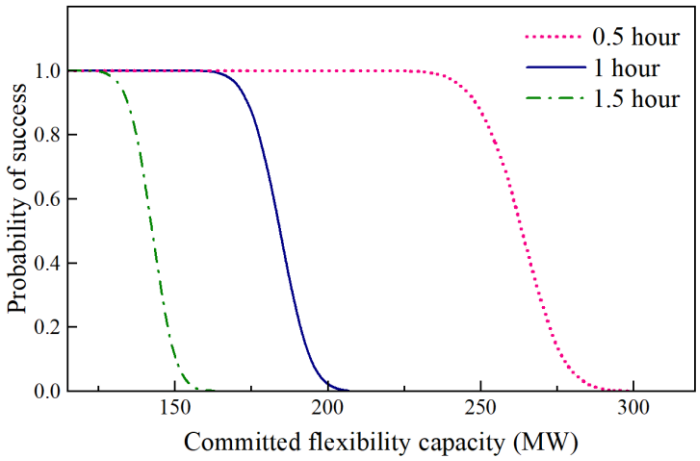

Figure 5.3 Probability-capacity curves for different demand response durations

The flexibility provided by buildings achieves a very high probability of success (i.e., 99.99%) when the committed capacity is below a certain threshold (e.g., 160 MW for a response duration of 1 hour). The success probability is even higher than that of most conventional generators (i.e., 99.9%) (Doherty and O'Malley 2005). This can be attributed to the aggregating effect of multiple buildings, which offers three significant benefits: *First*, it mitigates the impact of uncertainties of individual buildings on their aggregated flexibility. *Second*, even if a subset of buildings cannot provide adequate flexibility, the other buildings can compensate for this temporary shortage (Zhang, Saloux, and Candanedo 2024). *Third*, the flexibility committed by buildings can be flexibly adjusted as needed, unlike conventional generators with fixed and large-rated capacities. Therefore, buildings can serve as a reliable complement to conventional generators for providing grid services in smart grids.

5.3.2 Accuracy and scalability of proposed model

The accuracy of the proposed probabilistic model is verified by comparing its output with that of the numerical probabilistic model commonly used in the literature, which relies on a numerical solution method to solve the building thermodynamic model. For this purpose, the time step of the numerical model is set to 1 second to obtain an

accurate solution. However, using such a small time step increases the computational intensity of the numerical model when applied to the 150 buildings. To simplify the comparison, a random sample of uncertainties is utilized. It is found that the difference between the aggregated flexibility obtained from the two models, using this sample, is less than 0.01%. This negligible difference confirms the accuracy of the proposed probabilistic model.

The scalability of the proposed model is demonstrated by applying it to quantify the aggregated flexibility of building clusters consisting of different numbers of buildings (i.e., 10, 100, 500, 1000, and 2000). Figure 5.4 illustrates the computational time measured under different numbers of buildings. It can be seen that even when dealing with 2000 buildings, the proposed model only takes about 140 seconds to give a solution, confirming its scalability. This means that even if we use ten second-order RC models for modeling the 150 buildings, the computation time of the proposed model is still very fast (less than 2 minutes). This computational time can satisfy the application requirements of power grid real-time dispatch and engaging building flexibility into real-time electricity market, which usually have a time interval of 15 minutes. Furthermore, the measured computational time exhibits a linear growth trend, which aligns with the theoretical trend inferred from the bottom-up structure of the proposed model.

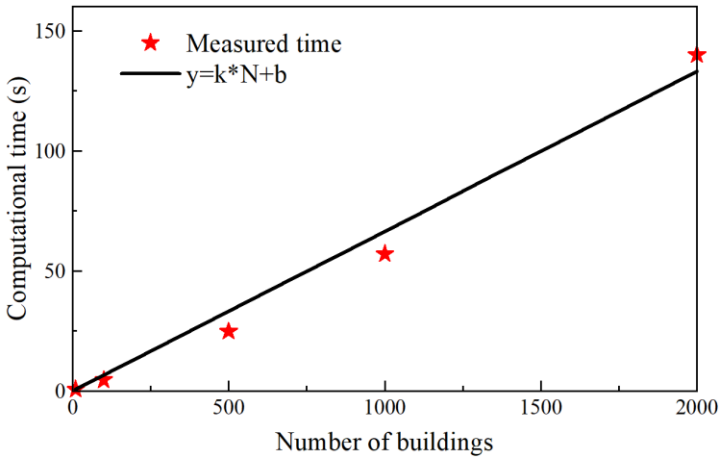

Figure 5.4 Computational time of the proposed model under different number of buildings

5.3.3 Comparison with existing probabilistic models

The superior computational accuracy and efficiency of the proposed probabilistic model is confirmed by comparing it with two existing probabilistic models, i.e., the probabilistic numerical model and the archetype-based model. The demand response duration is set to 1 hour for comparison.

The time step of the probabilistic numerical model is set to 1 and 5 minutes, respectively. The probabilistic numerical model with a 1-minute time step takes 3605.6 seconds to give a solution, as shown in Table 5.2. In contrast, the proposed model only takes 6.7 seconds, which is 537 times faster than the numerical model. The probability-capacity curves given by these two probabilistic models are very close, as shown in Figure 5.5. Their differences in flexibility capacities at success probabilities of 0.999 and 0.95 are less than 1.8%. For the probabilistic numerical model with a 5-minute time step, the computational time is 1503.2 seconds, and the estimated flexibility capacity at a success probability of 0.999 is 4.4% lower compared to that of the proposed model. Although this deviation may seem small on its own, it may significantly affect power grid scheduling. It could lead grid operators to schedule an

additional large-scale conventional generator to meet the flexibility requirement, increasing the operational cost of the power system. Note that these differences are attributed to the discrete-time state space formulation of the probabilistic numerical model. The outputs of the proposed model have been demonstrated to be accurate and correct in Section 5.3.2.

Table 5.2 Computational results of different probabilistic models

Model	Capacity at Prob. 0.999 (MW)	Capacity at Prob. 0.95 (MW)	Computational time (s)
Proposed	160	171	6.7
Prob. Numerical (1-min step)	162	174	3605.6
Prob. Numerical (5-min step)	153	165	1503.2
Archetype-based	141	147	54.5

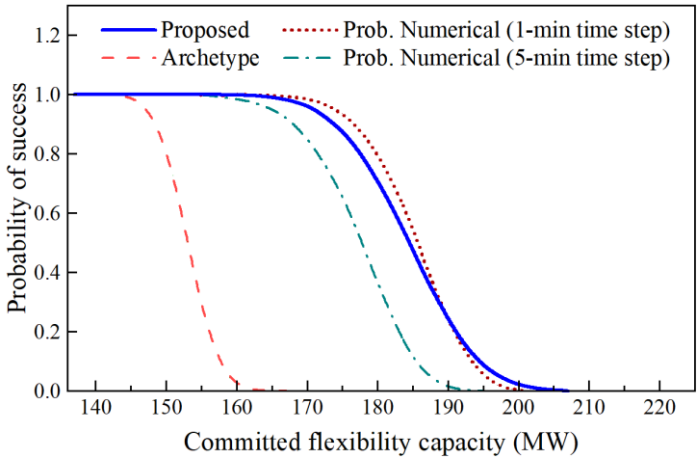

Figure 5.5 Probability-capacity curves given by different probabilistic models

The performance of the archetype-based model, as adopted in (Martinez et al. 2022a) (Wang et al. 2018) (Hu and Xiao 2020), is also tested and compared. The archetype-based model has been extended to incorporate the building response failures. In this model, 150 buildings in the building cluster are classified into 5 groups based on their characteristics. The numerical time step is set to 5 minutes. As shown in Table 5.2, although the archetype-based model reduces the computational time by using a few

building archetypes to represent the entire building cluster, it still requires 54.5 seconds to give a solution. This computational time is about 8 times that of the proposed model (6.7 seconds). Moreover, the archetype-based model generates a probability-capacity curve that significantly deviates from the correct curve, as shown in Figure 5.5. It gives a flexibility capacity of 147 MW for a success probability of 0.95, which is 14% lower than the correct value. The lower accuracy of the archetype-based model is due to its inadequate consideration of the characteristics of individual buildings. In summary, the proposed model outperforms the existing models in terms of both accuracy and computational efficiency.

5.4 Real-world implementation feasibility analysis

This study presents a novel probabilistic model for real-time quantification of the aggregated flexibility of buildings under uncertainties. The model can be used by load aggregators to quantify the flexibility of a building cluster and perform bidding in the real-time electricity and grid service markets, which requires flexibility providers to have a minimum reliability of 95%. Additionally, the outputs of this probabilistic model can be directly used by grid operators for optimized power grid scheduling and real-time dispatch incorporating building flexibility, as widely studied in smart grid fields. For instance, the quantified distribution of the aggregated flexibility of buildings under uncertainties can serve as a basis for risk assessment and stochastic scheduling of the power system adopting building flexibility as operating reserve.

To implement this model on a building cluster, the following steps are required. Firstly, smart devices should be installed in each building to enable effective communication and interaction between the power grid and the buildings. Secondly, the parameters

(e.g., thermal resistance and thermal capacitance) of each building are required. These parameters can be identified either locally by individual buildings or centrally by grid operators. Existing software tools (e.g., CTSM-R) can be employed to facilitate parameter estimation based on the measured data in each building (Bacher and Madsen 2011). Finally, the proposed model is applied to quantify the aggregated building flexibility based on the collected information. The probability-capacity curves of the aggregated building flexibility can then be utilized by load aggregators or power grid operators.

There are several potential challenges related to the real-time application of the proposed model for building flexibility quantification. First, the model requires each building to communicate its operational parameters to grid operators or load aggregators. This may raise concerns regarding the reliability of communication protocols and the privacy of the data being transmitted. Second, the thermal zones within a building may be highly diverse, necessitating the use of multiple thermodynamic models to represent each zone. In such cases, the proposed model can still provide real-time flexibility quantification due to its verified scalability, but obtaining the cooling load of each thermal zone for training the thermodynamic model is challenging, because typically only the HVAC operating power is measured. Third the thermal parameters of a building may change over time. Ignoring this issue in model development can compromise the accuracy of energy flexibility quantification. To tackle this issue, the thermodynamic models should be trained adaptively in real-time application to continuously update their parameters and accommodate the time-varying conditions (Hua et al. 2023).

5.5 Summary

This chapter presents a novel probabilistic model for real-time quantification of the aggregated flexibility of buildings under uncertainties. The model applies an explicit equation to analytically quantify the flexibility of individual buildings, eliminating the need for time-consuming iterative and finite difference computations. The uncertainty analysis accounts for the major uncertainties in flexibility quantification, including model inputs, model bias, and building response failures. Validation tests are conducted using a building cluster consisting of 150 buildings. Based on the test results, main conclusions are drawn as follows:

- The proposed probabilistic model can provide a more robust quantification of the aggregated building flexibility by considering uncertainties, compared to the deterministic model. For a demand response duration of 1 hour, the flexibility capacity estimated by the deterministic model has a high probability of 52.5% of being overestimated.
- The proposed model outperforms the existing probabilistic models in terms of both accuracy and computational efficiency. It can accurately quantify the aggregated flexibility in 6.7 seconds, which is 535 times faster than the probabilistic model solved numerically. Furthermore, it is 8 times faster than the archetype-based model while offering significantly higher accuracy.
- The scalability of the proposed probabilistic model is validated. The proposed model only takes 140 seconds to quantify the aggregated flexibility of 2000 buildings, which can satisfy the real-time application requirements of power grid scheduling and dispatch.
- The aggregated flexibility of buildings has a very high success probability (e.g.,

99.99%) when the committed capacity is below a certain threshold (e.g., 160 MW for a 1-hour response duration). This reliability level is even higher than that of conventional generators (i.e., 99.9%). Therefore, buildings can provide reliable grid services by properly setting their committed flexibility capacity.

The proposed model can quickly and accurately generate probability-capacity curves for the aggregated building flexibility in real-time applications, facilitating the active engagement of building energy flexibility into electricity and grid service markets.

CHAPTER 6 A RISK-AVERSE RESERVE SCHEDULING RAMEWORK FOR POWER SYSTEMS ENGAGING BUILDING FLEXIBILITY

This chapter presents a risk-averse day-ahead reserve scheduling framework for power systems engaging building energy flexibility. The framework leverages the outputs of the probabilistic model of building energy flexibility, as presented in Chapter 5, to provide a risk-averse reserve schedule. In this framework, a set of alternative reserve schedules with different levels of building reserve commitment are generated. The best reserve schedule is identified by balancing the power system operation cost and risk under alternative reserve schedules. A new risk indicator, namely the expected reserve shortage, is proposed for more accurate and efficient risk assessment.

Section 6.1 presents the outline of the framework. Section 6.2 presents the generation procedures of alternative reserve schedules. Section 6.3 presents the proposed risk indicator and risk assessment method. Section 6.4 presents the validation test arrangement. Section 6.5 presents the test results to evaluate the performance of the proposed framework. Section 6.6 gives a summary of this chapter.

6.1 Outline of the framework

There are various alternative day-ahead reserve schedules incorporating building energy flexibility, each of which has a specific combination of reserve commitments from buildings and conventional generators, as illustrated in Figure 6.1. All of these schedules can meet the power system reserve requirement in the day-ahead reserve commitment stage, but they have different risk levels concerning real-time power

system operation. This is because that buildings may fail to realize their committed reserve provision in the real-time operation stage due to various uncertainties, which could adversely affect power system reliability. Therefore, it is essential to identify the best reserve schedule that properly balances the operation cost and risk of the power system using building energy flexibility.

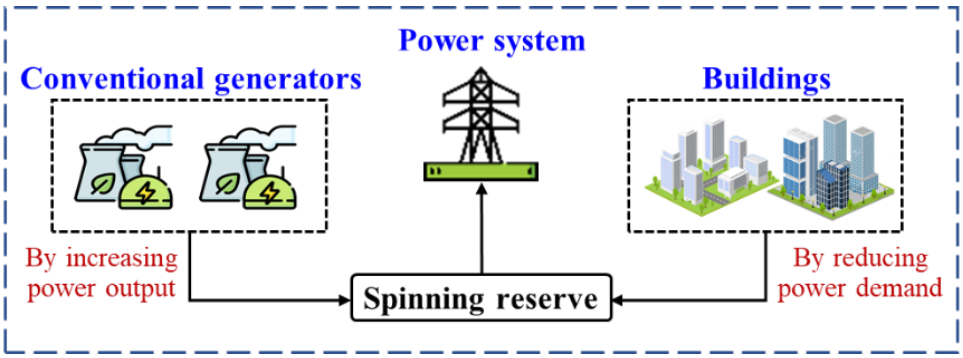

Figure 6.1 Reserve balance of a power system engaging building flexibility

To identify the best reserve schedule among various alternative reserve schedules, four main functional components or steps are involved in the proposed risk-averse reserve scheduling framework, as illustrated in Figure 6.2.

In Step 1, the probability distribution of building energy flexibility under uncertainties is obtained using the probabilistic building flexibility model introduced in Chapter 5. For spinning reserve provision, the building demand response duration is chosen as one hour, according to the typical requirement of power grid operation.

In Step 2, a set of alternative reserve schedules is generated by incorporating the probabilistic forecasts of building energy flexibility into the existing deterministic reserve scheduling model. The power system operation cost under each schedule is also obtained.

In Step 3, the risk associated with each reserve schedule is assessed using the proposed risk indicator, namely the expected reserve shortage, considering uncertainties of both buildings and conventional generators.

In Step 4, the best reserve schedule is identified by balancing the power system operation cost and risk under alternative schedules.

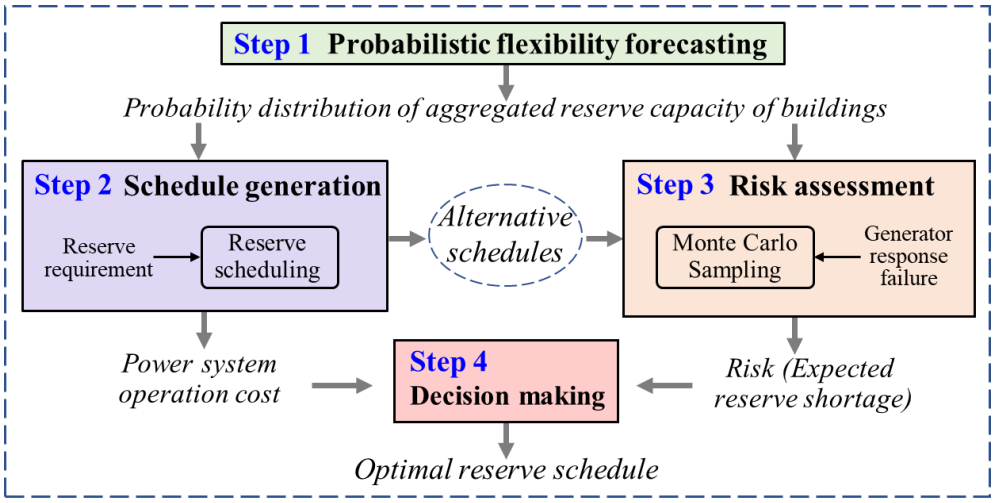

Figure 6.2 Main steps of the risk-averse reserve scheduling framework

The details on *Step 1* has been presented in Chapter 5. The *Step 4*, as a decision-making component, depends on the specific preference of power grid operators on cost saving and risk management. The *Step* 2 and *Step* 3 are elaborated in the following sections.

6.2 Alternative schedule generation

Based on the probabilistic quantification results of building energy flexibility, a set of alternative reserve schedules with different levels of building reserve commitment can be obtained. This can be achieved using two approaches. The first approach, as found in (Wang, Wang, and Guan 2013), relies on stochastic optimization to solve the reformulated stochastic reserve scheduling problem, where demand flexibility is described by stochastic variables. This approach often requires complex modifications

to existing deterministic reserve scheduling problem, which hinders their practical engineering application.

The second approach, as suggested in (Q. Wang et al. 2023), transforms probabilistic information (e.g., renewable generation forecasts) into multiple deterministic values, each of which corresponds to a certain confidence threshold, i.e., satisfying a certain confidence level. In this study, the second approach is used because it offers greater ease of implementation and avoids the complex modification to the existing deterministic reserve scheduling problem.

The detailed procedures of alternative schedule generation are as follows. First, the probabilistic building energy flexibility is transformed into multiple deterministic building flexibility capacities for providing spinning reserve, each of which corresponds to a certain confidence threshold (e.g., 99.9%) of building reserve commitment. Second, the deterministic building flexibility capacities are respectively incorporated into the deterministic reserve scheduling problem through the reserve balance constraints. An alternative reserve schedule, along with the corresponding power system operation cost, is obtained by solving the reformulated deterministic reserve scheduling problem that includes the cost of engaging buildings. By varying the confidence level with a certain interval (e.g., 5%) and repeating the above process, a set of alternative reserve schedules can be obtained.

The confidence level of buildings in achieving a specific reserve commitment ($SR^{\mathrm{bui,com}}$) when the reserve is called on in real-time operation is determined using Eq. (6.1). Where, $p^{\mathrm{SR,bui}}$ is the probability distribution of building energy flexibility for providing spinning reserve under uncertainties.

$$P(SR^{\mathrm{bui}} \geq SR^{\mathrm{bui,\,com}}) = \int_{SR^{\mathrm{bui,\,com}}}^{+\infty} p^{\mathrm{SR,bui}} \tag{6.1}$$

Reformulation of the deterministic reserve scheduling problem

To consider the cost of engaging building energy flexibility, the deterministic reserve scheduling problem is formulated as shown in Eqs. (6.2) and (6.3), based on the typical deterministic reserve scheduling problem for determining the commitment status of conventional generators. The revised objective is to minimize the total expected power system cost, including the operation cost of conventional generators (C^{gen}) and the cost of using building energy flexibility (C^{bui}), subject to reserve balance constraints.

$$min(C^{\text{gen}} + C^{\text{bui}}) \tag{6.2}$$

$$SR_j^{\text{gen}} + SR_j^{\text{bui,com}} = SR_j^{\text{req}} \tag{6.3}$$

where, j represents the time interval. SR^{gen} and $SR^{\text{bui,com}}$ is the spinning reserve committed by conventional generators and buildings respectively. SR^{req} is the power system spinning reserve requirement.

Note, in Eq. (6.3), $SR^{\text{bui,com}}$ is a deterministic value when generating each alternative schedule, without introducing additional stochastic variables. Therefore, the above problem reformulation is minor and suitable for engineering practice.

The cost of using building flexibility is determined by Eq. (6.4). Where, p^{SR} is the activation probability of power system spinning reserve, which can be derived from historical data of power system operation. *rc* and *ra* are reserve commitment and activation price of buildings, respectively.

$$C^{\text{bui}} = \sum_j SR_j^{\text{bui,com}}(rc + ra \cdot p^{\text{SR}}) \tag{6.4}$$

The operation cost and constraints of conventional generators are determined using a commonly used power grid dispatch model, as presented in Section 4.3.2.

6.3 Risk assessment and risk-averse reserve scheduling

The power system operation risk associated with each alternative reserve schedule is assessed based on a newly proposed risk indicator, i.e., expected reserve shortage (ERS). The main novelties and advantages of this indicator are as follows.

- ERS is based on the amount of spinning reserve, rather than power imbalance. Therefore, it can efficiently quantify the risk of adopting building energy flexibility for providing spinning reserve, even in cases where the reserve activation is infrequent.
- ERS quantifies the *expected* amount of reserve shortage, rather than a deterministic amount. Therefore, it can effectively consider the risk due to uncertain provision of spinning reserve. Moreover, the proposed formulation focuses on the uncertainty in reserve provision rather than the uncertainty in power system reserve requirement.
- ERS considers the uncertainty in reserve provision from both conventional generators and buildings, enabling a more accurate and realistic risk assessment of adopting building energy flexibility as spinning reserve, compared to that solely focusing on the risk resulting from using building energy flexibility.

ERS can be quantified using Eqs. (6.5)-(6.7). A higher value of ERS indicates a higher operation risk, and vice versa. To quantify ERS under a given alternative reserve schedule, random samples for the reserve commitment of buildings and conventional generators under this schedule are generated using Monte Carlo simulation, based on the quantified distribution of building energy flexibility under uncertainties and the response failure probabilities of conventional generators. A two-state model is used to describe the response failures of conventional generators, similar to that of buildings (Qi et al. 2022). Here, m and N represent the index and total number of samples,

respectively. I represents the reserve shortage under a sample. SR^{ava} is the total spinning reserve actually provided by conventional generators and buildings under a sample.

$$ERS \approx \frac{1}{N}\sum_{m=1}^{N} I_m \tag{6.5}$$

$$I_{j,m} = \begin{cases} SR_{j,m}^{\text{req}} - SR_{j,m}^{\text{ava}}, & SR_{j,m}^{\text{ava}} < SR_{j,m}^{\text{req}} \\ 0, & SR_{j,m}^{\text{ava}} \geq SR_{j,m}^{\text{req}} \end{cases} \tag{6.6}$$

$$SR_{j,m}^{\text{ava}} = SR_{j,m}^{\text{gen}} + SR_{j,m}^{\text{bui}} \tag{6.7}$$

6.4 Validation test arrangement

6.4.1 Description of the power system

The proposed strategy is tested on a power system modified from the existing Hong Kong power system. The supply side contains twenty combined cycles gas turbines (CCGT), eight open cycle gas turbines (OCGT), 1577 MW of nuclear power, and 4000 MW of wind power. The response failure probability of each conventional generator is chosen as 0.1% (Herre et al. 2022) (Doherty and O'Malley 2005). The spinning reserve requirement of the power system is set as the capacity of the largest conventional generator (600 MW) plus a specific proportion of day-ahead renewable generation forecasts (Mallapragada et al. 2020). Such arrangements align with common practice in utility management. The day-ahead forecasts of electricity demand and wind power on the test day are shown in Figure 6.3. Based on the day-ahead forecasts, power grid operators determine the power system reserve requirement at each time interval of the next day, as well as the reserve commitment of buildings and conventional generators.

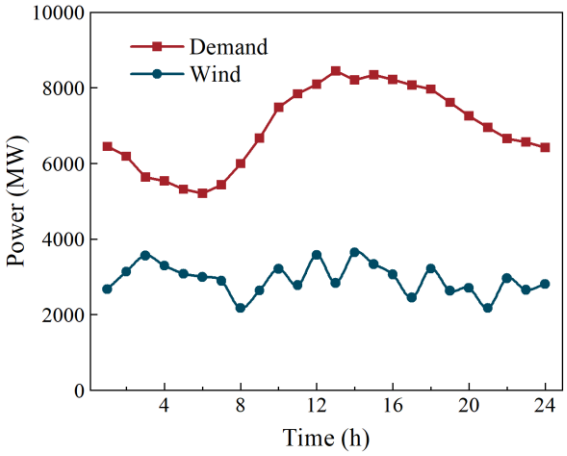

Figure 6.3 Day-ahead forecasts of electricity demand and wind power

6.4.2 Description of reference buildings

On the demand side, 150 large and high-rise commercial buildings are selected to participate in spinning reserve provision. The parameters of these buildings and the distribution of uncertainties have been introduced in Section 5.1.2. The planned indoor air temperature offset for each building during spinning reserve provision is set at 2 K. The buildings can provide spinning reserve during occupancy hours (8:00-20:00) while their HVAC systems are operating. The reserve commitment and activation prices of buildings are set at 3 €/MWh and 80 €/MWh. The controls of individual buildings are assumed to be independent, allowing them to respond to power grid request independently.

6.4.3 Outline of the tested cases

Three cases are tested to validate the performance of the proposed risk-averse reserve scheduling framework, as listed below.

- *Base case*: Only conventional generators are used to provide spinning reserve. The energy flexibility of buildings is not used.

- *Deterministic case*: Both conventional generators and buildings are used to provide spinning reserve. Building energy flexibility is predicted without considering the impact of uncertainties, i.e., using the deterministic flexibility model presented in Chapter 5.
- *Risk-averse case*: Both conventional generators and buildings are used to provide spinning reserve. Building energy flexibility is quantified while considering the impact of uncertainties. The best reserve schedule is determined using the proposed risk-averse scheduling framework.

Both building energy flexibility models and reserve scheduling problems are programmed using Matlab on a computer with an eight-core Intel Core i7 CPU. The reserve scheduling horizon is 24 hours for the next day and the time interval is 1 hour. For comparison, the confidence threshold is set at 95% in the risk-averse case to properly balance the operation cost and risk of the power system. The impact of varying the confidence threshold setting is analyzed in Section 6.5.4.

6.5 Performance evaluation of proposed framework

This section presents the test results to evaluate the performance of the proposed risk-averse reserve scheduling framework. The deterministic reserve scheduling model is programmed using Matlab on a computer with an eight-core Intel Core i7 CPU. The scheduling horizon is 24 hours for the next day and the time interval is 1 hour. For risk assessment, 10,000 samples are used to obtain a converged ERS. In contrast, more than 10^7 samples are required to obtain a converged EENS. This shows the higher computational efficiency of using ERS for risk assessment.

6.5.1 Power system risk of using building flexibility as spinning reserve

A major concern when leveraging building energy flexibility to provide spinning reserve is its potential impact on power system reliability. Therefore, it is essential to consider the impact of uncertainties on building energy flexibility. The distribution of building energy flexibility for providing spinning reserve on the test day is shown in Figure 6.4. It can be seen that the flexibility capacity of buildings for providing spinning reserve is higher during midday hours due to the greater occupancy and cooling load, compared to the early morning and night time periods.

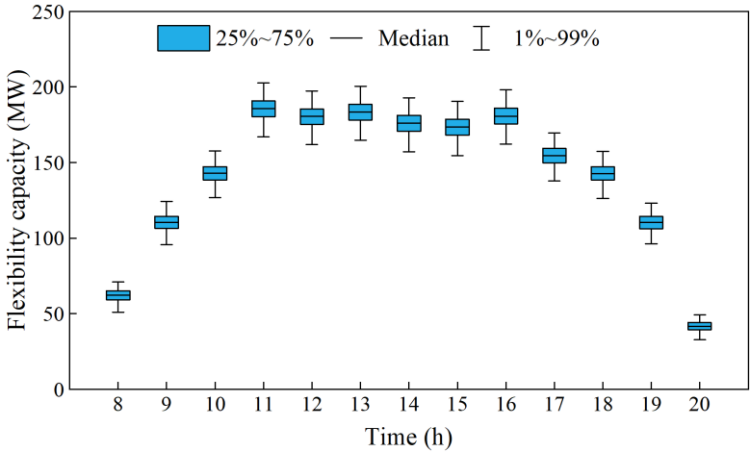

Figure 6.4 Distribution of building energy flexibility for spinning reserve

The power system operation risk is assessed by setting different confidence thresholds for building reserve commitment. The total expected reserve shortage (ERS) accumulated over the next 24 hours is used as the risk indicator. Figure 6.5 shows the impact of varying thresholds on the operation risk. The baseline risk level corresponds to that in the base case where only conventional generators are providing spinning reserve. When appropriate confidence thresholds are set for building reserve commitment, the total ERS is lower than the baseline level (13.95 MWh), indicating a lower power system operation risk.

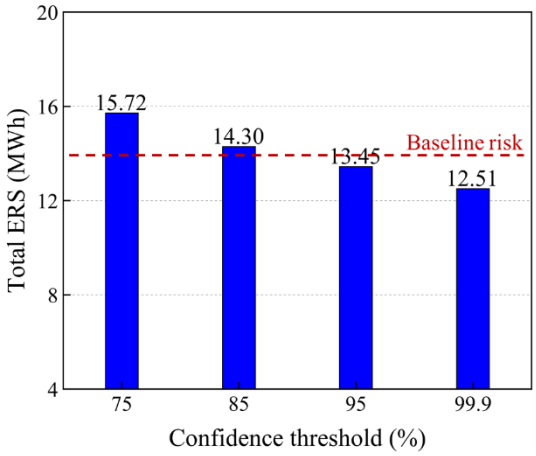

Figure 6.5 Power system operation risk under different confidence thresholds for building reserve commitment

Compared to the baseline risk level, procuring spinning reserve from buildings with confidence thresholds of 99.9% and 95% achieves a risk reduction of 9.51% and 2.70%, respectively. When the confidence threshold is set even lower, i.e., at 85%, the total ERS is 14.30 MWh, which is higher than the baseline risk level (13.95 MWh). In summary, the power system operation risk is manageable and acceptable when using building energy flexibility as spinning reserve.

6.5.2 Comparison with solely using conventional generators

Figure 6.6 shows the scheduling of conventional generators in different cases. Compared to the base case, where only conventional generators are providing spinning reserve, fewer conventional generators are committed from 8:00 to 20:00 in the risk-averse case due to the adoption of building energy flexibility. This leads to a lower power system operation cost because of the reduced part-load efficiency losses and lower start-up costs of conventional generators.

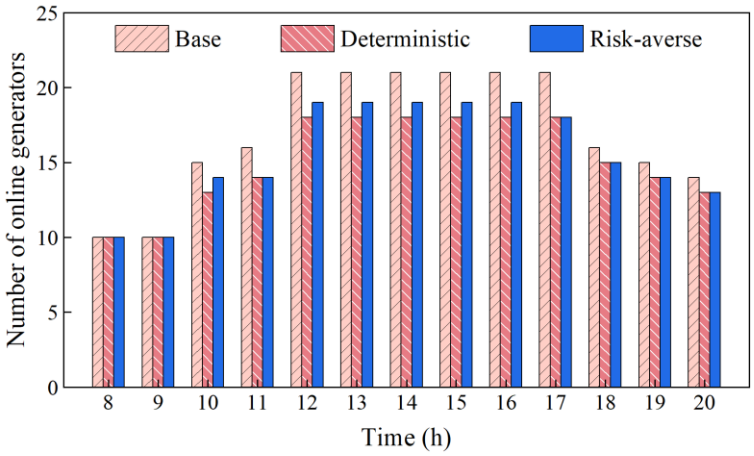

Figure 6.6 Scheduling of conventional generators in different cases

Figure 6.7 compares the hourly ERS in these two cases. The adoption of building energy flexibility leads to a reduction in hourly ERS by up to 28% because the reserve committed by buildings is below the quantified flexibility capacity with a high confidence level of 99.99% at most time intervals. Using a large number of less reliable reserve providers (i.e., buildings) mitigates the operation risk of relying on a few conventional generators, even though conventional generators have much lower response failure probabilities than individual buildings. This also highlights the importance of considering response failures of conventional generators when assessing the risk of alternative reserve schedules.

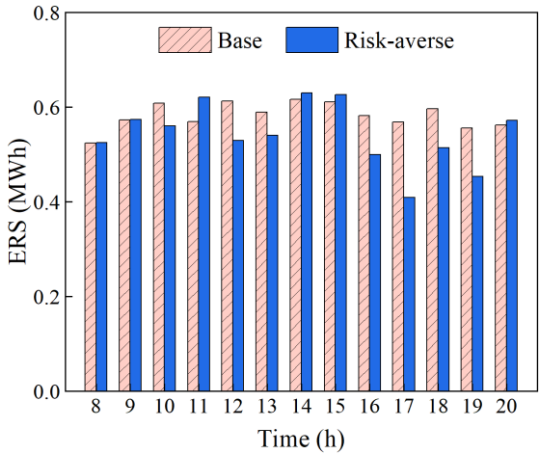

Figure 6.7 Hourly ERS in the base case and risk-averse case

The hourly ERS in the risk-averse case is slightly higher at 11:00, 14:00, and 15:00, because ERS is influenced by both buildings and conventional generators, while fewer conventional generators are committed at these time intervals in the risk-averse case. Despite this, a 2.70% reduction in the total accumulated ERS is achieved on the test day using the proposed risk-averse reserve scheduling framework.

6.5.3 Comparison with using deterministic reserve scheduling

Figure 6.8 shows the reserve committed by buildings in the deterministic case and risk-averse case, respectively. Both cases consider adopting building energy flexibility to provide spinning reserve. In the risk-averse case, buildings provide spinning reserve together with conventional generators at 10:00, 12:00-13:00, and 16:00-20:00. No spinning reserve is committed by buildings at other time intervals, while online conventional generators can fulfill the power system reserve requirement solely due to their required electricity power supply.

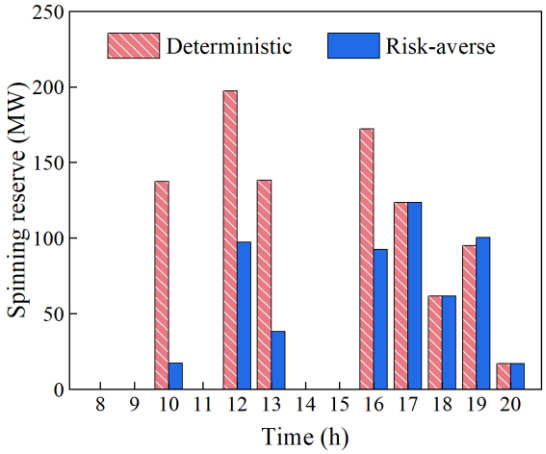

Figure 6.8 Reserve committed by buildings in the risk-averse and deterministic cases

It can be seen in Figure 6.8 that a lower amount of spinning reserve is committed by buildings in the risk-averse case. This is because a high confidence threshold (95%) is imposed for building reserve commitment, resulting in a smaller portion of building energy flexibility being qualified for spinning reserve. In contrast, the confidence level

of the reserve committed by buildings is significantly overestimated in the deterministic case. For instance, 197 MW of spinning reserve is committed by buildings at 12:00, which has a confidence level of 16.8%.

As shown in Figure 6.9, significant hourly ERS occurs at 10:00, 12:00, and 18:00 in the deterministic case. In contrast, the hourly ERS is controlled at a relatively low level (below 0.6 MW) in the risk-averse case, where the impact of uncertainties on building energy flexibility is considered. The total accumulated ERS is reduced by 59.9% on the test day due to the high confidence level of building reserve commitment, which effectively maintains power system reliability.

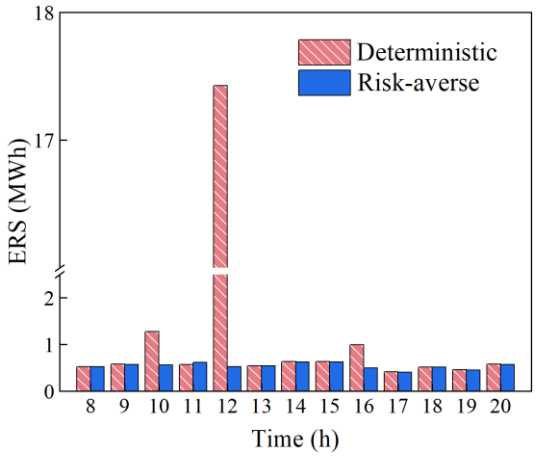

Figure 6.9 Hourly ERS in the risk-averse and deterministic cases

In the risk-averse case, more conventional generators are committed for spinning reserve at 10:00, 12:00, and 18:00, as shown in Fig. 6.6. This ensures that adequate spinning reserve is available even when a subset of buildings fails to provide their committed reserve capacity due to uncertainties. The conventional generators remain online from 13:00 to 15:00 to avoid high generator startup/shutdown costs, which leads to a lower amount of building reserve commitment at 13:00, as shown in Fig. 6.8.

Table 6.1 shows the power system operation cost and risk in different cases. By adopting building flexibility as spinning reserve using the proposed risk-averse framework, a 0.28% reduction in power system operation cost is achieved compared to the base case, which uses conventional generators solely. It also achieves the lowest operational risk among these cases.

Table 6.1 Power system operation cost and risk in different cases

Case	Operation cost (€)	Total ERS (MWh)	Reserve committed by buildings (MW)	Cost saving (%)
Base	3547,755	13.95	0	/
Deterministic	3531,434	31.56	942.1	0.46%
Risk-averse	3537,924	13.45	547.5	0.28%

6.5.4 Effectiveness in balancing power system cost and risk

In practical applications, power grid operators may wish to adjust the operation cost by slightly compromising power system reliability, given that spinning reserve is activated infrequently. In this section, the impact of varying confidence threshold settings is analyzed.

As shown in Figure 6.10, the power system operation cost increases when the confidence threshold increases. This is because that a lower portion of building energy flexibility is qualified for spinning reserve, leading to a decrease in the reserve commitment from buildings. As shown in Figure 6.11, more conventional generators are committed to meet the power system spinning reserve requirement, resulting in a higher operation cost. On the other hand, increasing the confidence threshold results in a more reliable reserve provision from buildings, which lowers the ERS due to uncertain demand response from buildings. In summary, a proper trade-off between the operation cost and risk can be achieved by adjusting the confidence threshold

settings. Grid operators can select a proper alternative schedule based on their specific preferences for operation cost saving and risk management.

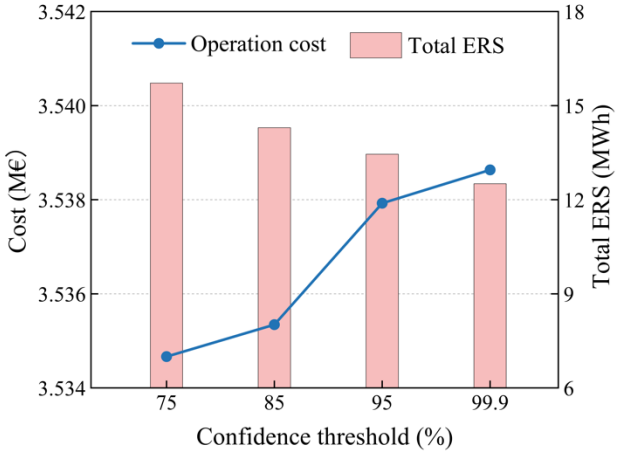

Figure 6.10 Power system operation cost and risk under different confidence thresholds

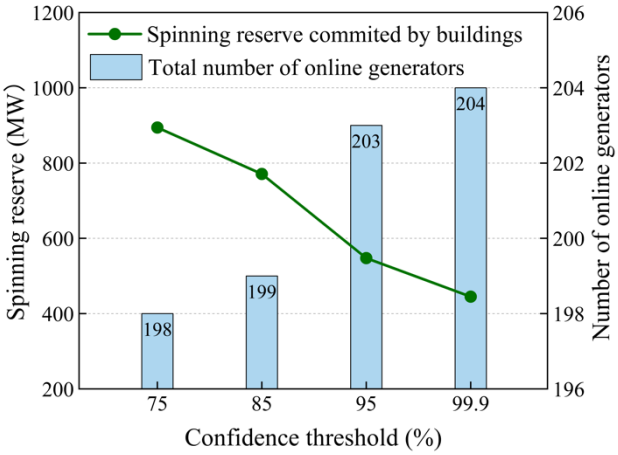

Figure 6.11 Reserve committed by buildings and the total number of online generators

6.6 Advantages of proposed framework

The proposed risk-averse reserve scheduling framework has several significant advantages and enhancements compared to existing reserve scheduling strategies presented in the literature.

- Applicability. The proposed framework directly incorporates the uncertainty in

building energy flexibility into existing deterministic reserve scheduling model, avoiding the need for complex stochastic optimization (Wang et al. 2017). This makes it highly suitable for implementation in real-world engineering practices.

- Interpretability. The framework provides quantified risk assessment of alternative reserve schedules, facilitating optimized decision-making for power grid operators. Compared to the uncertainty sets used by (Poorvaezi Roukerd, Abdollahi, and Rashidinejad 2020), the confidence threshold for building reserve commitment is easily understandable and acceptable for building users and load aggregators, which enhances market transparency.
- Accuracy. Unlike existing studies that only consider the uncertainties in buildings, the proposed framework also accounts for the uncertain response of conventional generators, enabling a comprehensive and precise assessment of the impact of engaging building energy flexibility.
- Generality. The decision-making process of the proposed framework is generic and adaptable to various application scenarios involving the uncertainty in demand response. For instance, to leverage updated intra-day forecasting information, the framework can be easily extended to an intra-day rescheduling scheme by adjusting the scheduling horizon to the upcoming few hours.

When implementing the proposed reserve scheduling in practice, the first step is to obtain a set of deterministic building flexibility capacities corresponding to different confidence thresholds for building energy flexibility. Power grid operators can then incorporate these deterministic building flexibility capacities in existing deterministic reserve scheduling model used in industry, and run the model to obtain alternative reserve schedules. Finally, power grid operators can assess the risk of these alternative schedules and select the best schedule based on their specific preference.

6.7 Summary

This chapter presents a risk-averse day-ahead reserve scheduling framework for power systems engaging building energy flexibility. It also presents a novel risk indicator and risk assessment method for power systems using building flexibility. Validation tests are conducted on a power system modified from the Hong Kong power system. Based on the test results, the main conclusions are drawn as follows.

- By using a larger number of less reliable reserve providers (buildings), the risk from solely relying on a few conventional generators can be mitigated. Compared to using conventional generators solely, both power system operation cost and risk can be reduced by procuring spinning reserve from buildings, when setting proper confidence thresholds for building reserve commitment. With a 95% confidence threshold, the operation cost and risk are reduced by 0.28% and 2.70%, respectively.
- Using the proposed risk-averse reserve scheduling framework, the uncertainties in buildings are accommodated effectively. The power system operation risk is reduced by 57.4% compared to that of using deterministic reserve scheduling.
- A proper trade-off between power system operation cost and risk can be achieved by using the proposed risk-averse framework. Increasing the confidence threshold leads to a higher operation cost but a lower operation risk. Grid operators can select a proper schedule according to their specific preferences for risk management.

CHAPTER 7 OPTIMAL RESERVE SCHEDULING OF POWER SYSTEMS ENGAGING BUILDING FLEXIBILITY CONSIDERING LOAD REBOUND

This chapter presents an optimal day-ahead reserve scheduling strategy for power systems engaging building energy flexibility. The proposed strategy considers the load rebound effect after demand response, which has been widely overlooked in the literature. It considers the uncertainties in both renewable forecasts and generator failures, enabling more effective utilization of building energy flexibility. A two-stage robust optimization problem is formulated for optimal reserve scheduling.

Section 7.1 presents the outline of the proposed strategy. Section 7.2 presents the mathematical formulation of the robust optimization problem, including the optimization objective and constraints. Section 7.3 presents the validation test arrangement. Section 7.4 presents the test results to evaluate the performance of the proposed strategy. Section 7.5 gives a summary of this chapter.

7.1 Outline of the proposed strategy

The proposed optimal day-ahead reserve scheduling strategy is formulated as a two-stage robust optimization problem, as illustrated in Figure 7.1. The inputs include the day-ahead forecasts of power system electricity demand, renewable generation, and the maximum flexibility capacity of buildings for providing spinning reserve. The first stage represents the day-ahead unit commitment, where the on-off status of conventional generators and the reserve capacity committed by buildings over the next 24 hours are determined. The decisions made in this stage cannot be changed and serve

as optimization constraints for the second stage. The second stage represents the real-time dispatch stage, which optimizes the spinning reserve that is activated in uncertain real-time scenarios of renewable generation for power balancing.

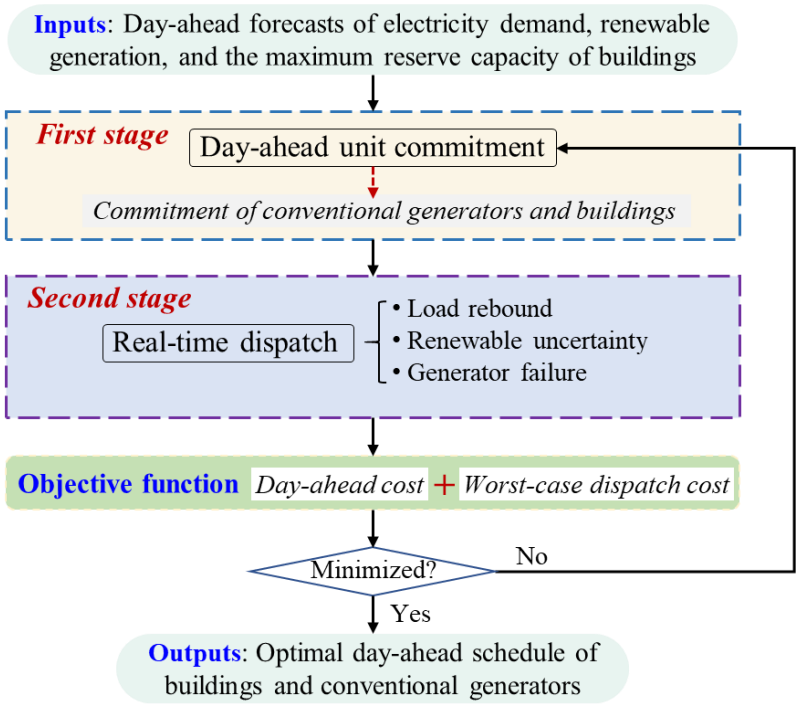

Figure 7.1 Outline of proposed reserve scheduling strategy

To comprehensively consider the impact of building energy flexibility, the aggregated load rebound of buildings is incorporated into the real-time dispatch stage through power balance constraints. The load rebound is modeled as a function of the previous load reduction (i.e., the building energy flexibility that is activated in the previous time interval). Specifically, the coupling between the aggregated load rebound and load reduction is explicitly quantified based on building thermal dynamics, which is more realistic compared to the hypothetical values used in most previous studies (Paterakis et al. 2018).

The robust optimization aims to minimize the total operation cost of the power system while ensuring the system power balance and operational security in the presence of

load rebound, uncertain renewable generation and unexpected generator failures. The optimization process iterates until it converges to the minimum total operation cost under the worst-case uncertainty scenario. The optimal day-ahead schedule of buildings and conventional generators will be output by the proposed strategy.

7.2 Optimization objective

The optimization objective is shown in Eq. (7.1). It is determined by the day-ahead commitment cost (C^{DA}) and the real-time dispatch cost (C^{RT}) under the worst-case realization of uncertainties (Bertsimas et al. 2013). Where x and y represent the variables to be optimized in the day-ahead and real-time stages, respectively. u represents the uncertainty parameters, e.g., the deviation of actual renewable generation from the day-ahead forecasted value. The max-min calculation is to determine the minimum real-time dispatch cost in the worst-case uncertainty scenario.

$$\min\{\, C^{\mathrm{DA}}(x) + \max_{u \in U} \min C^{\mathrm{RT}}(x, u, y)\} \tag{7.1}$$

The day-ahead commitment cost (C^{DA}) and real-time dispatch cost (C^{RT}) are calculated using Eq. (7.2) and (7.3), respectively, according to the day-ahead commitment and real-time dispatch decisions of conventional generators and buildings.

$$C^{\mathrm{DA}} = C^{\mathrm{gen,com}} + \sum_{j} SR_j^{\mathrm{bui,com}} rc^{\mathrm{bui}} \tag{7.2}$$

$$C^{\mathrm{RT}} = C^{\mathrm{gen,RT}} + \sum_{j} SR_j^{\mathrm{bui,act}} ra^{\mathrm{bui}} \tag{7.3}$$

Where j represents the time interval. $C^{\mathrm{gen,com}}$ and $C^{\mathrm{gen,RT}}$ are the day-ahead commitment and real-time dispatch cost of conventional generators. $SR^{\mathrm{bui,com}}$ is the reserve capacity committed by buildings in the day-ahead stage. $SR^{\mathrm{bui,act}}$ is the reserve activation of

buildings in the real-time stage. rc^{bui} and ra^{bui} are the unit price of committing and activating building energy flexibility, respectively.

A typical clustered unit commitment model is applied to simulate the operation of conventional generators, which has been elaborated in Chapter 4. The day-ahead commitment cost of conventional generators is determined using Eq. (7.4). Where i represents the generator cluster type. SC, MC and VC are the startup cost, operating cost at minimum power output, and output-dependent operating cost of generators. N^{start} and N^{on} are the number of generators being started and online, respectively. P^{gen} is the power output of generators.

$$C^{\text{gen,com}} = \sum_{i}\sum_{j}(SC_i N_{i,j}^{\text{start}} + MC_i N_{i,j}^{\text{on}} + VC_i P_{i,j}^{\text{gen}}) \tag{7.4}$$

The real-time dispatch cost of conventional generators ($C^{\text{gen,RT}}$) is determined using Eq. (7.5), based on the measures taken to restore power balance. Where ΔP^{gen} is the extra power output of online conventional generators for power balancing. P^{em} is the high-cost emergency actions, such as dispatching fast-start peaking generators or reducing interruptible loads, which are activated to ensure spinning reserve adequacy (Lavin et al. 2020) (Bertsimas et al. 2013). ra^{em} is the unit cost of using emergency actions to restore power balance.

$$C^{\text{gen,RT}} = \sum_{i}\sum_{j}(\Delta P_{i,j}^{\text{gen}} VC_i + P_j^{\text{em}} ra^{\text{em}}) \tag{7.5}$$

7.3 Optimization constraints

A key challenge in formulating the optimization problem is the simultaneous presence of load rebound, renewable forecast uncertainties and unexpected generator failures.

In this study, uncertainties in renewable forecast and generator failures are considered separately in the real-time stage, because they are statistically uncorrelated (Xiong and Jirutitijaroen 2013). An adjustable uncertainty set is used to consider renewable forecast uncertainties, while the reserve for generator failures is enforced as security constraints under each renewable scenario. The separate formulation is also adopted in (Roos and Bolkesjø 2018) (Liu and Conejo 2024).

The real-time dispatch after generator failures is not modeled to avoid an overly conservative reserve schedule. In practice, generator failure is a low-probability (below 0.4%) contingency event. Therefore, the primary concern is the pre-contingency adequacy of reserve capacity for generator failures rather than the cost minimization of post-contingency operation (Chen et al. 2017). The power imbalance can be managed using fast-start generators once a generator failure occurs. More details can be found in (Trovato 2023).

7.3.1 Constraints for renewable forecast uncertainties

Adjustable uncertainty set

To control the conservativeness level of the optimized reserve schedule (the solution of the robust optimization problem), a widely used adjustable uncertainty set U is adopted to constrain renewable forecast uncertainties (forecast deviations) (Bertsimas et al. 2013), as shown in Eq. (7.6).

$$U = \begin{cases} u_j \in \left(-u_{max,j}, u_{max,j}\right) \\ \dfrac{1}{24}\displaystyle\sum_j u_j / \, u_{max,j} <= \sigma \end{cases} \tag{7.6}$$

Where $u_{max,j}$ represents the maximum deviation at each time step, which is usually chosen as a certain percentage of the day-ahead forecasts of renewable generation

(Roos and Bolkesjø 2018) (Chyong and Newbery 2022).

An uncertainty budget, σ, is used to bound the total deviations of actual renewable generation from the forecasted value. A value of σ=0 indicates no uncertainty in renewable forecast. A larger value of σ corresponds to more renewable deviations and leads to a more conservative solution. A value of σ=1 indicates that the renewable deviation at each time interval reaches their respective maximum deviation. Power grid operators can choose a proper value of σ based on their specific risk preference and operational requirement.

7.3.2 Constraints for load rebound

Coupling between load rebound and previous load reduction

After reserve activation (load reduction) of buildings, the indoor air temperature is higher than the baseline setting. To restore the indoor air temperature, the HVAC system needs to provide additional cooling to indoor space compared to that in the baseline scenario with normal cooling supply. The HVAC operating power will exceed the baseline level until the indoor air temperature resumes to the baseline setting, which is referred to as load rebound.

Chapter 3 presents the analytical solutions for energy flexibility modelling of building HVAC systems, where the aggregated load reduction and load rebound of buildings are quantified using two analytical equations.

The coupling between the aggregated load reduction ($P^{\text{bui,act}}$) and load rebound (P^{reb}) of buildings can be explicitly represented by Eq. (7.7).

$$P_{j+1}^{\text{reb}} = \frac{\sum_k \beta_k \left(\Delta t_{\text{s}}, \Delta t_{\text{r}}\right) \Delta T_k^{\text{in,max}}}{\sum_k \alpha_k \left(\Delta t_{\text{s}}\right) \Delta T_k^{\text{in,max}}} P_j^{\text{bui,act}} \tag{7.7}$$

where, k represents the index of buildings. $\Delta T^{\text{in,max}}$ is the maximum allowable indoor air temperature offset of a building. Δt_{s} and Δt_{s} are the durations of load reduction and load rebound periods, respectively.

$$\alpha(\Delta t_{\text{s}}) = \frac{(r_1 - r_2) C^{\text{in}} \Delta T^{\text{in}}}{[e^{r_1 \Delta t} - e^{r_2 \Delta t} + C^{\text{in}} R^{\text{out}} (r_1 - r_2 + r_2 e^{r_1 \Delta t} - r_1 e^{r_2 \Delta t})] \cdot COP}$$

$$\beta(\Delta t_{\text{s}}, \Delta t_{\text{r}}) = \frac{[C^{\text{in}} \alpha(\Delta t_{\text{s}}) \cdot p(\Delta t_{\text{s}}) \cdot c \cdot COP / a - h]\left(e^{r_1 \Delta t_{\text{r}}} - e^{r_2 \Delta t_{\text{r}}}\right) + C^{\text{in}} q(\Delta t_{\text{r}})}{\left[e^{r_1 \Delta t_{\text{r}}} - e^{r_2 \Delta t_{\text{r}}} + C^{\text{in}} R^{\text{out}} (r_1 - r_2 - q(\Delta t_{\text{r}}))\right] \cdot COP}$$

$$p(\Delta t_{\text{s}}) = \frac{\left(1 - e^{r_1 \Delta t_{\text{s}}}\right)\left(\frac{1}{C^{\text{in}}} + r_2 R^{\text{out}}\right)}{(r_1 - r_2) r_1} + \frac{\left(1 - e^{r_2 \Delta t_{\text{s}}}\right)\left(\frac{1}{C^{\text{in}}} + r_1 R^{\text{out}}\right)}{(r_2 - r_1) r_2}$$

$$q(\Delta t_{\text{r}}) = r_1 e^{r_2 \Delta t_{\text{r}}} - r_2 e^{r_1 \Delta t_{\text{r}}},\ h = \frac{C^{\text{in}}}{C^{\text{m}} R^{\text{m}}} - \frac{1}{R^{\text{out}}} - \frac{1}{R^{\text{m}}}$$

Power balance constraint considering load rebound

The power balance constraint of the power system in real-time dispatch stage is shown in Eq. (7.8). Both renewable forecast deviation and load rebound are considered as sources of power imbalance. This ensures the power balance even in the presence of load rebound of buildings.

$$P_j^{\text{RE,dev}} + P_j^{\text{reb}} = \Delta P_j^{\text{gen}} + SR_j^{\text{bui,act}} + P_j^{\text{em}} \tag{7.8}$$

where, $P^{\text{RE,dev}}$ is the renewable deviation from the forecasted value. P^{reb} is the load rebound of buildings. ΔP^{gen} is the extra power output of online conventional generators for power balancing. P^{em} is the high-cost emergency actions in power systems.

7.3.3 Constraints for generator failures

Security constraints are enforced in each renewable generation scenario to ensure that the power system has sufficient reserve capacity to handle unexpected generator failures after managing the renewable forecast deviation and load rebound (Liu and Conejo 2024). The constraints are shown in Eqs. (7.9)-(7.11). Eq. (7.9) indicates that

the spinning reserve committed for generator failures must be equal to or greater than the required amount. Eqs. (7.10) and (7.11) indicate that the total spinning reserve provision of buildings and conventional generators must not exceed their technical flexibility capacity for providing reserve, respectively.

$$SR_{j,s}^{\text{bui, GF}} + SR_{j,s}^{\text{gen, GF}} \geq SR_{j}^{\text{req,GF}} \tag{7.9}$$

$$SR_{j,s}^{\text{bui, GF}} + SR_{j,s}^{\text{act, bui}} \leq SR_{j}^{\text{com, bui}} \tag{7.10}$$

$$SR_{j,s}^{\text{gen, GF}} + \Delta P_{j,s}^{\text{gen}} \leq SR_{j}^{\text{gen}} \tag{7.11}$$

where, $SR^{\text{bui,GF}}$ and $SR^{\text{gen,GF}}$ are the spinning reserve committed by buildings and online generators for generator failures respectively. $SR^{\text{req,GF}}$ is the reserve requirement for generator failures. $SR^{\text{gen}}{}_{j}$ is the allowable maximum increase in power output of online generators.

7.3.4 Constraints for generator dispatch

The operational constraints of conventional generators are described by Eqs. (7.12)-(7.19). The number of online generators (N^{on}) is constrained by Eq. (7.12). The constraints for generator startup and shutdown actions are shown in Eq. (7.13). The maximum and minimum power output constraints for each cluster are given by Eq. (7.14). The minimum up and down time constraints for each generator cluster are shown in Eqs. (7.15) and (7.16), respectively. The technical capacity of each cluster for providing spinning reserve is constrained by Eq. (7.17). The ramping up and down capacity of each cluster between two consecutive time intervals is constrained by Eqs. (7.18) and (7.19), respectively. More details can be found in Chapter 4.

$$N_{i,j}^{\text{on}} \leq N_{i}^{\text{install}} \tag{7.12}$$

$$N_{i,j}^{\text{on}} = N_{i,j-1}^{\text{on}} + N_{i,j}^{\text{start}} - N_{i,j}^{\text{shut}} \tag{7.13}$$

$$N_{i,j}^{\text{on}} P_i^{\min} \leq P_{i,j} \leq N_{i,j}^{\text{on}} P_i^{\max} \tag{7.14}$$

$$N_{i,j}^{\text{on}} \geq \sum_{j=j+1-MUT_i}^{j} N_{i,j}^{\text{start}} \tag{7.15}$$

$$N_i^{\text{install}} - N_{i,j}^{\text{on}} \geq \sum_{t=j+1-MDT_i}^{j} N_{i,j}^{\text{shut}} \tag{7.16}$$

$$SR_{i,j}^{\text{gen}} \leq min\left(N_{i,j}^{\text{on}} P_i^{\max} - P_{i,j}, N_{i,j}^{\text{on}} RU_i^{10\text{min}}\right) \tag{7.17}$$

$$P_{i,j+1}^{\text{gen}} - P_{i,j}^{\text{gen}} \leq N_{i,j}^{\text{on}} RU_i + N_{i,j+1}^{\text{start}} P_i^{\min} - N_{i,j}^{\text{shut}} P_i^{\min} \tag{7.18}$$

$$P_{i,j}^{\text{gen}} - P_{i,j+1}^{\text{gen}} \leq (N_{i,j}^{\text{on}} - N_{i,j}^{\text{start}} + N_{i,j}^{\text{shut}}) RD_i - N_{i,j}^{\text{start}} P_i^{\min} \tag{7.19}$$

7.4 Validation test arrangement

7.4.1 Description of the power system

The proposed strategy is tested on a power system modified from the existing Hong Kong power system. The supply side contains twenty combined cycles gas turbines (CCGT), eight open cycle gas turbines (OCGT), 1577 MW of nuclear power, and 4000 MW of wind power. For simplicity, it is assumed that all CCGTs have a rated capacity of 350 MW. Two sources of uncertainties are considered, including renewable forecast uncertainties and unexpected generator failures. It is assumed that the electricity demand of the power system and the energy flexibility capacity of buildings can be forecasted accurately.

A typical uncertainty set is used to describe renewable forecast uncertainties. The maximum deviation of actual renewable generation from the forecasted value is chosen as 10% of the forecasted value. For infrequent generator failures, the typical N-1 criterion of 350 MW is adopted as a security constraint, which ensures that the reserve committed for generator failures is sufficient. The cost of dispatching emergency actions is chosen as 2000 €/MWh (Bertsimas et al. 2013). The day-ahead

forecasts of electricity demand and wind power on the test day are shown in Figure 7.2.

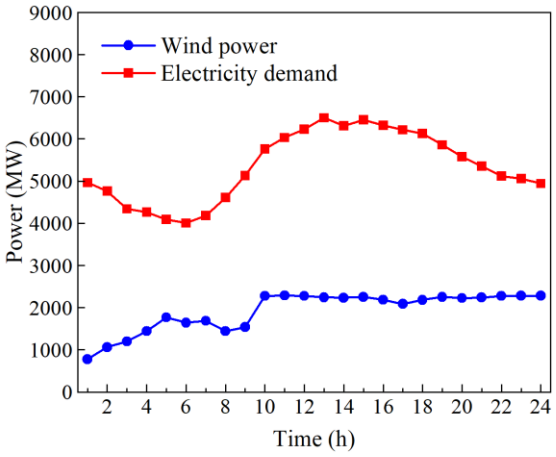

Figure 7.2 Day-ahead forecasts of electricity demand and wind power

7.4.2 Description of reference buildings

On the demand side, 500 high-rise commercial buildings are engaged in spinning reserve provision. The building cluster is generated based on a prototype commercial building in Hong Kong, as detailed in Section 5.2.1.The baseline setting of indoor air temperature in each building is chosen as 24 ℃. When the reserve is activated, the indoor air temperature can be increased by up to 2 K from the baseline setting. The aggregated power demand and reserve capacity of these buildings are about 1600 MW and 500 MW, respectively. The unit cost of reserve commitment and activation of buildings are chosen as 3 €/MWh and 80 €/MWh respectively. The time duration of reserve provision is chosen as 1 hour based on the technical requirement of spinning reserve. The time duration of load rebound is also chosen as 1 hour. The above settings are in line with the typical settings in the literature (Paterakis et al. 2018) (Karangelos and Bouffard 2012). In practice, the duration of load rebound should be predefined by both power grid operators and building owners to avoid either a high load rebound for power grid or a slow temperature restoration for buildings. Note, load rebound

duration is chosen as a consensus setting for all buildings in this study to ensure fairness in thermal comfort sacrifice due to reserve provision.

7.4.3 Outline of the tested strategies

Three day-ahead reserve scheduling strategies are tested to validate the performance of the proposed optimal reserve scheduling strategy, as listed below.

- *Strategy 1*: Only conventional generators are used for spinning reserve. The energy flexibility of buildings is not utilized.
- *Strategy 2*: Both conventional generators and buildings are used for spinning reserve. The load rebound effect is overlooked in reserve scheduling.
- *Proposed strategy*: Both conventional generators and buildings are used for spinning reserve. The load rebound effect is considered in reserve scheduling.

All reserve scheduling strategies are programmed using Matlab on a computer with an eight-core Intel Core i7 CPU. The reserve scheduling horizon is 24 hours for the next day and the time interval is 1 hour. The two-stage robust optimization problem is decomposed into a master problem and a subproblem, which are solved using the column and constraint generation algorithm.

7.5 Performance evaluation of proposed strategy

In this section, the performance of the proposed optimal reserve scheduling strategy is evaluated by conducting a comparison with two existing strategies. The budget of the renewable uncertainty set is chosen as 1 to align with the typical reserve requirement of power systems without incorporating building energy flexibility (Roos and

Bolkesjø 2018). The impact of varying the uncertainty budget on the performance of the proposed strategy is analyzed in Section 7.5.3.

7.5.1 Reserve schedule given by the proposed strategy

Figure 7.3 shows the spinning reserve committed by buildings and conventional generators using the proposed strategy. As shown in Figure 7.3 (a), most spinning reserve for generator failures is allocated to buildings during office hours (8:00 to 20:00) when their energy flexibility is available. This type of spinning reserve has a very low probability of actual activation and typically requires the reserve providers to be on a standby state. Buildings are suitable for this type of reserve due to their much lower standby cost than that of conventional generators. On the other hand, conventional generators inherently have a certain amount of reserve capacity due to their power supply requirements at specific time intervals. It can be seen that no spinning reserve is committed by buildings at 20:00 when online generators solely can fulfill the system reserve requirement. Therefore, it is important to coordinate the scheduling of buildings and conventional generators for providing spinning reserve.

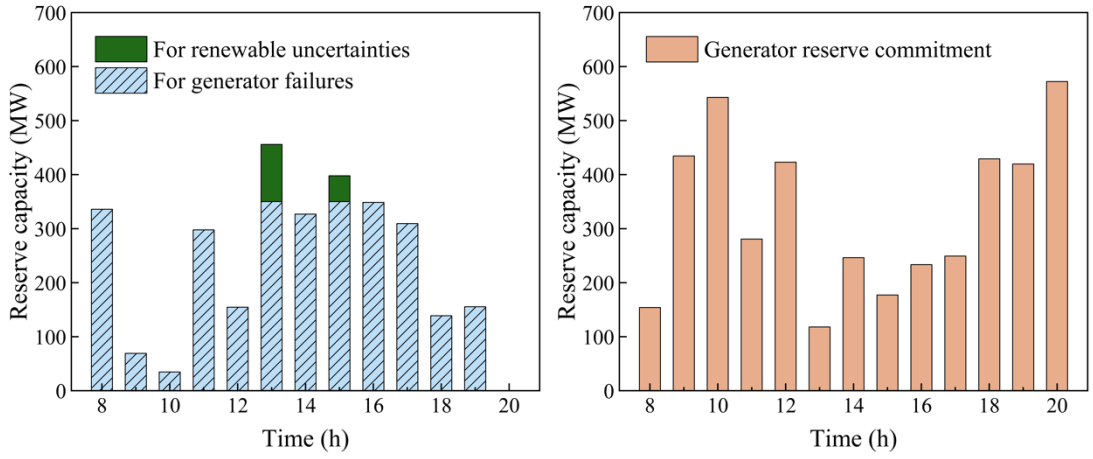

(a) Buildings (b) Conventional generators

Figure 7.3 Reserve schedule given by the proposed strategy

Buildings are providing spinning reserve for renewable forecast uncertainties at specific time intervals, i.e., 13:00 and 15:00, although they have a large reserve capacity available at other time intervals. It is more cost-effective to commit conventional generators rather than buildings to provide this type of spinning reserve, which has a relatively high probability of activation. Notably, buildings mainly provide spinning reserve for generator failures rather than for renewable uncertainties. These findings have two significant implications. Firstly, it is essential to consider the reserve for generator failures when leveraging the flexibility of HVAC systems in buildings, which is often overlooked in the literature. Secondly, the cost of utilizing building flexibility should be considered in reserve scheduling to avoid the uneconomic dispatch of building energy flexibility.

7.5.2 Comparison with existing strategies

Figure 7.4 shows the optimal schedules of buildings and conventional generators obtained from different strategies. Compared to the strategy 1 using conventional generators solely, the proposed strategy utilizes building energy flexibility as an alternative spinning reserve resource, resulting in fewer conventional generators being committed online. The part-load efficiency losses and the startup costs of conventional generators are therefore reduced. Table 7.1 presents the total power system cost under different strategies. The proposed strategy achieves the lowest total power system operation cost among these strategies, with a cost saving of 2.29% compared to the strategy 1.

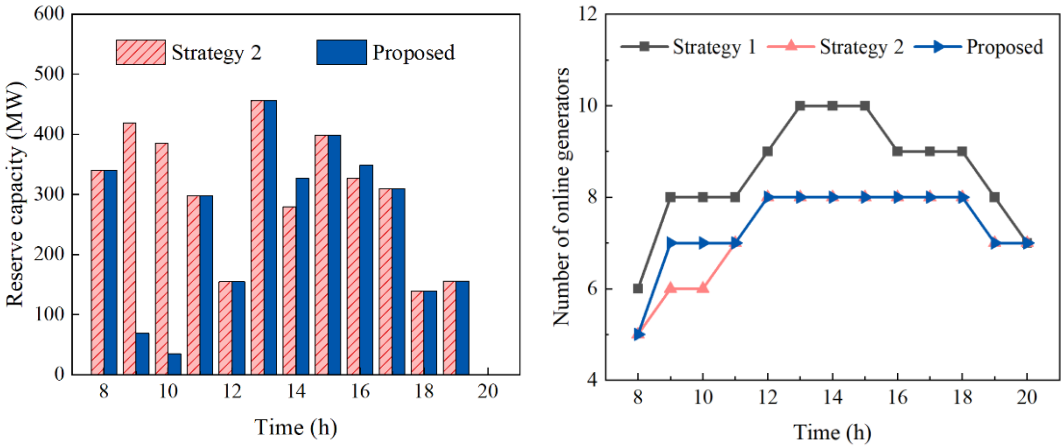

(a) Buildings (b) Conventional generators

Figure 7.4 Reserve schedules given by different strategies

Table 7.1 Power system cost under different strategies

Strategy	Total cost (€)	Day-ahead cost (€)	Real-time cost (€)	Emergency actions (MWh)	Cost variation
Strategy 1	2856,626	599,200	2257,426	0	/
Strategy 2	3019,033	536,298	2482,735	101	+5. 69%
Proposed	2791,250	538,745	2252,505	0	-2.29%

The Strategy 2, which overlooks the load rebound in reserve scheduling, leads to a 5.69% higher operation cost compared to the baseline strategy. Using the conventional strategy, buildings are committed to providing spinning reserve for renewable forecast uncertainties at 9:00, 10:00, 13:00, and 15:00. Load rebound events occur in subsequent time steps, as shown in Figure 7.5. To maintain an adequate reserve capacity for generator failures, expensive emergency actions such as dispatching fast-start generators are required, resulting in a higher real-time operation cost. On the test day, the strategy 2 leads to total accumulated emergency actions of 116 MWh. This finding highlights the importance of considering load rebound effect in reserve scheduling.

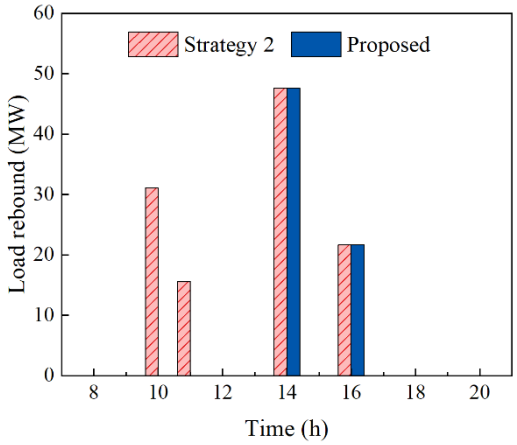

Figure 7.5 Load rebound events using different strategies

Using the proposed strategy, more conventional generators but fewer building energy flexibilities are committed to providing spinning reserve at 9:00 and 10:00, compared to the strategy 2, as seen from Figure 7.6. This is because the cost of extra power output of conventional generators for managing the load rebound outweighs the cost savings obtained from committing buildings for spinning reserve. By reducing building reserve commitment, the load rebound events at 10:00 and 11:00 are avoided, as shown in Figure 7.5.

On the other hand, more building energy flexibilities are committed at 14:00 and 16:00 to balance the load rebound resulting from the load reduction at 13:00 and 15:00. This avoids the high startup cost of committing additional conventional generators to provide spinning reserve for managing load rebound. Consequently, the proposed strategy achieves a significantly lower real-time dispatch cost by proactively managing the load rebound, while it leads to a slightly higher day-ahead commitment cost due to its more robust day-ahead reserve schedule. On the test day, the proposed strategy reduces the total operation cost of the power system by 7.54% compared to the strategy 2 without considering load rebound.

7.5.3 Adjusting the robustness level of the optimal schedule

The conservativeness level of the optimal schedule given by the proposed strategy can be controlled by adjusting the setting of the uncertainty budget. Fig. 7.6 shows the total reserve capacity and worst-case operation cost of the power system under different uncertainty budgets. As the uncertainty budget increases, more renewable deviations from the forecasted values are considered in the day-ahead reserve scheduling. Therefore, a larger reserve capacity is scheduled to cover renewable forecast uncertainties, which corresponds to a more robust reserve schedule. However, increasing the system reserve capacity also leads to a higher power system operation cost, because more conventional generators and/or building energy flexibility are committed. By adjusting the uncertainty budgets, power grid operators can achieve a proper trade-off between economy and robustness based on their preference.

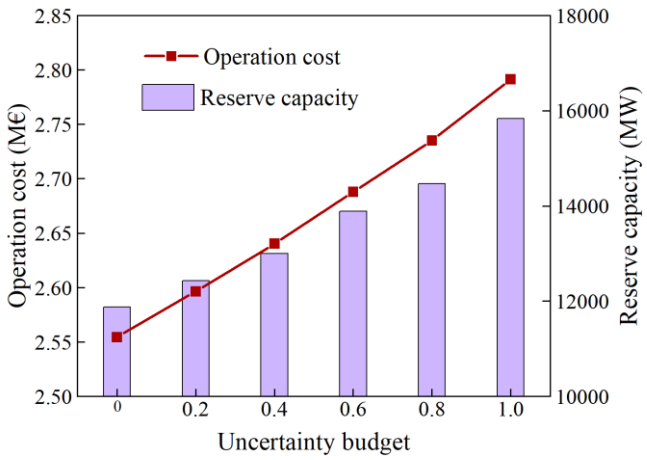

Figure 7.6 Power system operation cost and reserve capacity under different uncertainty budgets

Fig. 7.7 shows the reserve commitment of buildings and conventional generators under different uncertainty budgets. When the uncertainty budget is low (e.g., 0 and 0.2), buildings only provide spinning reserve for unexpected generator failures, since conventional generators can solely manage renewable forecast uncertainties. However,

as the uncertainty budget increases, it is cost-effective to utilize buildings to manage renewable forecast uncertainties, which can avoid the high cost of committing additional conventional generators. It can also be seen in Figure 7.7 that the total numbers of online conventional generators are the same under certain uncertainty budgets (e.g., 0.6 and 0.8). This can be attributed to the fact that each conventional generator has a large rated capacity, while the amount of reserve committed by buildings can be flexibly adjusted as needed, which provides a cost-effective complementation to conventional generators.

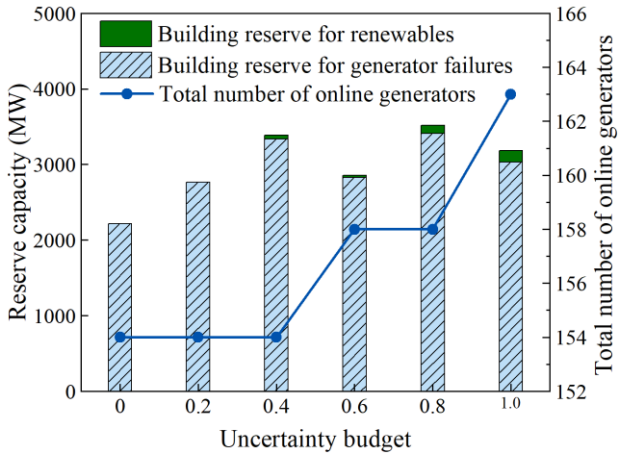

Figure 7.7 Reserve commitment under different uncertainty budgets

7.6 Summary

This chapter presents an optimal day-ahead reserve scheduling strategy for power systems engaging building energy flexibility. The strategy considers the uncertainties in both renewable forecasts and generator failures, as well as the effect of load rebound after the demand response of buildings. A simple and effective representation of the coupling between aggregated load rebound and load reduction of buildings is developed, which enables the convenient incorporation of building flexibility into reserve scheduling. The effectiveness and advantages of the proposed strategy are

validated on the Hong Kong power system. Based on the test results, the main conclusions are drawn as follows.

- The proposed optimal robust strategy achieves a 2.29% power system operation cost saving by incorporating the energy flexibility of buildings as spinning reserve, compared to using conventional generators solely.
- The strategy without considering load rebound effect leads to a 116 MWh reserve shortage in real-time operation. The proposed strategy can effectively avoid the reserve shortage and achieve a reduced operation cost of 7.54% by managing load rebound proactively.
- Using the proposed strategy, grid operators can achieve a proper trade-off between the economy and robustness of the power system. A larger uncertainty budget results in a more robust reserve schedule but a higher power system operation cost.

CHAPTER 8 CONCLUSIONS AND FUTURE WORK

This chapter presents the conclusions and future work of this thesis. Section 8.1 presents a summary of the main contributions of this PhD study. Section 8.2 presents the main conclusions based on the study presented in this thesis. The recommendations for future work are presented in Section 8.3.

8.1 Main contributions of this study

This PhD study conducted a comprehensive and systematic study on using building energy flexibility as spinning reserve in the context of smart grids, including: (1) modeling and quantification of building energy flexibility; (2) impact assessment of using building energy flexibility for providing spinning reserve; (3) optimized reserve scheduling of power systems engaging building energy flexibility. The main contributions of this PhD study are summarized as follows:

1. Analytical solutions for energy flexibility modelling and quantification of building air-conditioning systems are developed, considering the load reduction and subsequent load rebound of buildings at both individual and aggregated levels. The analytical solutions eliminate the need for time-consuming finite difference and iterative computations, facilitating the integration of building energy flexibility quantification in power grid scheduling and real-time dispatch.
2. A comprehensive impact assessment of using building energy flexibility as spinning reserve is conducted. The assessment covers the operation of both power grids and buildings, using the Hong Kong power system in 2035 as a reference case. An integrated grid-buildings model is developed for impact assessment. A

systematic and quantitative comparison of using building energy flexibility for providing spinning reserve and load shifting is conducted.

3. A probabilistic model is developed for real-time quantification of building energy flexibility. The model comprehensively considers major uncertainties involved in flexibility quantification, including uncertainties in model inputs, model bias, and building response failures, while capturing the diversity of individual buildings. The model is highly computationally efficient which facilitates the participation of building energy flexibility in grid service markets.
4. A risk-averse day-ahead reserve scheduling framework is proposed for power systems engaging building energy flexibility. The framework can provide quantified power system operation cost and risk for identifying the best reserve schedule. A new risk indicator, namely expected reserve shortage, is proposed for accurate and computationally efficient risk assessment, considering the uncertain responses of both buildings and conventional generators.
5. An optimal day-ahead reserve scheduling strategy is proposed for power systems engaging building energy flexibility. The strategy considers the load rebound effect, which maintains power system reliability. A two-stage robust optimization problem is formulated to incorporate load rebound effect in reserve scheduling, considering uncertainties in both renewable forecasts and generator failures.

8.2 Conclusions

Conclusions on analytical solutions of energy flexibility modelling of buildings

- The analytical solutions consist of five straightforward equations derived from a second-order building thermodynamic model. The first two equations quantify the load reduction and the subsequent load rebound of individual buildings,

respectively, as functions of regulation durations and indoor air temperature offset. The next two equations allocate the aggregated load reduction and rebound tasks, respectively, among buildings. The fifth equation explicitly represents the coupling between the aggregated load reduction and load rebound of buildings.

- The accuracy and correctness of analytical solutions are verified through numerical simulations under time-varying boundary conditions (e.g., outdoor temperature). The differences between the indoor air temperatures and aggregated energy flexibility of buildings computed by the analytical solutions and numerical solution methods are less than 0.0001 K and 0.01%, respectively.
- The analytical solutions can accurately quantify the energy flexibility of buildings at both individual and aggregated levels with dramatically reduced computation time. The analytical solutions only take 0.000009 seconds for quantifying the load reduction and rebound of 5000 buildings, which is 980,000 times faster than the existing numerical solution method.

Conclusions on the impact of using building energy flexibility for spinning reserve

- The commercial building sector in Hong Kong can contribute up to 520 MW of spinning reserve during cooling seasons, which meets up to 86.7% of the spinning reserve required to manage unexpected generator failures. Using building energy flexibility for spinning reserve can reduce the efficiency losses and startup costs of conventional generators and reduce renewable curtailment.
- Adopting the flexibility of commercial buildings in Hong Kong for spinning reserve can reduce the annual operating cost of the power system by 0.60%-1.55% (5.7-16.9 M€), compared to using conventional generators solely. The cost saving

increases as renewable energy penetration increases, but decreases after the adoption of utility-scale energy storage.

- The annual cost saving from using building flexibility for spinning reserve is up to 4.9 times that for load shifting, while the total accumulated amount of activated building flexibility for spinning reserve provision is only 2.4% of that for load shifting. Spinning reserve provision not only offers higher cost savings for the power system but also has much less interference with building operation compared to load shifting. Therefore, spinning reserve is proposed as a priority use of building energy flexibility in smart grids.

Conclusions on the probabilistic model of building energy flexibility

- The proposed probabilistic model can provide more robust quantification of building energy flexibility by considering the impact of uncertainties, compared to the deterministic flexibility quantification model. For a demand response duration of 1 hour, the flexibility capacity estimated by the deterministic model has a high probability of 52.5% of being overestimated.
- The proposed model outperforms the existing probabilistic models in terms of both accuracy and computational efficiency. It can accurately quantify the aggregated flexibility of 150 buildings in 6.7 seconds, which is 535 times faster than the probabilistic model solved numerically. Furthermore, it is 8 times faster than the archetype-based model while offering significantly higher accuracy.
- The aggregated flexibility of buildings has a very high success probability (e.g., 99.99%) when the committed capacity is below a certain threshold (e.g., 160 MW for a 1-hour response duration). This reliability level is even higher than that of

conventional generators (i.e., 99.9%). Therefore, buildings can provide reliable grid services by properly setting their committed flexibility capacity

- The scalability of the proposed probabilistic model is validated. The model only takes 140 seconds to quantify the aggregated flexibility of 2000 buildings, which can satisfy the real-time application requirements of grid scheduling and dispatch.

Conclusions on the risk-averse reserve scheduling framework

- By using a larger number of buildings as reserve providers, the risk from solely relying on a few conventional generators can be mitigated. Compared to using conventional generators solely, both power system operation cost and risk can be reduced when setting proper confidence thresholds for building spinning reserve commitment. With a 95% confidence threshold, the operation cost and risk are reduced by 0.28% and 2.70%, respectively.
- Using the proposed risk-averse day-ahead reserve scheduling framework, the uncertainties in buildings are accommodated effectively. The power system operation risk is reduced by 57.4% compared to that using deterministic reserve scheduling.
- A proper trade-off between power system operation cost and risk can be achieved by using the proposed risk-averse framework. Increasing confidence threshold leads to a higher operation cost but a lower operation risk. Grid operators can select a proper schedule according to their specific preference on risk management.

Conclusions on the optimal reserve scheduling strategy considering load rebound

- The proposed optimal day-ahead strategy achieves a 2.29% power system operation cost saving by incorporating the energy flexibility of buildings as

spinning reserve, compared to using conventional generators solely.

- The conventional strategy without considering load rebound effect leads to 116 MWh reserve shortage in real-time operation. The proposed strategy can effectively avoid the reserve shortage and achieve a reduced operation cost of 7.54% by managing load rebound proactively.
- Using the proposed strategy, grid operators can achieve a proper trade-off between the economy and robustness of the power system. A larger uncertainty budget of renewable forecasts results in a more robust reserve schedule with increased reserve capacity but a higher power system operation cost.

8.3 Recommendations for future work

The major efforts of this PhD study have been devoted to modeling, impact assessment and scheduling of building energy flexibility for providing spinning reserve in power systems. In future studies, further efforts can be made on the following aspects to improve the quality of the research.

- This study focuses on the energy flexibility potential of passive thermal mass storage of buildings, without detailed modelling of HVAC systems. Future work could incorporate component-level details of HVAC systems for more realistic flexibility quantification. A second-order building thermodynamic model is used for buildings in cooling-dominated regions in this study. The model overlooks the effect of humidity on building cooling load. Future work could consider humidity when determining the operating power of HVAC systems.
- This study focuses on the technical energy flexibility capacity of buildings. In reality, actual flexibility provision depends on the incentives that building owners

can obtain. Characterizing the flexibility function of a building cluster under both uncertainties and incentives will be an interesting research direction.

- The impact assessment in this study assumes that the entire commercial building sector participates in grid service provision. The actual cost saving greatly depends on the real-world participation rates of building users and needs further investigation. Moreover, this study focuses on the flexibility of building HVAC systems. Future work could consider other flexibility resources (e.g., electric vehicles) to provide a more comprehensive assessment of demand flexibility.
- The reserve scheduling framework and optimization strategy are conducted in a centralized manner in this study. The information of buildings needs to be communicated and shared with grid operators. This may raise concerns regarding communication protocols and data privacy. Future work could consider using distributed optimization to address these concerns.
- With a shorter predictive horizon, the forecast accuracy of renewable generation and building energy flexibility improves. Therefore, proper adjustment of the day-ahead reserve schedules according to the updated intra-day forecasts is of great benefit and needs further exploration.

REFERENCES

Amadeh, Ali, Zachary E. Lee, and K. Max Zhang. 2023. "Building Cluster Demand Flexibility: An Innovative Characterization Framework and Applications at the Planning and Operational Levels." *Energy Conversion and Management* 283:116884. doi: 10.1016/j.enconman.2023.116884.

Amadeh, Ali, Zachary E. Lee, and K. Max Zhang. 2022. "Quantifying Demand Flexibility of Building Energy Systems under Uncertainty." *Energy* 246:123291. doi: 10.1016/j.energy.2022.123291.

Aryandoust, Arsam, and Johan Lilliestam. 2017. "The Potential and Usefulness of Demand Response to Provide Electricity System Services." *Applied Energy* 204:749–66. doi: 10.1016/j.apenergy.2017.07.034.

Bacher, Peder, and Henrik Madsen. 2011. "Identifying Suitable Models for the Heat Dynamics of Buildings." *Energy and Buildings* 43(7):1511–22. doi: 10.1016/j.enbuild.2011.02.005.

Bampoulas, Adamantios, Fabiano Pallonetto, Eleni Mangina, and Donal P. Finn. 2023. "A Bayesian Deep-Learning Framework for Assessing the Energy Flexibility of Residential Buildings with Multicomponent Energy Systems." *Applied Energy* 348:121576. doi: 10.1016/j.apenergy.2023.121576.

Barani, Mostafa, Stian Backe, Ryan O'Reilly, and Pedro Crespo del Granado. 2023. "Residential Demand Response in the European Power System: No Significant Impact on Capacity Expansion and Cost Savings." *Sustainable Energy, Grids and Networks* 101198. doi: 10.1016/j.segan.2023.101198.

Bertsimas, Dimitris, Eugene Litvinov, Xu Andy Sun, Jinye Zhao, and Tongxin Zheng. 2013. "Adaptive Robust Optimization for the Security Constrained Unit Commitment Problem." *IEEE Transactions on Power Systems* 28(1):52–63. doi: 10.1109/TPWRS.2012.2205021.

Bünning, Felix, Philipp Heer, Roy S. Smith, and John Lygeros. 2023. "Increasing Electrical Reserve Provision in Districts by Exploiting Energy Flexibility of Buildings with Robust Model Predictive Control." *Advances in Applied Energy* 10:100130. doi: 10.1016/j.adapen.2023.100130.

Burgio, Alessandro, Domenico Cimmino, Mohammad Dolatabadi, Michal Jasinski, Zbigniew Leonowicz, and Pierlugi Siano. 2023. "Virtual Energy Storage System for Peak Shaving and Power Balancing the Generation of a MW Photovoltaic Plant." *Journal of Energy Storage* 71:108204. doi: 10.1016/j.est.2023.108204.

Chen, Richard Li-Yang, Neng Fan, Ali Pinar, and Jean-Paul Watson. 2017. "Contingency-Constrained Unit Commitment with Post-Contingency

Corrective Recourse." *Annals of Operations Research* 249(1):381–407. doi: 10.1007/s10479-014-1760-x.

Chyong, Chi Kong, and David Newbery. 2022. "A Unit Commitment and Economic Dispatch Model of the GB Electricity Market – Formulation and Application to Hydro Pumped Storage." *Energy Policy* 170:113213. doi: 10.1016/j.enpol.2022.113213.

Dai, Mingkun, Hangxin Li, Xiuming Li, and Shengwei Wang. 2024. "Reconfigurable Supply-Based Feedback Control for Enhanced Energy Flexibility of Air-Conditioning Systems Facilitating Grid-Interactive Buildings." *Advances in Applied Energy* 14:100176. doi: 10.1016/j.adapen.2024.100176.

Ding, Yi, Wenqi Cui, Shujun Zhang, Hongxun Hui, Yiwei Qiu, and Yonghua Song. 2019. "Multi-State Operating Reserve Model of Aggregate Thermostatically-Controlled-Loads for Power System Short-Term Reliability Evaluation." *Applied Energy* 241:46–58. doi: 10.1016/j.apenergy.2019.02.018.

Doherty, R., and M. O'Malley. 2005. "A New Approach to Quantify Reserve Demand in Systems with Significant Installed Wind Capacity." *IEEE Transactions on Power Systems* 20(2):587–95. doi: 10.1109/TPWRS.2005.846206.

Dong, Bing, Zhaoxuan Li, Ahmad Taha, and Nikolaos Gatsis. 2018. "Occupancy-Based Buildings-to-Grid Integration Framework for Smart and Connected Communities." *Applied Energy* 219:123–37. doi: 10.1016/j.apenergy.2018.03.007.

Dong, Lianxin, Qing Wu, Juhua Hong, Zhihua Wang, Shuai Fan, and Guangyu He. 2023. "An Adaptive Decentralized Regulation Strategy for the Cluster with Massive Inverter Air Conditionings." *Applied Energy* 330:120304. doi: 10.1016/j.apenergy.2022.120304.

Dong, Zihang, Xi Zhang, Linan Zhang, Spyros Giannelos, and Goran Strbac. 2024. "Flexibility Enhancement of Urban Energy Systems through Coordinated Space Heating Aggregation of Numerous Buildings." *Applied Energy* 374:123971. doi: 10.1016/j.apenergy.2024.123971.

Frew, Bethany, Brian Sergi, Paul Denholm, Wesley Cole, Nathaniel Gates, Daniel Levie, and Robert Margolis. 2021. "The Curtailment Paradox in the Transition to High Solar Power Systems." *Joule* 5(5):1143–67. doi: 10.1016/j.joule.2021.03.021.

Gade, Peter A. V., Trygve Skjøtskift, Charalampos Ziras, Henrik W. Bindner, and Jalal Kazempour. 2024. "Load Shifting versus Manual Frequency Reserve: Which One Is More Appealing to Thermostatically Controlled Loads in Denmark?" *Electric Power Systems Research* 232:110364. doi: 10.1016/j.epsr.2024.110364.

Georges, Emeline, Bertrand Cornélusse, Damien Ernst, Vincent Lemort, and Sébastien Mathieu. 2017. "Residential Heat Pump as Flexible Load for Direct

Control Service with Parametrized Duration and Rebound Effect." *Applied Energy* 187:140–53. doi: 10.1016/j.apenergy.2016.11.012.

Guo, Zhong, Austin R. Coffman, Jeffrey Munk, Piljae Im, Teja Kuruganti, and Prabir Barooah. 2021. "Aggregation and Data Driven Identification of Building Thermal Dynamic Model and Unmeasured Disturbance." *Energy and Buildings* 231:110500. doi: 10.1016/j.enbuild.2020.110500.

Hao, He, Di Wu, Jianming Lian, and Tao Yang. 2018. "Optimal Coordination of Building Loads and Energy Storage for Power Grid and End User Services." *IEEE Transactions on Smart Grid* 9(5):4335–45. doi: 10.1109/TSG.2017.2655083.

Herding, Robert, Emma Ross, Wayne R. Jones, Elizabeth Endler, Vassilis M. Charitopoulos, and Lazaros G. Papageorgiou. 2024. "Risk-Aware Microgrid Operation and Participation in the Day-Ahead Electricity Market." *Advances in Applied Energy* 100180. doi: 10.1016/j.adapen.2024.100180.

Herre, Lars, Pierre Pinson, and Spyros Chatzivasileiadis. 2022. "Reliability-Aware Probabilistic Reserve Procurement." *Electric Power Systems Research* 212:108345. doi: 10.1016/j.epsr.2022.108345.

Hu, Maomao, and Fu Xiao. 2020. "Quantifying Uncertainty in the Aggregate Energy Flexibility of High-Rise Residential Building Clusters Considering Stochastic Occupancy and Occupant Behavior." *Energy* 194:116838. doi: 10.1016/j.energy.2019.116838.

Hua, Yuchao, Lingai Luo, Steven Le Corre, and Yilin Fan. 2023. "An Online Learning Framework for Self-Adaptive Dynamic Thermal Modeling of Building Envelopes." *Applied Thermal Engineering* 232:121032. doi: 10.1016/j.applthermaleng.2023.121032.

Ji, Yongli, Qingshan Xu, Jun Zhao, Yongbiao Yang, and Lu Sun. 2021. "Day-Ahead and Intra-Day Optimization for Energy and Reserve Scheduling under Wind Uncertainty and Generation Outages." *Electric Power Systems Research* 195:107133. doi: 10.1016/j.epsr.2021.107133.

Jia, Heping, Yi Ding, Yonghua Song, Chanan Singh, and Maozhen Li. 2019. "Operating Reliability Evaluation of Power Systems Considering Flexible Reserve Provider in Demand Side." *IEEE Transactions on Smart Grid* 10(3):3452–64. doi: 10.1109/TSG.2018.2827670.

Karangelos, Efthymios, and François Bouffard. 2012. "Towards Full Integration of Demand-Side Resources in Joint Forward Energy/Reserve Electricity Markets." *IEEE Transactions on Power Systems* 27(1):280–89. doi: 10.1109/TPWRS.2011.2163949.

Lavin, Luke, Sinnott Murphy, Brian Sergi, and Jay Apt. 2020. "Dynamic Operating Reserve Procurement Improves Scarcity Pricing in PJM." *Energy Policy* 147:111857. doi: 10.1016/j.enpol.2020.111857.

Le, Lingling, Jiakun Fang, Xiaomeng Ai, Shichang Cui, and Jinyu Wen. 2022. "Aggregation and Scheduling of Multi-Chiller HVAC Systems in Continuous-Time Stochastic Unit Commitment for Flexibility Enhancement." *IEEE Transactions on Smart Grid* 1–1. doi: 10.1109/TSG.2022.3227390.

Li, Han, and Tianzhen Hong. 2022. "A Semantic Ontology for Representing and Quantifying Energy Flexibility of Buildings." *Advances in Applied Energy* 8:100113. doi: 10.1016/j.adapen.2022.100113.

Liang, Wei, Han Li, Sicheng Zhan, Adrian Chong, and Tianzhen Hong. 2024. "Energy Flexibility Quantification of a Tropical Net-Zero Office Building Using Physically Consistent Neural Network-Based Model Predictive Control." *Advances in Applied Energy* 14:100167. doi: 10.1016/j.adapen.2024.100167.

Liu, G., and K. Tomsovic. 2014. "A Full Demand Response Model in Co-Optimized Energy and Reserve Market." *Electric Power Systems Research* 111:62–70. doi: 10.1016/j.epsr.2014.02.006.

Liu, Jia, Yuekuan Zhou, Hongxing Yang, and Huijun Wu. 2022. "Net-Zero Energy Management and Optimization of Commercial Building Sectors with Hybrid Renewable Energy Systems Integrated with Energy Storage of Pumped Hydro and Hydrogen Taxis." *Applied Energy* 321:119312. doi: 10.1016/j.apenergy.2022.119312.

Liu, Jingguan, Xiaomeng Ai, Jiakun Fang, Shichang Cui, Shengshi Wang, Wei Yao, and Jinyu Wen. 2024. "Continuous-Time Aggregation of Massive Flexible HVAC Loads Considering Uncertainty for Reserve Provision in Power System Dispatch." *IEEE Transactions on Smart Grid* 1–1. doi: 10.1109/TSG.2024.3398627.

Liu, Jingjing, Rongxin Yin, Lili Yu, Mary Ann Piette, Marco Pritoni, Armando Casillas, Jiarong Xie, Tianzhen Hong, Monica Neukomm, and Peter Schwartz. 2022. "Defining and Applying an Electricity Demand Flexibility Benchmarking Metrics Framework for Grid-Interactive Efficient Commercial Buildings." *Advances in Applied Energy* 8:100107. doi: 10.1016/j.adapen.2022.100107.

Liu, Xuan, and Antonio J. Conejo. 2024. "Day-Ahead Reserve Determination in Power Systems with High Renewable Penetration." *International Journal of Electrical Power & Energy Systems* 156:109703. doi: 10.1016/j.ijepes.2023.109703.

Luo, Zhengyi, Jinqing Peng, and Rongxin Yin. 2023. "Many-Objective Day-Ahead Optimal Scheduling of Residential Flexible Loads Integrated with Stochastic Occupant Behavior Models." *Applied Energy* 347:121348. doi: 10.1016/j.apenergy.2023.121348.

MacDonald, Jason. 2014. "Commercial Building Loads Providing Ancillary Services in PJM."

Mallapragada, Dharik S., Nestor A. Sepulveda, and Jesse D. Jenkins. 2020. "Long-Run System Value of Battery Energy Storage in Future Grids with Increasing Wind and Solar Generation." *Applied Energy* 275:115390. doi: 10.1016/j.apenergy.2020.115390.

Martinez, S., M. Vellei, and J. Le Dréau. 2022a. "Demand-Side Flexibility in a Residential District: What Are the Main Sources of Uncertainty?" *Energy and Buildings* 255:111595. doi: 10.1016/j.enbuild.2021.111595.

Martinez, S., M. Vellei, and J. Le Dréau. 2022b. "Demand-Side Flexibility in a Residential District: What Are the Main Sources of Uncertainty?" *Energy and Buildings* 255:111595. doi: 10.1016/j.enbuild.2021.111595.

Mimica, Marko, Ivan-Pavao Boras, and Goran Krajačić. 2023. "The Integration of the Battery Storage System and Coupling of the Cooling and Power Sector for Increased Flexibility under the Consideration of Energy and Reserve Market." *Energy Conversion and Management* 286:117005. doi: 10.1016/j.enconman.2023.117005.

Müller, F. L., and B. Jansen. 2019. "Large-Scale Demonstration of Precise Demand Response Provided by Residential Heat Pumps." *Applied Energy* 239:836–45. doi: 10.1016/j.apenergy.2019.01.202.

Müller, Theresa, and Dominik Möst. 2018. "Demand Response Potential: Available When Needed?" *Energy Policy* 115:181–98. doi: 10.1016/j.enpol.2017.12.025.

Navidi, Thomas, Abbas El Gamal, and Ram Rajagopal. 2023. "Coordinating Distributed Energy Resources for Reliability Can Significantly Reduce Future Distribution Grid Upgrades and Peak Load." *Joule* 7(8):1769–92. doi: 10.1016/j.joule.2023.06.015.

Paterakis, Nikolaos G., Madeleine Gibescu, Anastasios G. Bakirtzis, and Joao P. S. Catalao. 2018. "A Multi-Objective Optimization Approach to Risk-Constrained Energy and Reserve Procurement Using Demand Response." *IEEE Transactions on Power Systems* 33(4):3940–54. doi: 10.1109/TPWRS.2017.2785266.

Patteeuw, Dieter, Kenneth Bruninx, Alessia Arteconi, Erik Delarue, William D'haeseleer, and Lieve Helsen. 2015. "Integrated Modeling of Active Demand Response with Electric Heating Systems Coupled to Thermal Energy Storage Systems." *Applied Energy* 151:306–19. doi: 10.1016/j.apenergy.2015.04.014.

Poorvaezi Roukerd, Saeed, Amir Abdollahi, and Masoud Rashidinejad. 2020. "Uncertainty-Based Unit Commitment and Construction in the Presence of Fast Ramp Units and Energy Storages as Flexible Resources Considering Enigmatic Demand Elasticity." *Journal of Energy Storage* 29:101290. doi: 10.1016/j.est.2020.101290.

Qi, Ning, Lin Cheng, Yingrui Zhuang, Yanglin Zhou, Yongmi Zhang, and Changyu Zhu. 2022. "Reliability Assessment and Improvement of Distribution System

with Virtual Energy Storage under Exogenous and Endogenous Uncertainty." *Journal of Energy Storage* 56:105993. doi: 10.1016/j.est.2022.105993.

Qi, Ning, Pierre Pinson, Mads R. Almassalkhi, Lin Cheng, and Yingrui Zhuang. 2023. "Chance-Constrained Generic Energy Storage Operations Under Decision-Dependent Uncertainty." *IEEE Transactions on Sustainable Energy* 14(4):2234–48. doi: 10.1109/TSTE.2023.3262135.

Qin, Xin, Bolun Xu, Ioannis Lestas, Ye Guo, and Hongbin Sun. 2023. "The Role of Electricity Market Design for Energy Storage in Cost-Efficient Decarbonization." *Joule* 7(6):1227–40. doi: 10.1016/j.joule.2023.05.014.

Reynders, G., J. Diriken, and D. Saelens. 2014. "Quality of Grey-Box Models and Identified Parameters as Function of the Accuracy of Input and Observation Signals." *Energy and Buildings* 82:263–74. doi: 10.1016/j.enbuild.2014.07.025.

Roos, Aleksandra, and Torjus Folsland Bolkesjø. 2018. "Value of Demand Flexibility on Spot and Reserve Electricity Markets in Future Power System with Increased Shares of Variable Renewable Energy." *Energy* 144:207–17. doi: 10.1016/j.energy.2017.11.146.

Salgado-Bravo, Marcelo, Matias Negrete-Pincetic, and Aristides Kiprakis. 2023. "Demand-Side Energy Flexibility Estimation for Day-Ahead Models." *Applied Energy* 347:121502. doi: 10.1016/j.apenergy.2023.121502.

Seatle, Madeleine, and Madeleine McPherson. 2024. "Residential Demand Response Program Modelling to Compliment Grid Composition and Changes in Energy Efficiency." *Energy* 290:130173. doi: 10.1016/j.energy.2023.130173.

Shamsi, Mohammad Haris, Usman Ali, Eleni Mangina, and James O'Donnell. 2021. "Feature Assessment Frameworks to Evaluate Reduced-Order Grey-Box Building Energy Models." *Applied Energy* 298:117174. doi: 10.1016/j.apenergy.2021.117174.

Song, Meng, Ciwei Gao, Huaguang Yan, and Jianlin Yang. 2018. "Thermal Battery Modeling of Inverter Air Conditioning for Demand Response." *IEEE Transactions on Smart Grid* 9(6):5522–34. doi: 10.1109/TSG.2017.2689820.

Song, Meng, Wei Sun, Yifei Wang, Mohammad Shahidehpour, Zhiyi Li, and Ciwei Gao. 2020. "Hierarchical Scheduling of Aggregated TCL Flexibility for Transactive Energy in Power Systems." *IEEE Transactions on Smart Grid* 11(3):2452–63. doi: 10.1109/TSG.2019.2955852.

Stover, Oliver, Pranav Karve, and Sankaran Mahadevan. 2023. "Reliability and Risk Metrics to Assess Operational Adequacy and Flexibility of Power Grids." *Reliability Engineering & System Safety* 231:109018. doi: 10.1016/j.ress.2022.109018.

Sun, Guoqiang, Sichen Shen, Sheng Chen, Yizhou Zhou, and Zhinong Wei. 2022. "Bidding Strategy for a Prosumer Aggregator with Stochastic Renewable

Energy Production in Energy and Reserve Markets." *Renewable Energy* 191:278–90. doi: 10.1016/j.renene.2022.04.066.

Tan, Jin, Qiuwei Wu, Menglin Zhang, Wei Wei, Feng Liu, and Bo Pan. 2021. "Chance-Constrained Energy and Multi-Type Reserves Scheduling Exploiting Flexibility from Combined Power and Heat Units and Heat Pumps." *Energy* 233:121176. doi: 10.1016/j.energy.2021.121176.

Tang, Hong, and Shengwei Wang. 2023. "Game-Theoretic Optimization of Demand-Side Flexibility Engagement Considering the Perspectives of Different Stakeholders and Multiple Flexibility Services." *Applied Energy* 332:120550. doi: 10.1016/j.apenergy.2022.120550.

Tang, Hong, Shengwei Wang, and Hangxin Li. 2021. "Flexibility Categorization, Sources, Capabilities and Technologies for Energy-Flexible and Grid-Responsive Buildings: State-of-the-Art and Future Perspective." *Energy* 219:119598. doi: 10.1016/j.energy.2020.119598.

Tina, Giuseppe Marco, Stefano Aneli, and Antonio Gagliano. 2022. "Technical and Economic Analysis of the Provision of Ancillary Services through the Flexibility of HVAC System in Shopping Centers." *Energy* 258:124860. doi: 10.1016/j.energy.2022.124860.

Trovato, Vincenzo. 2023. "Optimal Coordination of Spinning and Standing Reserve with Energy Payback of Thermostatically Controlled Loads." *International Journal of Electrical Power & Energy Systems* 149:109041. doi: 10.1016/j.ijepes.2023.109041.

Trovato, Vincenzo, Fei Teng, and Goran Strbac. 2018. "Role and Benefits of Flexible Thermostatically Controlled Loads in Future Low-Carbon Systems." *IEEE Transactions on Smart Grid* 9(5):5067–79. doi: 10.1109/TSG.2017.2679133.

Vindel, Elvin, Mario Bergés, Burcu Akinci, Olga Kavvada, and Valentin Gavan. 2023. "AlphaShed: A Scalable Load Flexibility Model for Shedding Potential in Commercial HVAC Systems." *Energy and Buildings* 279:112686. doi: 10.1016/j.enbuild.2022.112686.

Wald, Dylan, Kathryn Johnson, Jennifer King, Joshua Comden, Christopher J. Bay, Rohit Chintala, Sanjana Vijayshankar, and Deepthi Vaidhynathan. 2023. "Shifting Demand: Reduction in Necessary Storage Capacity through Tracking of Renewable Energy Generation." *Advances in Applied Energy* 10:100131. doi: 10.1016/j.adapen.2023.100131.

Wang, Andong, Rongling Li, and Shi You. 2018. "Development of a Data Driven Approach to Explore the Energy Flexibility Potential of Building Clusters." *Applied Energy* 232:89–100. doi: 10.1016/j.apenergy.2018.09.187.

Wang, Beibei, Xuechun Yang, Taylor Short, and Shengchun Yang. 2017. "Chance Constrained Unit Commitment Considering Comprehensive Modelling of Demand Response Resources." *IET Renewable Power Generation* 11(4):490–500. doi: 10.1049/iet-rpg.2016.0397.

Wang, Huilong, Shengwei Wang, and Rui Tang. 2019. “Development of Grid-Responsive Buildings: Opportunities, Challenges, Capabilities and Applications of HVAC Systems in Non-Residential Buildings in Providing Ancillary Services by Fast Demand Responses to Smart Grids.” *Applied Energy* 250:697–712. doi: 10.1016/j.apenergy.2019.04.159.

Wang, Qianfan, Jianhui Wang, and Yongpei Guan. 2013. “Stochastic Unit Commitment With Uncertain Demand Response.” *IEEE Transactions on Power Systems* 28(1):562–63. doi: 10.1109/TPWRS.2012.2202201.

Wang, Qin, Aidan Tuohy, Miguel Ortega-Vazquez, Mobolaji Bello, Erik Ela, Daniel Kirk-Davidoff, William B. Hobbs, David J. Ault, and Russ Philbrick. 2023. “Quantifying the Value of Probabilistic Forecasting for Power System Operation Planning.” *Applied Energy* 343:121254. doi: 10.1016/j.apenergy.2023.121254.

Wang, Shengwei, and Rui Tang. 2017. “Supply-Based Feedback Control Strategy of Air-Conditioning Systems for Direct Load Control of Buildings Responding to Urgent Requests of Smart Grids.” *Applied Energy* 201:419–32. doi: 10.1016/j.apenergy.2016.10.067.

Wang, Zhaohua, Bin Lu, Bo Wang, Yueming (Lucy) Qiu, Han Shi, Bin Zhang, Jingyun Li, Hao Li, and Wenhui Zhao. 2023. “Incentive Based Emergency Demand Response Effectively Reduces Peak Load during Heatwave without Harm to Vulnerable Groups.” *Nature Communications* 14(1):6202. doi: 10.1038/s41467-023-41970-8.

Wei, Congying, Qiuwei Wu, Jian Xu, Yuanzhang Sun, Xiaolong Jin, Siyang Liao, Zhiyong Yuan, and Li Yu. 2020. “Distributed Scheduling of Smart Buildings to Smooth Power Fluctuations Considering Load Rebound.” *Applied Energy* 276:115396. doi: 10.1016/j.apenergy.2020.115396.

Xiong, Peng, and Panida Jirutitijaroen. 2013. “A Stochastic Optimization Formulation of Unit Commitment With Reliability Constraints.” *IEEE Transactions on Smart Grid* 4(4):2200–2208. doi: 10.1109/TSG.2013.2278398.

Xue, Xue, Shengwei Wang, Chengchu Yan, and Borui Cui. 2015. “A Fast Chiller Power Demand Response Control Strategy for Buildings Connected to Smart Grid.” *Applied Energy* 137:77–87. doi: 10.1016/j.apenergy.2014.09.084.

Yang, Shiyu, H. Oliver Gao, and Fengqi You. 2024. “Demand Flexibility and Cost-Saving Potentials via Smart Building Energy Management: Opportunities in Residential Space Heating Across the US.” *Advances in Applied Energy* 100171. doi: 10.1016/j.adapen.2024.100171.

Zhan, Sicheng, Bing Dong, and Adrian Chong. 2023. “Improving Energy Flexibility and PV Self-Consumption for a Tropical Net Zero Energy Office Building.” *Energy and Buildings* 278:112606. doi: 10.1016/j.enbuild.2022.112606.

Zhang, Jiangmeng, and Alejandro. D. Domínguez-García. 2018. “Evaluation of Demand Response Resource Aggregation System Capacity Under

Uncertainty." *IEEE Transactions on Smart Grid* 9(5):4577–86. doi: 10.1109/TSG.2017.2663780.

Zhang, Kun, Etienne Saloux, and José A. Candanedo. 2024. "Enhancing Energy Flexibility of Building Clusters via Supervisory Room Temperature Control: Quantification and Evaluation of Benefits." *Energy and Buildings* 302:113750. doi: 10.1016/j.enbuild.2023.113750.

Zhang, Menglin, Qiuwei Wu, Jinyu Wen, Bo Zhou, Qinyue Guan, Jin Tan, Zhongwei Lin, and Fang Fang. 2022. "Day-Ahead Stochastic Scheduling of Integrated Electricity and Heat System Considering Reserve Provision by Large-Scale Heat Pumps." *Applied Energy* 307:118143. doi: 10.1016/j.apenergy.2021.118143.

Zhang, Wei, Jianming Lian, Chin-Yao Chang, and Karanjit Kalsi. 2013. "Aggregated Modeling and Control of Air Conditioning Loads for Demand Response." *IEEE Transactions on Power Systems* 28(4):4655–64. doi: 10.1109/TPWRS.2013.2266121.

Zhao, Chaoyue, Jianhui Wang, Jean-Paul Watson, and Yongpei Guan. 2013. "Multi-Stage Robust Unit Commitment Considering Wind and Demand Response Uncertainties." *IEEE Transactions on Power Systems* 28(3):2708–17. doi: 10.1109/TPWRS.2013.2244231.

Zhou, Ella, Elaine Hale, and Elaina Present. 2022. "Building Flexibility Revenue in Modeled Future Bulk Power Systems with Varying Levels of Renewable Energy." *Heliyon* 8(7):e09865. doi: 10.1016/j.heliyon.2022.e09865.